DEVELOPING PLATINUM NANOPARTICLES FOR ACTIVE TARGETING OF LIVER CANCER IN ZEBRAFISH

TEOW YIWEI

NATIONAL UNIVERSITY OF SINGAPORE

2012

DEVELOPING PLATINUM NANOPARTICLES FOR ACTIVE TARGETING OF LIVER CANCER IN ZEBRAFISH

TEOW YIWEI

B.Sc.(Hons.), NUS

A THESIS SUBMITTED

FOR THE DEGREE OF DOCTOR OF PHILOSOPHY

NUS GRADUATE SCHOOL FOR

INTEGRATIVE SCIENCES AND ENGINEERING

NATIONAL UNIVERSITY OF SINGAPORE

2012

DECLARATION

I hereby declare that the thesis is my original work and it has been written by me in its entirety. I have duly acknowledged all the sources of information which have been used in the thesis.

This thesis has also not been submitted for any degree in any university previously.

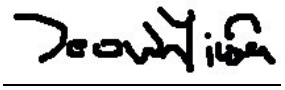

Teow Yiwei

12 March 2013

ACKNOWLEDGEMENTS

It is an honour to thank the following people, for if not for them, the thesis would not have been possible. Firstly, I am grateful to my mentor Associate Professor Suresh Valiyaveettil, for his funding, resources and timely discussions. Secondly, I thank Professor Gong Zhiyuan (also the TAC Chairman) from the Department of Biological Sciences for his supervision and resources in the Zebrafish Laboratory. Thirdly, I thank Associate Professor Xu Qing-Hua (TAC member) for his advice.

Special thanks to my colleagues from other departments: Dr. Chew Tiweng, Ms. Zhou Li and Mr. Yan Chuan for their advices on experimental techniques; my lab mates Dr. Brahathees, Kiruba, Ramakrishna, Ashok, Chunyan, Daisy, Nizar, Roshan and Madhuvanthi for all the fun, laughter and wonderful discussions.

I also appreciate the help from the following administrative and laboratory staff: Madam Loy Gek Luan, Mr. Chong Ping Lee and Mr. Subhas Balan.

Last but not least, I thank my loving wife Teng Chew Ping and our parents for their kind understanding, love and support. This thesis is dedicated to my baby boy Teow Jun Yang Davien. Daddy hopes that you will have a better future with the submission of this thesis.

TABLE OF CONTENTS

CHAPTER 1

CHAPTER 2

CHAPTER 3

CHAPTER 4

CHAPTER 5

SUMMARY

Many engineered nanomaterials (NMs) are being synthesized and explored for potential use in consumer and medical products. Already, nanoparticles (NPs) of titanium dioxide (TiO_2), zinc oxide (ZnO), silver (Ag) and other metals or their oxides are present in commercial products such as sunscreens, cosmetics, wound dressings, surgical tools, detergents, automotive paints and tires. More recent and advanced FDA-approved use of NPs includes quantum dots (QDs) in live cell imaging, zirconium oxides in bone replacement and prosthetic devices and nanocarriers in drug delivery. The benefits from nanotechnology are aplenty, comprising antimicrobial activities, scratch- and water-resistance, long-lasting shine, improved processor speeds and better display resolution, to name a few.

In the following chapters, we explore the use of NPs in the field of drug delivery, especially in cancer. Conventional drugs are governed by Absorption, Distribution, Metabolism and Excretion (ADME) and these dictates concentrations, kinetics and performance of a drug. Often, simple issues like poor solubility, stability, high metabolism and toxicity can prevent a New Chemical Entity (NCE) from reaching the market in the long and arduous process of drug discovery. Cleverly designed functional NPs can avoid these issues and aid in the development of more successful NCEs.

Cancer is a disease which involves unregulated cell growth. Treatment methods include surgery, radiation therapy and alternative medicine. Newer methods developed in recent years also include employing ultrasound, laser and heat. However, the most common and easiest method is chemotherapy. Chemotherapeutic drugs kill cancer cells which are dividing rapidly but in the process, also harm normal cells and could result in serious side effects. Targeted drug delivery vehicles can help overcome

toxicity by delivering the drug to the target of interest. NPs emerge as a useful delivery vehicle for poorly soluble drugs and at the same time, also exhibit targeting properties. Abraxane (albumin-bound paclitaxel) was the first particulate drug to be approved by the US-FDA in 2005.

In Chapter 1, a detailed introduction was given to discuss the current issues and problems faced by chemists during drug development. Nanotechnology offers an attractive solution and the advantages and disadvantages will be discussed. A review of current literature explores the mechanisms and success stories of using NPs, followed by the rationale of this study. Chapter 2 contains the detailed experimental procedures for the studies carried out.

Interaction of nanoparticles with human cells is an interesting topic for understanding toxicity and developing potential drug candidates. In Chapter 3, water soluble platinum nanoparticles (Pt-nps) were synthesized *via* reduction of hexachloroplatinic acid using sodium borohydride in the presence of capping agents. A thorough characterization was carried out before *in vitro* studies in human cell lines (HeLa, MCF7, HepG2 and IMR90). The toxicity of Pt-nps, combined with the possibility to incorporate functional organic molecules as capping agents, meant that Pt-nps were suitable for developing new drug candidates.

In Chapter 4, zebrafish (*Danio rerio*) was used as an *in vivo* model which developed liver cancer. Designed Pt-nps which target the liver was used for treatment of liver cancer. The liver size of Pt-nps treated fish larvae were compared against untreated control larvae and the uptake of Pt-nps by larvae were studied.

ABBREVIATIONS

ATP	Adenosine triphosphate
Au	Gold
BBB	Blood brain barrier
CNTs	Carbon nanotubes
DLS	Dynamic light scattering
DMEM	Dulbecco's modified eagle medium
DNA	Deoxyribonucleic acid
EDX	Electron dispersive X-ray spectroscopy
EPR	Enhanced permeability and retention effect
FA	Folic acid
H	Hours
HPF	Hours post fertilisation
HPT	Hours post treatment
ICP-OES	Inductively coupled plasma optical emission spectrometry
MEM	Minimal essential medium
MTT	3-(4,5-dimethylthiazole-2-yl)-2,5-biphenyl tetrazolium bromide)
MTS	3-(4,5-dimethylthiazole-2-yl)-5-(3-carboxymethoxyphenyl)-2-(4-sulfophenyl)-2*H* tetrazolium)
NMs	Nanomaterials
NPs	Nanoparticles
PCNA	Proliferating cell nuclear antigen
Pt	Platinum
PEG	Poly(ethylene glycol)
PVA	Poly(vinyl alcohol)

PVP	Poly(vinyl pyrrolidone)
RES	Reticuloendothelial system
RNA	Ribonucleic acid
ROS	Reactive oxygen species
RPM	Revolutions per minute
SOP	Standard operating procedures
TEM	Transmission electron microscopy
UV-Vis	Ultraviolet-visible spectroscopy
5FU	5-Fluorouracil

LIST OF TABLES AND FIGURES

LIST OF PUBLICATIONS AND CONFERENCES ATTENDED

Publications (attached in APPENDIX)

[1] N. Mahanta, Yiwei Teow and S. Valiyaveettil, "Fabrication and characterization of hybrid nanofibers from poly(vinyl alcohol), milk protein and metal carbonates", Journal of Nanoscience and Nanotechnology, 2012, 12, 1–7 (1 citation)

[2] Yiwei Teow, P. V. Asharani, M. Prakash Hande and Suresh Valiyaveettil, "Health impact and safety of engineered nanomaterials", Chemical Communications, 2011, 47, 7025–7038 (Cover article) (9 citations)

[3] Yiwei Teow and Suresh Valiyaveettil, "Active targeting of cancer cells using folic acid-conjugated platinum nanoparticles", Nanoscale, 2010, 2, 2607–2613 (Cover article) (4 citations)

Submitted/under preparation

[1] Yiwei Teow, Boon Chuan Low, Zhiyuan Gong and Suresh Valiyaveettil, "Active targeting of liver cancer in zebrafish (*Danio rerio*) using platinum nanoparticles"

[2] Yiwei Teow, Nuraini binte Supaat, Liwen Neo, Zhiyuan Gong and Suresh Valiyaveettil, "Protective effects of plant extracts against silver nanoparticle toxicity in zebrafish (*Danio rerio*) embryos"

Conferences

[1] 2012 5th MRS-S Conference on Advanced Materials (NTU, Singapore)

Poster Presentation: Functionalized platinum nanoparticles as an active targeting drug for cancer in zebrafish

[2] 2011 Materials Research Society (MRS) Fall Meeting & Exhibit (Hynes Convention Centre, Boston)

Poster Presentation: Functionalized platinum nanoparticles as an active targeting drug for cancer in zebrafish

[3] 2010 Materials Research Society (MRS) Spring Meeting (San Francisco, California)

Oral Presentation: 1) Structural Damage in Erythrocytes Exposed Nanomaterials (Asha); 2) Azide Functionalization on Graphene Nanosheets (Sajini).

Poster Presentation: Folate-functionalized Platinum Nanoparticles for Tumour Targeting

[4] 2010 NUSSNI-BMRC Workshop on Nanotoxicity and Nanomedicine (NUS, Singapore)

Oral Presentation: Cytotoxicity of Silver Nanoparticles in Human Cell Lines and Zebrafish Embryos

[5] 2010 NGS Symposium 2 (NUS, Singapore)

Poster Presentation: Folate-Capped Platinum Nanoparticles For Cancer Targeting

[6] 2009 SICC6 (Suntec Convention Centre, Singapore)

Poster Presentation: Folic Acid-Conjugated Platinum Nanoparticles for the Active Targeting of Cancer

[7] 2009 ICMAT (Suntec Convention Centre, Singapore)

Student volunteer

CHAPTER 1

INTRODUCTION

Publication from this chapter:

Yiwei Teow, P. V. Asharani, M. Prakash Hande and Suresh Valiyaveettil, "Health impact and safety of engineered nanomaterials", Chemical Communications, 2011, 47, 7025–7038 (Cover article)

1. Introduction

1.1 Nanotechnology

The word "nano", derived from Greek, means "dwarf" and represents one-billionth of a unit. The oldest and most famous example of nanotechnology is probably the Lycurgus Cup that was made in the 5th century B.C. (Daniel and Astruc 2004). The cup is ruby red in transmitted light and green in reflected light due to the presence of gold and silver colloids. The cup's composition is an alloy of 70 nm nanoparticles (NPs) containing 70% silver and 30% gold. Soluble gold was used in the Middle Ages because of its curative powers for diseases such as heart and venereal problems, dysentery, epilepsy, tumours and for diagnosis of syphilis. Modern nanotechnology started in 1959, where physicist Richard P. Feynman championed the arrival of nanotechnology (Arvizo, Bhattacharyya et al. 2012). In his famous lecture to the American Physical Society at Caltech, he said, "There's plenty of room at the bottom", hinting at the potential for nanoscale design to influence a wide range of fields such as optics and electronics.

Nanotechnology has enormous potential to affect the society. In 2007, US$60 billion worth of nanotechnology-incorporated products were sold and this figure rose to US$150 billion in 2008 (Scholars). Global research and development is anticipated to lead to new medical treatments and tools; more efficient energy production, storage and transmission; better access to clean water; more effective pollution reduction and prevention; and stronger, lighter materials. It is expected that the sale of products employing nanotechnology may reach US$1 trillion per year by 2015 (Xia, Li et al. 2009), with medical-related products alone occupying US$53 billion in this market (Jones and Grainger 2009). Today, there are more than 1000 nanotechnology

incorporated products marketed by 587 companies in 30 countries (Scholars ; Xia, Li et al. 2009).

Figure 1.1: The Lycurgus Cup (© Trustees of the British Museum) in reflected (left) and transmitted (right) light, displaying the dichroic effect (Daniel and Astruc 2004).

1.2 Classification and synthesis of nanomaterials

Nanomaterials (NMs) are mainly classified based on their composition and shape (Huczko 2000; Rodriguez-Hernandez, Checot et al. 2005; Wang and Cao 2006; Byrappa and Adschiri 2007; Hussain, Braydich-Stolle et al. 2009). A few examples would include NPs, nanowires, nanotubes, nanofibers and nanohydrogels. The most commonly synthesized are NPs owing to their versatility in terms of shapes, sizes, functionalities and compositions. Based on composition, NPs can be grouped into the following categories:

1. Organic NMs (polymers, polymeric micelles, dendrimers);
2. Organic–inorganic hybrids (nanocomposites);

3. Carbon-rich NMs (carbon nanotubes (CNTs), C_{60});
4. Liposome NMs (generally used for drug delivery);
5. Biological NMs (proteins, lipids, carbohydrates);
6. Inorganic NMs (Ag, Au, Pt, Fe, TiO_2, $CaCO_3$, QDs, silica).

NPs can be synthesized by using either (Wiley, Sun et al. 2007; Zhou, Ralston et al. 2009; Misra and Sahoo 2010):

1. a "top-down" approach, where bulk materials are broken down to nanometre scale by milling, grinding, etching and pyrolysis; or
2. a "bottom-up" approach, which creates nano-objects by combining atomic scale materials (**Figure 1.2**).

In the top-down approach, a suitable starting material is reduced in size using mechanical or chemical methods. Silicon micro-fabrication and photolithography are two processes often prepared using the top-down approach (Mishra, Patel et al. 2010). An advantage of this method is the possibility of mass production in the industrial setting. The major disadvantages of the top-down approach include lengthy, time consuming processes, generation of a broad feature size distribution and imperfections or defects of the surface morphology generated. Surface deformations can have a significant impact on its physical properties and surface chemistry of the NPs (Thakkar, Mhatre et al. 2010). In pyrolysis, an organic precursor is burnt after forcing through an orifice at high pressure. The resulting ash is processed in order to recover the oxidized NPs which have a wide particle size distribution (Thakkar, Mhatre et al. 2010). This process consumes enormous amounts of energy to sustain the high pressure and temperature. On the contrary, the bottom-up method operates under ambient conditions which leads to high energy savings.

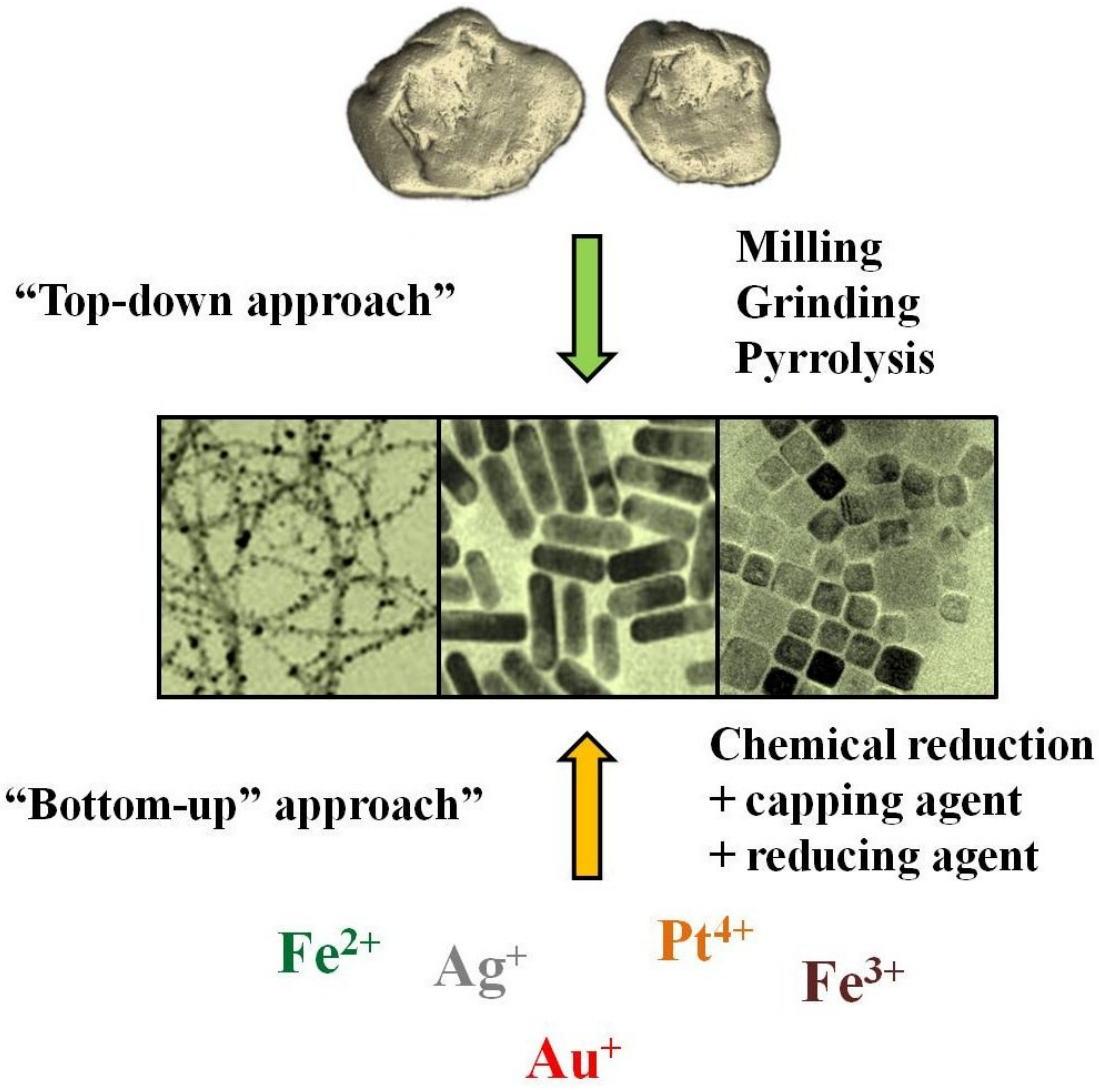

Figure 1.2: Nanoparticles of different sizes and morphologies can be synthesized *via* top-down mechanical methods or a bottom-up approach using metal salts (Teow, Asharani et al. 2011).

A variety of bottom-up approaches exist, comprising complex coacervation of two oppositely-charged polyelectrolytes, co-precipitation, salting-out from an aqueous–organic mixture, nanoprecipitation or solvent displacement, solvent emulsification–diffusion using an oil–water emulsion and using supercritical fluids. These techniques can be used to generate a variety of NMs including liposomes, nanoemulsions, polymeric micelles, polymeric NPs, protein NPs, solid lipid NPs and carbohydrate (chitosan, alginate, hyaluronic acid, dextran) NPs (Liu, Jiao et al. 2008; Szarpak, Cui et al. 2010). The most commonly employed and reported method is the

chemical reduction of metal ions using a suitable reducing agent in the presence of stabilizing or capping agent(s). The metal ions are reduced to yield corresponding metal atoms that aggregate to form a metal particle. The growth of the metal particle is inhibited by the addition of capping agents. The capping agent works either by conferring a charge (carboxylic acids and amines) on the surface which helps repel neighbouring NPs, or by sterically preventing the agglomeration of two NPs (Thanh and Green 2010). Apart from preventing NPs from precipitation, capping agents also serve other important functions such as controlling particle size, shape, charge and surface functionality which can confer special properties and which behave differently from their bulk materials (Liang, Lin et al. 2010).

Recently, there has been a growing interest in biological synthesis of metallic NPs using bacteria (Reddy, Chen et al. 2010), yeast (Kowshik, Ashtaputre et al. 2003), fungi, plants and algae (Thakkar, Mhatre et al. 2010). Such methods offer advantages over conventional chemical methods which avoid the use of toxic organic solvents and reagents, generation of hazardous side-products, high cost and energy consumption as well as producing NPs which are relatively non-toxic and biocompatible. Different NPs from Ag, Au, CdS, magnetite and uranium were made using biological processes (Nanda and Saravanan 2009). A similar method has been used in the synthesis of Ag NPs using fungal cell filtrate (Gajbhiye, Kesharwani et al. 2009).

1.3 Development of nanomaterials

Nanotechnology has captured both the commercial and academic research interests. According to Nel et al., it is expected to advance in four phases (Nel, Xia et al. 2006). The first phase of nanotechnology aims to develop passive nanostructures

for specific applications such as for use in sunscreens, wound dressings and other commercial products. The success and advancement of the first phase offers many promising future opportunities. The second phase relies on active NMs that can perform multiple tasks (e.g., biodevices and multifunctional drug delivery systems). The third phase will comprise nanosystems with a large number of interacting components acting together in a robotic manner, while the fourth and final phase will open up more complex systems that can function like living systems in a coordinated hierarchical way to provide better understanding of the processes under study.

Indeed, the applications of nanotechnology in modern day products are aplenty, especially from the first and second phase. The term "nano" has been used widely and even unrelated products such as "iPod nano" and "Tata Nano" have adopted this word in their names (Asharani 2009). NPs, especially, are being commercialised at a fast pace. Titanium dioxide NPs are being incorporated in sunscreen lotions to provide protection against harmful UV-rays. Gold NPs and nanorods are investigated for the diagnosis and treatment of cancer (Boisselier and Astruc 2009). Silver NPs, owing to their broad spectrum antimicrobial actions, are widely used in antiseptics, wound dressings, components in food containers, detergents, cosmetics and in many other consumer products (Edwards-Jones 2009; Rai, Yadav et al. 2009). Polymeric NPs are used as nanocarriers transport therapeutic agents directly to the target site with high efficiency (Mandal and Kundu 2009). CNTs can be used in electronics due to their excellent conductivity (Kang, Kocabas et al. 2007). Medicine is one of the areas where extensive research is ongoing for development of better therapeutics. Approximately 160 nanodrugs are currently in market with many more in clinical trials (Peer, Karp et al. 2007). Nanotechnology has also attracted the defence force, where NMs-based rocket fuel and wear and tear resistant coating on warships were

developed. NASA is actively developing NPs-based systems in their space shuttles for better performance (Asharani 2009).

1.4 Factors affecting biological properties of nanomaterials

1.4.1 Morphology (size and shape)

The small size of NMs has created opportunities for them to interact with biological entities such as cells, cellular components, bacteria and viruses which are never possible at the bulk scale. Cells were found to internalize NMs in a size-dependant manner, where smaller NPs were found to be better taken up and more toxic (Pan, Neuss et al. 2007; He, Zhang et al. 2009), but with a few exceptions (Waters, Masiello et al. 2009). In terms of *in vivo* uptake, 1.4 nm Au NPs were found to be able to translocate the air–blood barrier in the rat lung, while 18 nm Au NPs were trapped by the lungs and did not enter the blood (Semmler-Behnke, Kreyling et al. 2008). Researchers have made use of such properties to design and develop drugs, drug carriers (Kim, Jang et al. 2010), anti-cancer agents (Kim, Rozhkova et al. 2010) and stains for cell imaging (Mang, Won et al. 2009).

Examples of metallic NMs include Au NPs, Au nanorods (Leonov, Zheng et al. 2008), Au nanoplates (triangles, pentagons, hexagons) (Das, Das et al. 2010), FePt stars (Pazos-Perez, Rodriguez-Gonzalez et al. 2010), FePt yolk–shell NPs (Gao, Liang et al. 2008), Pt cubes, Pt polypods, Pt raspberries (Lim, Ojea-Jimenez et al. 2010), Pt nanodendrites (Wang, Wang et al. 2010), Pt nanowires and Pt–MWCNT composites (Chen and Holt-Hindle 2010), to name a few (**Figure 1.3**). Even though NMs with different morphologies may find different applications, spherical NPs are the most studied NMs. The shapes of Pt NPs were also found to cause a variation in their toxicity (Elder, Yang et al. 2007). Amongst nanoflowers, spheres and multipods,

nanoflowers showed the highest reactive oxygen species (ROS)-generating capacity on the same mass basis and therefore has higher toxic potential.

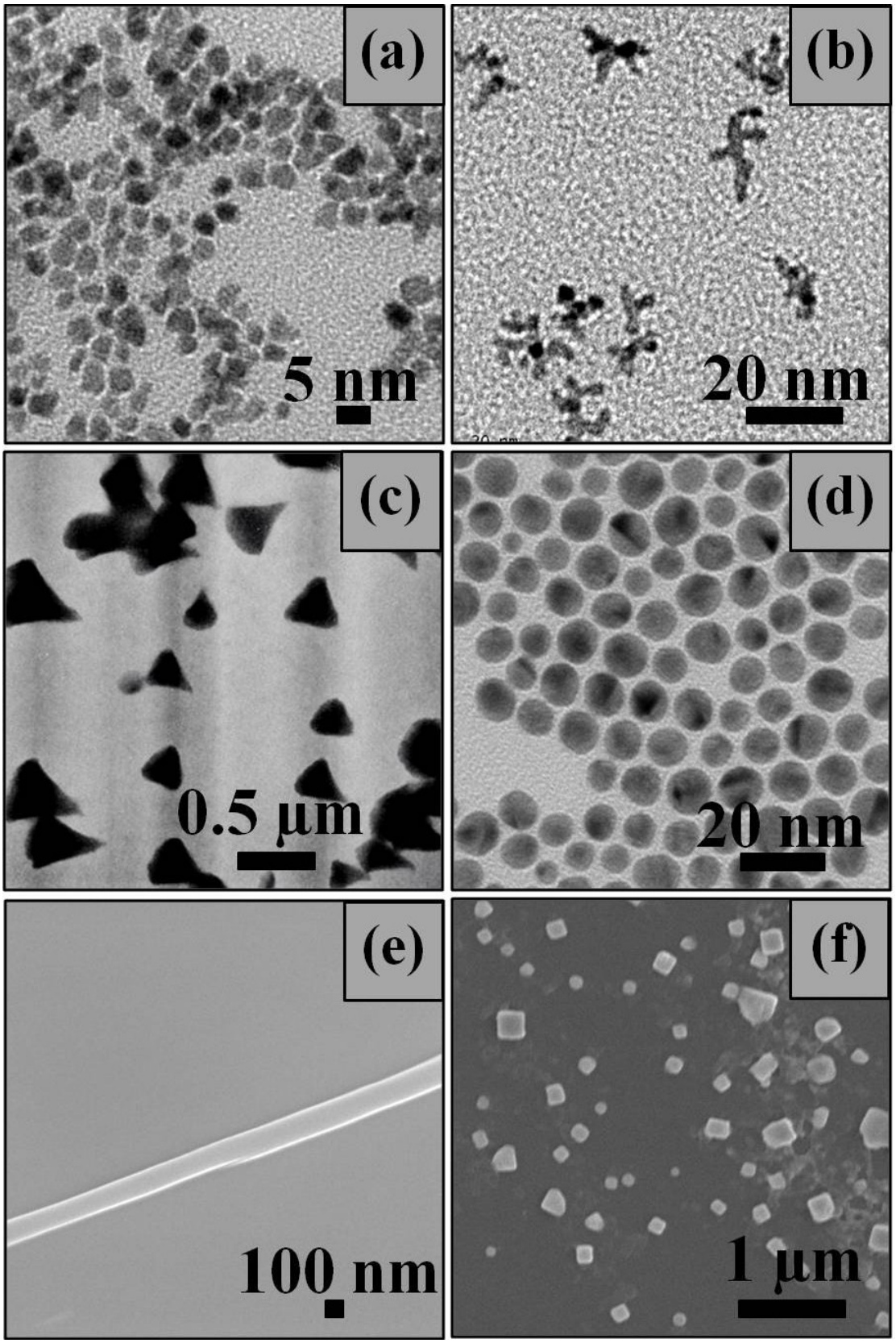

Figure 1.3: Morphological variants of inorganic NMs. Platinum NPs with random shapes (a), platinum multipods (b), titanium dioxide nanotriangles (c), gold nanospheres (d), silver nanowire (e) and silver nanocubes (f) (Teow, Asharani et al. 2011).

1.4.2 Surface functionalization

Surface functionalization confers stability and interesting properties such as surface charges, hydrophilicity or hydrophobicity to NPs. This has an effect on biocompatibility, subsequent uptake and downstream processing by cells. Cationic NPs enter cells more efficiently than neutral or anionic NPs (Thevenot, Cho et al. 2008). Secondly, the capping agent can influence solubility and stability of NPs in a solvent. Water-soluble molecules (e.g. poly(ethylene glycol)) are frequently used as capping agent which offers various advantages, including water solubility, increased blood circulation time, decreased enzymatic degradation and immunogenicity, avoiding removal by the reticuloendothelial system (RES), as well as increasing uptake by cancer cells through high permeability and retention effect (EPR) (Zalipsky 1995). Doxil is a FDA-approved PEGylated liposomal formulation of the anticancer drug doxorubicin which makes use of such properties. Organic micro- and nano-particles have been investigated in the area of drug delivery. Most of these NPs are prepared from non-toxic natural polymers by choice. Besides hydrophilic polymers such as PEG, amphiphilic polymers are also useful for synthesizing drug delivery vehicles (Torchilin 2007). Polymeric micelles can be made from these polymers for encapsulating hydrophobic cancer drugs such as tamoxifen, paclitaxel and camptothecin (Chen 2010). When synthetic polymers were used, the inherent toxicity was examined at an early stage to avoid problems at the final application stage. Because of the inherent biocompatibility and biodegradability of the material itself,

polymeric micelles are non-toxic or mildly-toxic at high concentrations, unlike NPs made from heavy metals.

Capping agents which bind weakly to the NPs surface can influence the fate of NPs *in vivo*. The blood plasma is a concoction of 3700 identified proteins and they compete to bind to the NPs surface (Lynch, Salvati et al. 2009). Proteins with high concentrations may first occupy the NPs surface, which are in turn replaced by proteins of lower concentrations and higher affinity (Lynch and Dawson 2008). Eventually, the cell "sees" and interact with NPs with a constantly changing protein corona that is not present on the NPs initially (Klein 2007). The exchange processes may also affect NPs redistribution from one compartment or organ to another inside a living organism (Lynch and Dawson 2008).

Often, it is a worry that engineered NPs are discharged or run-off into water sources and later be found in our drinking water. Jarvie et al. have shown that the stability of NPs in water can be heavily influenced by surface coatings (Jarvie and King 2010). Using silica NPs as the model, they showed that NPs coated with the surfactant, Tween 20, rapidly aggregated and sedimentated to form solid sewage sludge after interacting with organic matter in the sewage wastewater. Owing to the presence of many organic compounds, NPs in wastewater can also lose, gain or change coatings with time (Jarvie and King 2010). Surprisingly, uncoated NPs which were originally stable and dispersed in ultrapure water remained stable in wastewater with no sedimentation, and therefore pose a larger threat to our water sources (Jarvie, Al-Obaidi et al. 2009).

1.5 Platinum nanoparticles (Pt-nps)

Platinum complexes such as cisplatin have been used for several decades to treat a number of conditions. However, the use of Pt-nps as therapeutics is still in its infancy. The most common method for the synthesis of Pt-nps is by chemical reduction of platinum salts; the most common of additional agents are ethylene glycol and sodium borohydride (Eklund and Cliffel 2004; Herricks, Chen et al. 2004). Guo et al. synthesized Pt-nps using borohydride as the reducing agent and citric acid as a stabilizer (Guo, Zhao et al. 2005). By varying the ratio of citric acid to the platinum salt, they synthesized Pt-nps with different sizes. The size and shape of Pt-nps can be controlled by the precursor reduction conditions while employing supercritical fluid reactive deposition (Gehrke, Pelka et al. 2011). Additionally, Pt-nps exhibit size and shape-dependent catalytic properties (Ahmadi, Wang et al. 1996).

One of the growing areas where potential applications are being explored is nanomedicine. Preliminary reports have shown that Pt-nps which formed complexes with other metals had remarkable anticancer properties (Gao, Liang et al. 2007). Scientists are exploring ways to exploit the potential of Pt-nps and to develop a highly specific targeted nano-platinum drug. Pt-nps complexed with CNTs, find other applications in medicine as DNA biosensors, owing to their superior catalytic properties (Wang, Liu et al. 2006).

1.6 Nanomedicine

Applications of nanotechnology for treatment, diagnosis, monitoring, and control of biological systems are referred to as "nanomedicine" by the National Institutes of Health (Moghimi, Hunter et al. 2005). Biomedical nanotechnology is an evolving field having enormous potential to positively impact the health care system

(Arvizo, Bhattacharyya et al. 2012). Important biomedical applications of nanotechnology that may have potential clinical applications include targeted drug delivery, detection, diagnosis and imaging. Basic understanding of how NMs, the building blocks of nanotechnology, interact with cells and their biological consequences are beginning to evolve.

Noble metal NPs such as gold, silver and platinum are particularly interesting due to their size and shape dependent unique optoelectronic properties. These noble metal NPs have elicited a lot of interest for important biomedical applications because of their ease of synthesis, characterization and surface functionalization. Drugs can be loaded onto NPs by methods such as encapsulation, surface attachment or entrapment. NPs can efficiently penetrate across barriers through small capillaries into individual cells, allowing efficient drug accumulation at the target site. Therefore, the unwanted side effects and toxicity of the therapeutic agent are greatly reduced (Yih and Al-Fandi 2006). NPs in the pharmaceutical biotechnology sector serve to improve the therapeutic index of drugs and provide solutions to future delivery problems for new and upcoming classes of biotechnological products such as recombinant proteins and oligonucleotides. New therapeutic opportunities are opened for therapeutic agents that cannot be used as conventional drug formulations due to poor bioavailability or drug instability. Advantages of nano-formulations include: (i) improving the solubility and stability of drugs, (ii) allowing a prolonged release of drugs, (iii) increasing bioavailability of drugs, (iv) providing a targeted release platform and (v) using lesser drugs and lowering toxicity of the formulation (Parveen, Misra et al. 2012). Because of these properties, diverse types of NPs can be used to deliver therapeutics to the site of action. In order to improve the stability of NPs, polymeric surfactants or other

modifiers are often added, forming a layer which offers repulsive force between NPs and preventing flocculation (Dutta and Green 2008).

1.7 Body portals of nanomaterials

Since many commercial products contain NMs, exposure of NMs to an organism can occur in various ways, with common routes of entry being inhalation, ingestion, dermal absorption and through therapeutic applications. A schematic map of portals of NMs entry is demonstrated in **Figure 1.4**.

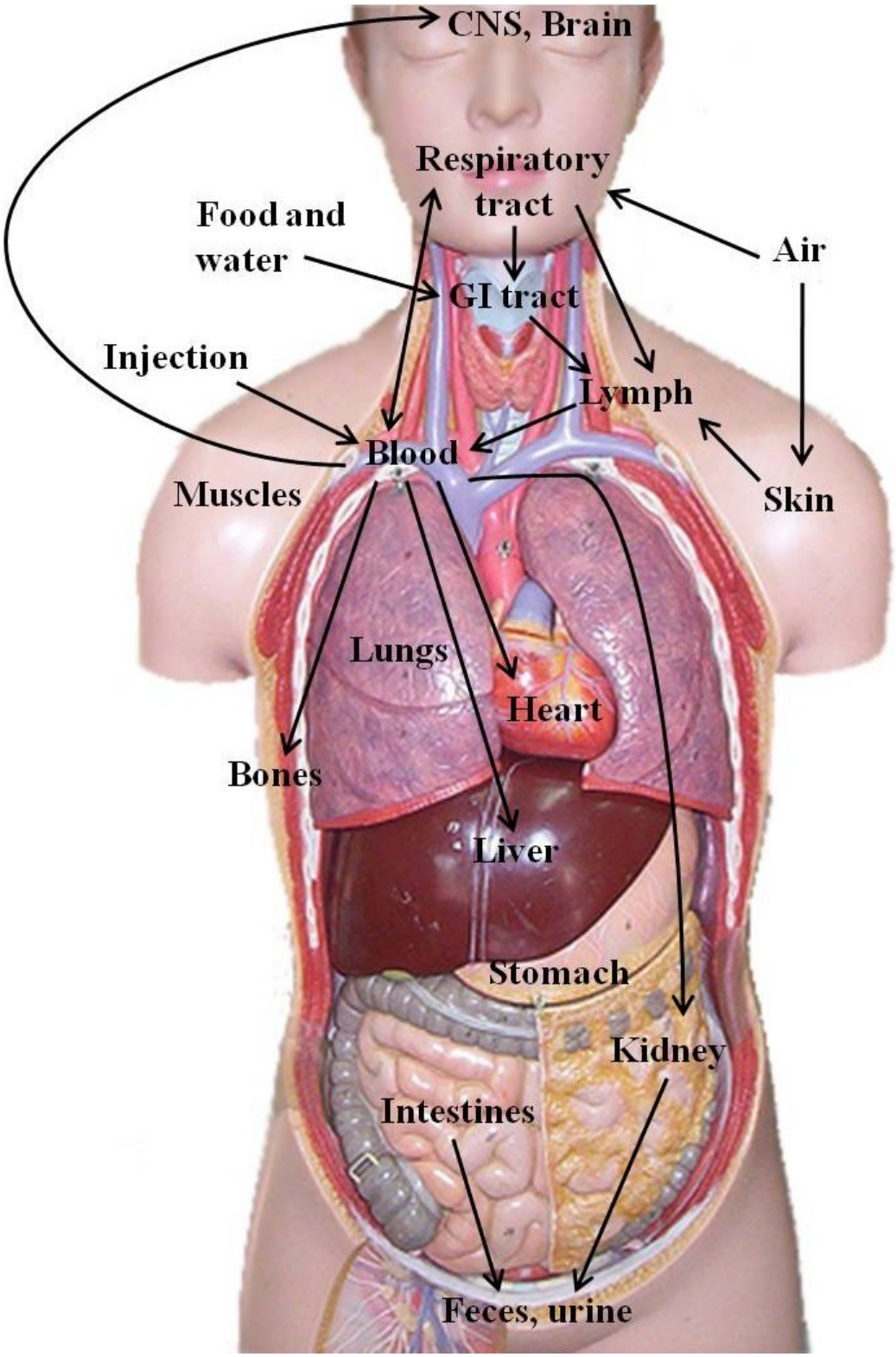

Figure 1.4: Potential routes of exposure, translocation and deposition sites of nanomaterials. Bold arrows refer to routes which have been demonstrated and reported. It should be noted that translocation, accumulation and retention rates may vary with physicochemical properties of the nanomaterials and the experimental organism (Teow, Asharani et al. 2011).

1.7.1 Inhalation

Systemic availability of NPs after inhalation is driven by factors such as the exposure time and concentration, method of NPs administration, NPs size and agglomeration state (Johnston, Hutchison et al. 2010). Ultrafine particles (UFPs, < 100 nm) were the crucial cause of respiratory disorders and these were more toxic and caused greater inflammation in test animals than larger particulates (Zhu, Feng et al. 2009). Moreover, the size distribution of the NPs affects the target regions of deposition in the respiratory tract, where smaller particles were found to penetrate deeper (Oberdorster, Oberdorster et al. 2005). NPs can penetrate the alveoli and get absorbed by the lung, or could be cleared by macrophages (Semmler-Behnke, Kreyling et al. 2008). This process is influenced by the size and shape of NMs (Elder, Yang et al. 2007).

CNTs were reported to impair phagocytosis, causing the release of chemokines and cytokines and impairing their functions (Shvedova, Fabisiak et al. 2008). On the other hand, smaller particles (less than 70 nm) are less efficiently phagocytosed, as macrophages cannot recognize ultra small particles below a phagocytic cut off size of 500 nm (Rupper and Cardelli 2001; Champion, Walker et al. 2008). In some cases, NPs can impair the phagocytic capacity of alveolar macrophages, leading to apoptosis (Oh, Kim et al. 2010). Occupational exposure of workers to NPs generated pleural granuloma formation characterized by shortness of breath and pulmonary fibrosis (Song, Li et al. 2009).

NPs of size below 400 nm have a high chance of crossing the lung–epithelial barrier and enter the blood or lymphatic systems which are subsequently transported to different organs. Also, particle-laden macrophages also play a part in distributing NPs to various organs (Furuyama, Kanno et al. 2009). Inhalation experiments of Au

(Semmler-Behnke, Kreyling et al. 2008) and Ag (Kim, Kim et al. 2009) NPs in animal models resulted in systemic distribution and subsequent deposition in various organs. Inhalation of Ag NPs was not found to cause any change to the nasal mucosal architecture significantly (Hyun, Lee et al. 2008). Nonetheless, inhalation of commercially available products such as "Magic Nano" sprays resulted in serious lung injury, haemorrhage and subsequent death in rat models (Pauluhn, Hahn et al. 2008).

1.7.2 Absorption through the skin

The human skin is an effective barrier against NPs and chemicals. The strongly keratinized stratum corneum (10 mm thickness) expels foreign bodies effectively. However, sweat glands and hair follicles could make this barrier more vulnerable and facilitate entry of NMs. TiO_2 NPs is an effective UV filter added to sunscreen lotions. Micron and sub-micron sized TiO_2 NPs were shown to cross the skin and reach hair follicles and dermis after the horny layer had been removed (Lademann, Weigmann et al. 1999). TiO_2 NPs were not detected in viable non-damaged skin layers (Mavon, Miquel et al. 2007). However, NPs can reach into the viable skin regions in the dermis and epidermis when the skin is wounded or abrased. Surface coatings on TiO_2 NPs can affect indirect skin damage by controlling the reactive surface available for photocatalysis, which generates harmful ROS (Carlotti, Ugazio et al. 2009).

Skin absorption of NMs was proposed to occur through interactions with lipid systems of the skin and subsequent phagocytosis by Langerhans cells (Hoet, Brüske-Hohlfeld et al. 2004). TiO_2 NPs are associated with exacerbation of atopic dermatitis and progression of other skin conditions *via* histamine release (Yanagisawa, Takano

et al. 2009). The uptake of metallic NPs through the skin has been considered more obscure than other routes of entry. Parameters such as clothing, dose, age, type and condition of the skin are expected to be involved in this process.

Ag NPs dissolved in synthetic sweat exhibited low penetration in intact and damaged human skin, suggesting their safe application on intact skin (Larese, D'Agostin et al. 2009). The damaged skin used in the experiment showed significant absorption of Ag NPs when compared to intact skin. Ag NPs are usually applied as wound dressings on damaged skin which may facilitate rapid penetrations. Filon et al. have studied the effect of cobalt NPs in human volunteers and established their skin penetration potentials (Filon, Maina et al. 2004). Skin irritations and ulcerations have been reported for ZnO NPs in *in vivo* models such as the zebrafish (Zhu, Zhu et al. 2008). Also, similar work on damaged rat skin showed increased penetration of QDs (Zhang and Monteiro-Riviere 2008). These reports emphasize that NPs could penetrate faster in a damaged skin under normal conditions. Concisely, NPs are capable of crossing both intact and damaged skin at different rates, a property which is controlled by intrinsic parameters of the material.

1.7.3 Ingestion

NPs which are employed as food additives and drugs are likely to get absorbed into the body through the gastrointestinal tract (GI), which is one of the potential routes for the entry of particles. From the GI tract, they can enter lymphatic tissues containing phagocytic cells. Multiple parameters such as size, surface charge, attachment to ligand or type of ligand could control their targeting and absorption in the GI tract (Hillyer and Albrecht 2001). Ingested NMs are likely to get expelled if they are unstable or undergo chemical changes in the GI tract. Change in pH may

trigger agglomeration of NMs inside the intestinal tract. If agglomerates are small enough, they can get expelled through faeces with little absorption. Bigger agglomerates can result in obstruction of GI tract and death. This idea was experimentally proven in mice fed with zinc NPs. Following exposure to these NPs, mice developed severe diarrhoea, vomiting and anorexia followed by death. Autopsy revealed clumps of particles blocking the intestine (Wang, Feng et al. 2006). Ingestion of polystyrene NPs by rats resulted in absorption through the GI tract (Jani, Halbert et al. 1990), whereas fullerenes were cleared within 48 h (Yamago, Tokuyama et al. 1995). On the other hand, 15 nm Au NPs showed higher penetration rates in rat intestinal models as compared to larger size (102 and 198 nm) Au NPs (Sonavane, Tomoda et al. 2008). These reports suggest that NPs could penetrate the GI tract, resulting in translocation to other organs.

1.7.4 Translocation

From the site of entry, NPs can enter the circulatory system (Furuyama, Kanno et al. 2009; Zhu, Feng et al. 2009). Intra-tracheal instillation of 30 nm Au NPs translocated to platelets within 30 min (Berry, Arnoux et al. 1977). Carbon NPs showed a rapid diffusion (5 min) from lung to blood in hamster models (Nemmar, Vanbilloen et al. 2001) and in human subjects (Oberdorster, Sharp et al. 2004). Many animal experiments have shown rapid translocation of NPs from the site of entry to target organs such as brain, spleen, liver, kidney and muscles through blood (Oberdorster, Sharp et al. 2004). Once in the blood stream, stable NPs can get distributed to various organs where they impart specific side effects. Ag NPs were observed to penetrate the chorion of zebrafish embryos and are distributed to the brain, heart, yolk and blood (Asharani, Wu et al. 2008). These embryos developed abnormal

body axes, twisted notochord, slow blood flow, pericardial oedema, cardiac arrhythmia and apoptosis of cells in various body parts (**Figure 1.5**). Similar phenotypic defects were also caused by multi-walled CNTs (MWCNTs) (Asharani, Serina et al. 2008). Recent evidences suggest that the NPs can cross the blood–brain barrier and affect brain functions (Sarin, Kanevsky et al. 2008). Many research groups have studied the effects of NPs on cardiovascular systems. Exposure of NPs in experimental animal models resulted in myocardial infarction (Nemmar, Al-Maskari et al. 2007).

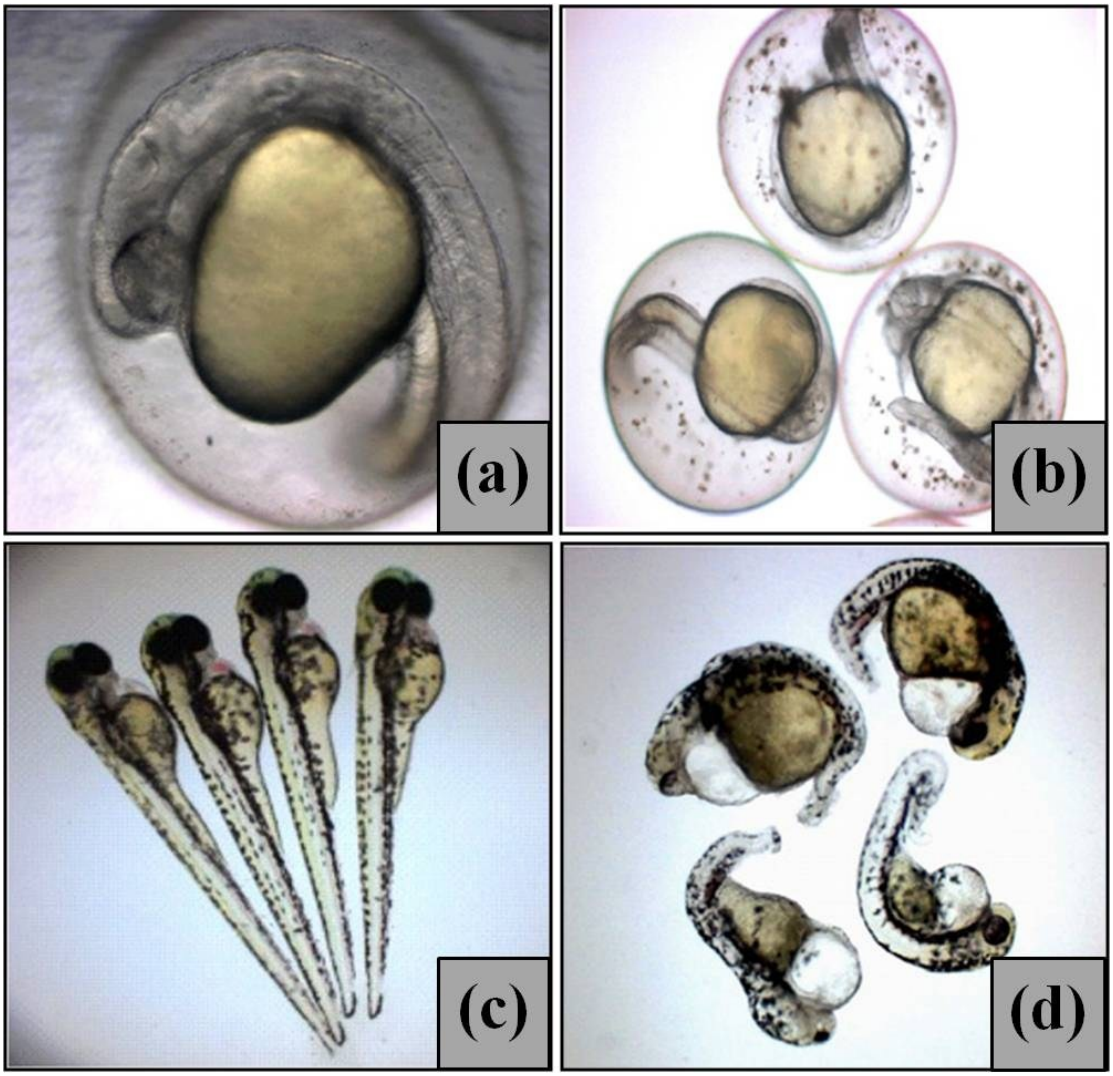

Figure 1.5: Optical micrographs of zebrafish embryos 24 hours post fertilization (hpf) (a, b) and 72 hpf (c, d). Untreated, healthy zebrafish embryo had a clear and transparent chorion (a), while Ag NPs (5 µg/ml) treated embryos had brown flakes (dead cells) suspended inside the chorion (b). At 72 hpf, untreated, control healthy

zebrafish larvae had normal development (c) and Ag NPs (100 µg/ml) treated embryos showed deformities such as bent notochord, pericardial oedema, enlarged yolk and abnormal eye formation (d) (Asharani, Wu et al. 2008).

Recent reports have shown anti-platelet properties by Ag NPs (Shrivastava, Bera et al. 2009). Our group has investigated the hemocompatibility of Ag, Au and Pt NPs with erythrocytes (Asharani, Sethu et al. 2010). Erythrocytes exhibited significant lyses, hemagglutination, membrane damage, detrimental morphological variations and cytoskeletal distortions following exposure to Ag NPs at a concentration of 100 µg/ml, while Au and Pt NPs remained hemacompatible at the same concentration (**Figure 1.6**).

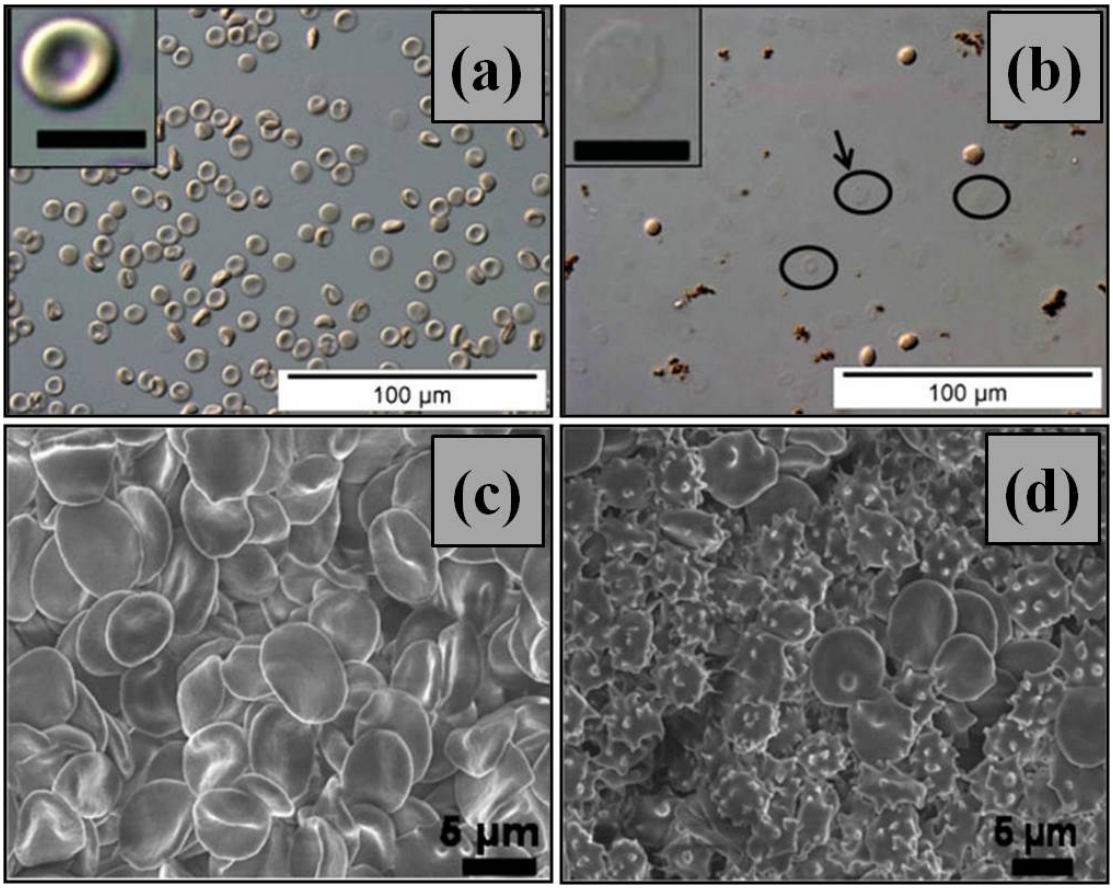

Figure 1.6: Optical micrographs of normal (a) and Ag NPs treated (b) erythrocytes. With Ag NPs (400 µg/ml) treatment, erythrocytes showed haemolyses and appeared as ghost cells (circled). SEM images of erythrocytes with normal biconcave structure (c), while Ag NPs (400 µg/ml) treatment induced aberrant morphology (d) (Asharani, Sethu et al. 2010).

Exposure of 23.5 nm copper NPs in mice *via* oral gavage damaged the liver, spleen and kidneys, while micron-sized particles did not show the same effect (Chen, Meng et al. 2006). Exposure to ZnO NPs resulted in necrosis of liver tissues and severe renal damage (Wang, Feng et al. 2006). The effects of long term deposition of metallic NPs in various organs are still largely unknown. They may lead to organ dysfunction at later stages, which can be dependent on various factors such as dose, mode of intake, stability and the properties of NPs.

1.7.5 Excretion of nanoparticles

Even though literature reports may suggest various routes for excretion of NPs, only a few have been proven experimentally. NPs are proposed to be expelled through urine, faeces, sweat, breast milk and saliva (Oberdorster, Oberdorster et al. 2005). However, experimental evidence support excretion only through urine (Burns, Vider et al. 2009) and faeces (Cho, Cho et al. 2009). Expulsion of NPs through the kidney (i.e. urine) is dependent on various parameters such as size, surface functionality and aspect ratio. The size of NPs can affect renal excretion and QDs (< 5.5 nm) were rapidly eliminated in the rat model, while renal excretion was prevented when proteins adsorbed on the surface of QDs, resulting in the hydrodynamic diameter to increase by more than 15 nm (Choi, Liu et al. 2007). Surface functionality also played an important role in regulating renal excretion. Souris et al. reported that highly-charged mesoporous silica NPs (+34.4 mV at pH 7.4) were rapidly excreted in the faeces as compared to lesser-charged particles (-17.6 mV at pH 7.4). However, it was unclear whether the magnitude of the charge or nature of the charge (+/-) had really caused the difference in excretion (Souris, Lee et al. 2010). NMs with high aspect ratios, for example MWCNTs, were also capable of renal clearance (Lacerda, Herrero

et al. 2008). Excretion of these NMs requires individualized, well-dispersed MWCNTs to align their longitudinal axis perpendicular to the endothelial fenestrations during translocation through the glomerular filtration barrier. This indicates that CNT dispersions that were not individualized, or that have aggregated *in vivo*, may be retained by the kidney.

The kidney therefore becomes one of the target organs for NP toxicity. Mice exposed to Cu NPs resulted in glomerulitis, degeneration, necrobiosis, oedema and discoloration of kidneys (Chen, Meng et al. 2006). Cu NPs also altered metabolic functions in the kidney leading to nephrotoxicity as well as hepatoxicity. These evidences suggest that NPs are able to damage the excretory systems, leading to NP retention and organ failure.

1.7.6 Biodistribution at the cellular level

Intracellular targets of NPs are largely unknown and can vary widely depending on particle functionalization, while target organs of NPs are well documented (Oberdorster, Oberdorster et al. 2005; Asharani, Wu et al. 2008; Semmler-Behnke, Kreyling et al. 2008; Johnston, Hutchison et al. 2010). Uptake kinetics of Au NPs were reported to occur *via* receptor mediated clathrin-dependant endocytosis (Chithrani, Ghazani et al. 2006; Chithrani and Chan 2007). Chithrani et al. have shown that the wrapping of plasma membranes is faster for 50 nm NPs as compared to NPs of other sizes, which resulted in their faster uptake. A shape-dependant study proved that spherical NPs are taken up faster than nanorods (Chithrani, Ghazani et al. 2006). However, study on the exocytosis kinetics showed an inverse relation, where 14 nm Au NPs were expelled much faster than 74 nm NPs (Chithrani and Chan 2007). Existing experimental data suggest endocytosis as a major

route for uptake of different NMs (Au, CNTs and silica) (Xing, He et al. 2005; Jin, Heller et al. 2009). However, clathrin-knockdown rabbit conjunctiva cells were also able to endocytose chitosan NPs efficiently, suggesting the involvement of other pathways in NP uptake process (Huang, Ma et al. 2002). Rejman et al. studied fluorescent latex particle uptake and suggested that smaller particles (< 200 nm) are internalized by clathrin-mediated endocytosis, whereas, particles larger than 500 nm are internalized by caveolae-mediated endocytosis (Rejman, Oberle et al. 2004). It is likely that mechanisms other than phagocytosis exist for the uptake of NPs, as most of the non-phagocytic cells were also taking up NPs efficiently. Macropinocytosis is also documented as one of the mechanisms for the uptake of NPs (Walsh, Tangney et al. 2006). Macropinosomes are larger structures (1 mm) as compared to clathrin pits (150 nm), but the selection between the two processes remain obscure (Nichols and Lippincott-Schwartz 2001). Due to the limited number of reports on the uptake of NPs, it is difficult to conclude at the current state on a common mechanism which regulates the uptake for all types of NMs.

Following uptake, Au NPs have been observed to interact with endosomal proteins, escaping from endosomes and cluster in the cytosol and perinuclear regions, while some NPs entered the nucleus (Thomas and Klibanov 2003). To enter the nucleus, NPs could pass through the nucleus envelope via the channels provided by nuclear pore complexes or by attachment with a nuclear localization signal (Misra and Sahoo 2010) in the cytosol. Au NPs in the nucleus induced cytokinesis arrest, causing binucleated cell formation to occur after mitosis has taken place which finally led to apoptosis (Kang, Mackey et al. 2010).

1.8 Passive targeting: Enhanced Permeability and Retention (EPR) effect

Solid tumours have unique pathophysiological characteristics which are not observed in normal tissues (Maeda, Wu et al. 2000). These include extensive angiogenesis, hypervasculature, defective vascular architecture, impaired lymphatic drainage-recovery system, and increased production of permeability mediators. This phenomenon is known as the enhanced permeability and retention (EPR) effect and has been observed to be universal in tumours. Enhanced vascular permeability helps sustain an adequate supply of nutrients and oxygen for rapid tumour growth. In addition, the lack of effective lymphatic drainage has allowed targeting using macromolecular drugs, lipids, liposomes, etc, which led to accumulation of drug delivery vehicles at the tumour.

The EPR effect has been observed in many experimental and human solid tumours, such as S-180 sarcoma, Meth-A, melanoma B16 and Ehrlich carcinoma; colon 38 adenocarcinoma in mice; Yoshida AH136B, Walker 256 carcinoma and LY tumours in rats; VX-2 carcinoma in rabbits; and many humans tumours, including hepatoma, renal cancer, lung cancer and brain tumours (Maeda, Wu et al. 2000). Small molecules such as molecular chemotherapeutic drugs are governed by free diffusion-dependent equilibrium and therefore do not discriminate tumour tissue from normal tissue (Maeda 2001). They do not exhibit the EPR effect.

NPs are usually be taken up by the liver, spleen and the RES depending on their surface characteristics (Brannon-Peppas and Blanchette 2004). Particles with more hydrophobic surfaces will be preferentially taken up by the liver, followed by the spleen and lungs (Brigger, Dubernet et al. 2002). Hydrophilic NPs such as those prepared from poly(vinyl pyrrolidone), show less than 1% uptake by the spleen and liver, and 8 h after injection, still showing 5–10% circulating in the bloodstream

(Gaur, Sahoo et al. 2000). NPs with longer circulation times and hence greater ability to target to the site of interest, should be smaller than 100 nm in diameter and have a hydrophilic surface in order to reduce clearance by macrophages (Storm, Belliot et al. 1995). Coatings of hydrophilic polymers can create a cloud of chains at the particle surface which will repel plasma proteins.

Systems that have been approved include liposomal doxorubicin (Myocet, Elan Pharmaceuticals), PEGylated liposomal doxorubicin (Doxil, Ortho Biotech and Caelyx, Schering Plough), PEGylated liposomal daunorubicin (DaunoXome, Diatos), and the recently approved albumin-bound paclitaxel-loaded NPs (Abraxane, Abraxis Bioscience) (Byrne, Betancourt et al. 2008).

1.9 Active targeting: Using biological molecules

Active targeting requires the conjugation of receptor-specific ligands that can promote site-specific targeting (Molema, Meijer et al. 1998; Thorpe 2004). The success of drug targeting depends on the selection of an appropriate targeting moiety. It should be highly abundant, having high affinity and specificity of binding to cell surface receptors and should be able to withstand chemical modification by conjugation. Active targeting can be achieved by molecular recognition of the diseased cells by the signature molecules over-expressed on their surface. The therapeutic agent can be actively targeted by conjugating the carrier with a cell- or tissue-specific ligand, thereby allowing a preferential accumulation of the drug at the diseased site. Using active targeting, efficient cellular uptake and intracellular internalization can be achieved. PEGylated Au NPs are decorated with various amounts of human transferrin to enhance active targeting (Choi, Alabi et al. 2010). Their results suggest that targeted NPs can provide enhanced intracellular delivery of

therapeutic agents to cancer cells than the non-targeted analogues. In another study, cancer cells were actively targeted using PLGA NPs that were surface-modified with monoclonal antibody (Kocbek, Obermajer et al. 2007). This demonstrated the superior capability of active recognition of the surface-modified NPs as they showed enhanced binding to the targeted cells than non-coated NPs. Examples of suitable ligands include proteins (antibodies and their fragments), nucleic acids (aptamers) and receptor ligands (peptides, vitamins, and carbohydrates) (Peer, Karp et al. 2007; Byrne, Betancourt et al. 2008).

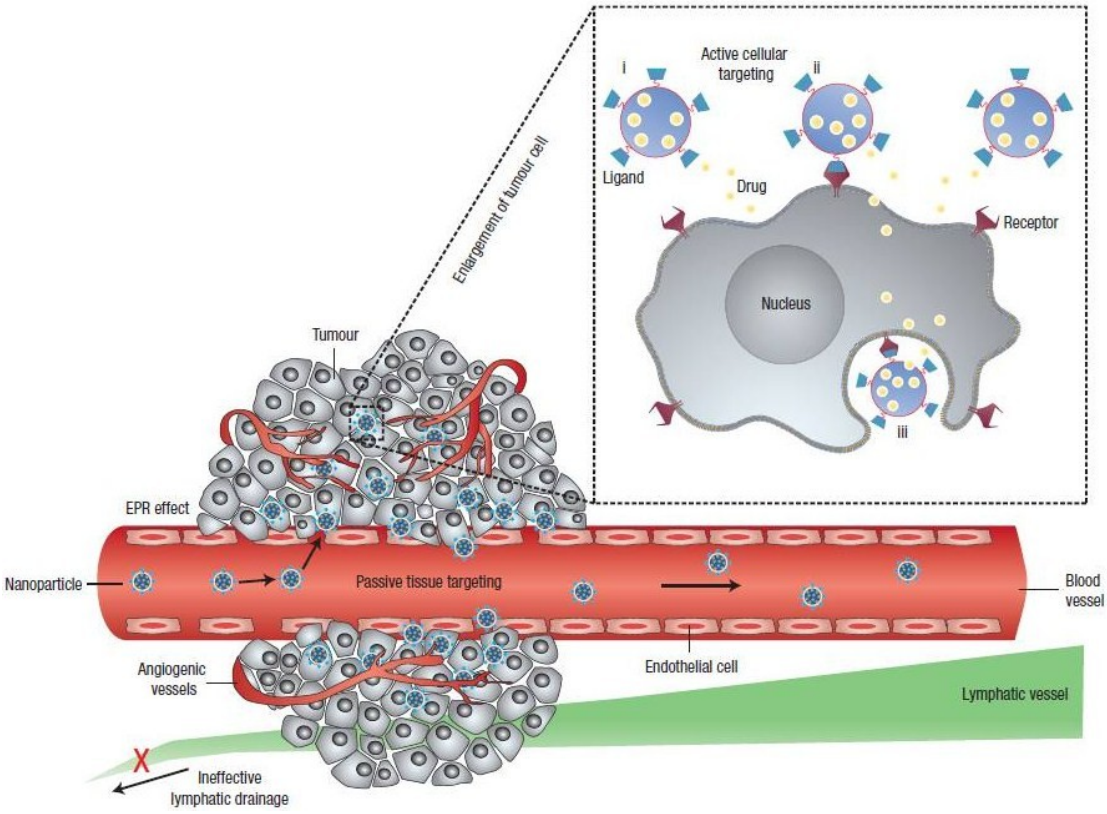

Figure 1.7: Schematic representation of different mechanisms by which nanocarriers can deliver drugs to tumours. Passive tissue targeting is achieved by extravasation of NPs through increased permeability of the tumour vasculature and ineffective lymphatic drainage (EPR effect). Active cellular targeting (inset) can be achieved by functionalizing the surface of NPs with ligands that promote cell-specific recognition and binding. NPs can (i) release their contents in close proximity to the target cells; (ii) attach to the membrane of the cell and act as an extracellular sustained-release drug depot and (iii) internalize into the cell (Peer, Karp et al. 2007).

1.10 Rationale of this study

The types of NPs currently used in research for cancer therapeutic applications include dendrimers, liposomes, polymeric micelles, protein NPs, ceramic NPs, viral NPs, metallic NPs and CNTs. Given the diverse variety of drug delivery vehicles to choose from, it is important to select one which is easy to synthesize, characterize, purify, non-toxic and could even exhibit therapeutic effects on its own. A careful survey of this long list of NMs revealed platinum nanoparticles (Pt-nps) as a potential candidate which fulfils all requirements. Although platinum (metal, salts and particles) is known for its catalytic properties in chemical reactions, little is known about its medical and biological properties. As mentioned earlier, few reports have indicated that Pt-nps can be easily synthesized *via* the bottom-up approach from its salts, relatively non-toxic, hemacompatible and may have anticancer properties.

Functionalization of NPs is necessary to create a stealth surface from opsonisation, the adherence of serum proteins to the NPs surface. This increases circulation time through avoidance of removal by the RES. Incorporation of a hydrophilic polymer, such PEG or PVP, to the surface of the NPs greatly improves solubility and a reduction in opsonisation. With increased circulation time, the tumour can have higher NPs uptake *via* passive targeting or EPR effect. For such reasons, PVP being biocompatible and water-soluble is employed.

To further improve site-specific targeting effects and reducing toxicity, active targeting can be used in conjunction with passive targeting. A careful analysis of available *in vitro* and *in vivo* models revealed folic acid and galactose as suitable receptor-specific ligands. Folic acid targets cancer cells which over-expressed folate receptors; while galactose targets cancer cells which over-expressed

asialoglycoprotein receptors. Folic acid and galactose were adsorbed onto Pt-nps to target the appropriate test model in our study.

5-Fluorouracil is chosen as the chemotherapeutic drug to be carried by Pt-nps. Its principal uses are in colorectal cancer, pancreatic cancer, breast cancer, head and neck cancer, liver cancer and ovarian cancer in the form of chemotherapy (intravenous injection). Cancerous tumours are characterized by uncontrolled cell division. Chemotherapy kills cancer cells by stopping cell division. 5-Fluoruracil is a pyrimidine analogue which works through irreversible inhibition of thymidylate synthase. In addition, 5-fluorouracil's anticancer activity was also tested separately in our test models so as to enable a comparison between Pt-nps and a commercially available drug.

Herein, we propose a systematic approach to analyse the feasibility of using Pt-nps as a drug delivery vehicle and to develop it into a nanomedicine:

1. Synthesis and purification methods of Pt-nps functionalized with a single capping agent or a combination of capping agents (PVP, folic acid, galactose and 5-fluorouracil), followed by experimental setups (Chapter 2);
2. Characterization and *in vitro* testing of Pt-nps in cancer and normal cell lines, in terms of uptake, viability and mechanism of cell death;
3. *In vivo* monitoring of zebrafish larvae liver size after exposure to Pt-nps.

CHAPTER 2

MATERIALS AND METHODS

2. Materials and Methods

2.1 Preparation for synthesis

All experiments were performed in a clean environment to eliminate the chances of endotoxin contamination that may interfere with the toxicity profile of the nanoparticles. Glassware used for synthesis were treated with piranha solution (3 : 1, concentrated sulphuric acid : 30% hydrogen peroxide) to remove contaminants prior to reaction, if necessary. Starting materials and purchased chemicals were used without further purification.

2.1.1 Synthesis of platinum nanoparticles functionalized with poly(vinyl pyrrolidone) (Pt-PVP)

PVP-capped platinum nanoparticles were synthesized *via* the reduction of $H_2PtCl_6.6H_2O$ (Sigma-Aldrich) as reported by van Rheenen et al. with some modifications (van Rheenen, McKelvy et al. 1987). $H_2PtCl_6.6H_2O$ (1 g) was dissolved in ultrapure water (19 ml, Millipore) to give a stock solution (100 mM). The stock solution (500 µl) was subsequently reduced under constant stirring using $NaBH_4$ (10 mg, Sigma-Aldrich) dissolved in ultrapure water (1 ml). Colloidal solution was then stabilized by the immediate addition of PVP (100 mg, Sigma-Aldrich) in ultrapure water (10 ml). Final volume of the reaction mixture was kept at 50 ml. The colour of the solution changed from yellow to dark brown during the reduction process, indicating nanoparticle formation. Stirring was continued for 3 days at room temperature.

A common purification method was used for all nanoparticles. The solution was centrifuged at 20000 rpm (JA-20, Beckman) for 45 min to obtain a pellet. The pellet was washed twice using ultrapure water (10 ml) to remove traces of unbound

capping agent and reducing agent. The purified solution was filtered using a 0.2 mm syringe filter to get rid of large particle aggregates. A known amount of dry solid obtained after freeze-drying was again resuspended in ultrapure water to get a stock solution (1 mg/ml) and subsequently stored at 4 °C.

2.1.2 Synthesis of platinum nanoparticles functionalized with folic acid (Pt-FA)

$H_2PtCl_6.6H_2O$ (500 µl, 100 mM) stock solution was stirred with folic acid dihydrate (200 mg, Alfa Aesar) solution for 5 min. This was subsequently reduced by adding a solution of $NaBH_4$ (2.5 mg) in a drop-wise manner. The final volume of the reaction mixture was kept at 50 ml and the final pH was adjusted to 7 and stirring was continued for 3 days.

Pt-FA was purified using a common purification method as mentioned in 2.1.1.

2.1.3 Synthesis of platinum nanoparticles functionalized with folic acid, 5-fluorouracil and PVP (Pt-FA/5FU/PVP)

$H_2PtCl_6.6H_2O$ stock solution (500 µl, 100 mM) was introduced into 48.5 ml ultrapure water, already pre-dissolved with folic acid (20 mg), 5-fluorouracil (100 mg, Sigma-Aldrich) and PVP (5 mg) under constant stirring at 700 rpm. After 15 min, this mixture was reduced using $NaBH_4$ (15 mg) dissolved in ultrapure water (1 ml). Final volume of the reaction mixture was kept at 50 ml. The final pH was adjusted to 7 and stirring was continued for 3 days.

Pt-FA/5FU/PVP was purified using a common purification method as mentioned in 2.1.1.

2.1.4 Synthesis of platinum nanoparticles functionalized with galactose, 5-fluorouracil and PVP (Pt-Gal/5FU/PVP)

$H_2PtCl_6.6H_2O$ stock solution (500 µl, 100 mM) was introduced into 48.5 ml ultrapure water, already pre-dissolved with D-galactose (20 mg, Duchefa Biochemie B. V.), 5-fluorouracil (100 mg) and PVP (5 mg) under constant stirring at 700 rpm. After 15 min, this mixture was reduced using $NaBH_4$ (15 mg) dissolved in ultrapure water (1 ml). Final volume of the reaction mixture was kept at 50 ml. The final pH was adjusted to 7 and stirring was continued for 3 days.

Pt-Gal/5FU/PVP was purified using a common purification method as mentioned in 2.1.1.

2.1.5 Synthesis of platinum nanoparticles functionalized with 5-fluorouracil and PVP (Pt-5FU/PVP)

$H_2PtCl_6.6H_2O$ stock solution (500 µl, 100 mM) was introduced into 48.5 ml ultrapure water, already pre-dissolved with 5-fluorouracil (100 mg) and PVP (5 mg) under constant stirring at 700 rpm. After 15 min, this mixture was reduced using $NaBH_4$ (15 mg) dissolved in ultrapure water (1 ml). Final volume of the reaction mixture was kept at 50 ml. The final pH was adjusted to 7 and stirring was continued for 3 days.

Pt-5FU/PVP was purified using a common purification method as mentioned in 2.1.1.

2.1.6 Synthesis of platinum nanoparticles functionalized with galactose and 5-fluorouracil (Pt-Gal/5FU)

$H_2PtCl_6.6H_2O$ stock solution (500 µl, 100 mM) was introduced into 48.5 ml

ultrapure water, already pre-dissolved with D-galactose (20 mg) and 5-fluorouracil (100 mg) under constant stirring at 700 rpm. After 15 min, this mixture was reduced using $NaBH_4$ (15 mg) dissolved in ultrapure water (1 ml). Final volume of the reaction mixture was kept at 50 ml. The final pH was adjusted to 7 and stirring was continued for 3 days.

Pt-Gal/5FU was purified using a common purification method as mentioned in 2.1.1.

2.1.7 Synthesis of platinum nanoparticles functionalized with galactose and PVP (Pt-Gal/PVP)

$H_2PtCl_6.6H_2O$ stock solution (500 µl, 100 mM) was introduced into 48.5 ml ultrapure water, already pre-dissolved with D-galactose (20 mg) and PVP (5 mg) under constant stirring at 700 rpm. After 15 min, this mixture was reduced using $NaBH_4$ (15 mg) dissolved in ultrapure water (1 ml). Final volume of the reaction mixture was kept at 50 ml. The final pH was adjusted to 7 and stirring was continued for 3 days.

Pt-Gal/PVP was purified using a common purification method as mentioned in 2.1.1.

2.1.8 Synthesis of platinum nanoparticles functionalized with galactose and cysteamine-AF594 (Alexa Fluor 594, fluorescent dye) conjugate (Pt-Gal/Dye)

The synthesis of a fluorescent Pt-np involves 3 steps: (a) synthesis of platinum nanoparticles capped with galactose (Pt-Gal); (b) synthesis of cysteamine-dye conjugate and (c) ligand exchange of cysteamine-dye conjugate with Pt-Gal.

Pt-Gal was synthesized by adding $H_2PtCl_6.6H_2O$ stock solution (500 µl) into

49.5 ml ultrapure water, already pre-dissolved with D-galactose (200 mg) under constant stirring at 700 rpm. The mixture was boiled to dryness in order to reduce Pt^{4+} into Pt^{0}. The resulting brown solid was resuspended in water, sonicated and filtered using a 0.2 mm syringe filter to get rid of large particle aggregates. The colloid was dialyzed using a semi-permeable membrane (MWCO 3200, Thermo Scientific) against ultrapure water to remove excess H_2PtCl_6 and galactose. A Benedict's test was carried out to confirm the presence of galactose on Pt-Gal.

Cysteamine acts as the linker to between platinum and the fluorescent dye. To synthesize the cysteamine-dye conjugate, cysteamine (12.5 mg, Sigma-Aldrich) was first dissolved in PBS (10 ml) to form a stock solution. The stock solution (0.1 ml) was diluted using PBS (4.9 ml) to get a 10 mM solution. Alexa Fluor 594 C_5 maleimide (1 mg, Life Technologies) was dissolved in DMSO (100 µl, Sigma-Aldrich) to form a 11 mM solution. The dye was added dropwise to a stirring solution of cysteamine at room temperature (25 ^{o}C), under N_2 atmosphere and protected from light. Stirring continued for 2 h in order for the nucleophilic reaction to complete.

To carry out ligand exchange, the cysteamine-dye conjugate (500 µl) was added to Pt-Gal (1 ml) and diluted with PBS (3.5 ml) to make up a final volume of 5 ml. The mixture was stirred for 2 days at room temperature. The colloid was dialyzed using a semi-permeable membrane against ultrapure water to remove excess reagents.

2.2 Characterization

2.2.1 UV-visible (UV-vis) spectroscopy

UV-visible measurement of stock solutions of Pt-nps and their capping agents were performed using a spectrophotometer (Shimadzu UV-1601PC) at room temperature.

2.2.2 Elemental analysis

Freeze-dried NPs were analyzed for their respective elemental composition. Carbon, hydrogen and nitrogen analysis were performed using Elementar Vario Microcube. Inductively-coupled plasma (ICP) analysis was used for the determination of platinum and silver levels in acid digested nanoparticles solutions. Sample preparation was done with a Milestone microwave laboratory system, while ICP was performed using Dual-view Optima 5300 DV ICPOES. A modular ion chromatography system was used for the determination of anions such as F^- with chemical suppression. Instrumentation includes Metrohm 818 IC Pump, 820 IC Separation Center, 830 Interface, 833 IC Liquid handling Unit, 732 IC Detector and 813 Compact Autosampler.

2.2.3 Transmission electron microscopy (TEM)

NPs were observed using JEOL 2010-F Field Emission Transmission Electron Microscope (FETEM) and JEOL 3010 High Resolution Transmission Electron Microscope (HRTEM). For sample preparation, a dilute solution of NPs dispersed in ultrapure water was placed onto a carbon-coated copper grid (400 mesh) supported on a clean filter paper and left to dry in an oven overnight. This was subsequently used for TEM.

2.2.4 Dynamic light scattering (DLS) and zeta potential measurements

To find out the hydrodynamic size and surface charge of NPs, dynamic light scattering (DLS) and zeta potential measurements were performed using Malvern Zetasizer Nano-ZS. Stock solutions were held in appropriate cuvettes or solution holders, measured at room temperature and diluted when necessary.

2.3 *In vitro* studies

2.3.1 Cell culture

Normal human lung fibroblast, IMR90, (Coriell Cell Repositories, USA, passage 18 ± 3) were cultured in minimum essential medium with glutamine (MEM, PAA Laboratories) supplemented with 15% foetal bovine serum (FBS, Standard Quality, EU-approved origin, PAA Laboratories), 1% each of penicillin, streptomycin, non-essential amino acids, vitamins and 2% essential amino acids (Gibco, Invitrogen). Human cervical cancer, HeLa; human hepatocellular carcinoma cells, HepG2, and human breast cancer cells, MCF7 were purchased from American Type Culture Collection (ATCC, USA). Cancer cell lines were maintained in Dulbecco's Modified Eagles Medium (DMEM) supplemented with 10% FBS and 1% penicillin–streptomycin. Cells were sub-cultured at 80 – 90% confluence and maintained at 37 °C in a humidified incubator supplied with 5% CO_2. IMR90 served as a representation of normal cell lines, while various cancer cell lines were studied because of different surface receptors.

2.3.2 Brightfield and darkfield (CytoViva) microscopy

To visualise cell lines under a microscope, the cell type of interest was cultured in a 24 - well plate (Griener Bio-one GmbH) where one sterilized VFM coverslip (CellPath) was laid at the bottom of the well. The coverslip was washed and soaked in sterile PBS for 10 min to condition before the addition of 10000 cells in media (1 ml), respectively, into each well. Spent media was aspirated the next day and replaced with fresh media. Coverslips were removed from the wells and rinsed with fresh media before placing facedown onto a clean glass slide for observation. Brightfield images of cell lines were captured using Olympus BX61 microscope with

cell^P imaging software (v3.0). Darkfield images were captured using Nikon E200 microscope with CytoViva ultra-high resolution illumination systems as the light source.

2.3.3 Cell viability assay (CellTiter-Glo)

The viability of Pt-nps treated cells was measured using CellTiter-Glo luminescent cell viability assay (Promega) following the manufacturer's instructions. This assay is a homogeneous method for determining the number of viable, metabolically-active cells in a culture based on the quantification of ATP concentration. The reagent contains detergents to break the cell membrane, causing ATP release into the medium and ATPase inhibitors to stabilize the released ATP. The addition of an equal volume of reagent to the cell medium generates a luminescent signal proportional to the concentration of ATP present in cells. The assay is based on the conversion of luciferin to oxyluciferin by a recombinant luciferase in the presence of ATP. The observed luminescence is proportional to the quantity of ATP where viable cells produce more ATP than non-viable cells. The experiments were performed in white, opaque-walled 96 - well plates (Corning, Costar). Additional controls were included in this test to rule out autoluminescence or quenching by Pt-nps. For the ATP assay, 5000 cells were plated per well and incubated in media (100 µl) overnight for cells to adhere to the bottom of the well. Spent media was aspirated the next day and replaced with fresh media and cells were treated with different concentrations of NPs (25, 50, 100, 200, and 400 µg/ml) for 24, 48 and 72 h for all cell types. At respective time points, CellTiter-Glo viability assay (100 µl) pre-warmed to room temperature was added into each well and mixed

properly. After 15 min, luminescence values were measured using Tecan Infinite F200 micro-plate reader.

2.3.4 Apoptosis assay

Annexin-V staining was performed to differentiate apoptosis from necrotic cell death induced by Pt-nps. Annexin-V has a high affinity for phosphatidylserine, which is translocated from the inner to the outer leaflet of the plasma membrane at early stages of apoptosis. Its conjugation with the fluorescent probe FITC facilitates measurement by cytometric analysis. Propidium iodide (PI) staining helps to distinguish between apoptosis and necrosis due to differences in permeability of PI through the cell membranes of live and damaged cells. Pt-nps treated cells were harvested and washed twice in DPBS (Sigma-Aldrich) and stained (Annexin-V FITC apoptosis detection kit, Sigma-Aldrich) as per manufacturer's instructions. Flow cytometry was performed using Epics Altra (Beckman and Coulter) at an excitation wavelength of 490 nm and emission wavelength of 610 nm. Data was collected for 10000 gated events and analyzed using Summit V4.3.02 software.

2.3.5 Drug (5FU) release kinetics of Pt-FA/5FU/PVP and Pt-Gal/5FU/PVP

Freeze-dried Pt-nps were used for preparation of stock solutions (1 mg/ml). Data were obtained from triplicates using the dialysis bag method following reported procedures (Cheng, Peng et al. 2009; Wilson, Samanta et al. 2010). 5FU release study was carried out in the dialysis membrane tubing (MWCO 3200, Thermo Scientific). Pt-nps cannot cross the membrane, while 5FU can easily diffuse out. Once the lyophilized Pt-nps were dispersed in water, they were immediately transferred into the dialysis membrane tubing. Typically, Pt-nps solution (1 ml) in dialysis membrane

tubing was incubated at 37 ± 0.5 °C in phosphate buffer saline (PBS, 20 ml). An aliquot (0.6 ml) was taken at pre-determined time intervals over the period of 24 h. The total volume of PBS was maintained by adding the same volume of fresh PBS after every aliquot removal. The cumulative release profile of 5FU from the Pt-nps was obtained via concentration correction (the amount of 5FU in each aliquot was calculated to correct the overall cumulative releasing of 5FU) of released 5FU based on the following equation: $C'_t = C_t + (v/V)\Sigma_0^{t-1}C_t$, where C'_t is the corrected concentration at time t, C_t is the apparent concentration at time t, v is the volume of the aliquots taken, and V is the total volume of buffer.

2.4 *In vivo* studies

2.4.1 Collection of zebrafish (*Danio rerio*) embryos

Zebrafish embryos were collected from the zebrafish aquarium in the Department of Biological Sciences, National University of Singapore and staged according to standard procedures (Westerfield 2000). For this study, 20 healthy embryos were placed in each well of a 24 - well plate along with embryo water (1 ml); or a 6 – well plate along with embryo water (6 ml). Healthy, fertilized embryos were selected at early stages (4 – 16 cell stage) with the aid of an optical microscope. Fertilized embryos are indicated by dividing blastomeres and transparency, while embryos with abnormalities such as asymmetry and presence of vesicles in the yolk were discarded.

2.4.2 Active Pt-nps delivery into transgenic zebrafish (Tet-on EGFP-kras^{v12}) liver (fluorescence microscopy)

Heterozygous transgenic embryos at 48 hours post fertilization (hpf) were treated with doxycycline (10 µg/ml, Sigma-Aldrich) for 48 h. Transgenic larvae which express oncogenic Kras in the liver after induction by doxycycline were identified by their GFP expression and randomized into a 6 - well plate (Griener Bio-one GmbH) with 20 larvae in each well. Doxycycline controls were given doxycycline (10 µg/ml) while the Pt-nps treatment groups were given either 25 µg/ml or 50 µg/ml nanoparticles solution, also with doxycycline (10 µg/ml). Preliminary experiments have shown that Pt-nps concentrations above 50 µg/ml could cause defects in larvae development and therefore concentrations were kept below this limit. LiPan transgenic zebrafish larvae displayed strong expression of Ds-Red RFP (red fluorescent protein) in the liver and were included to give an indication of the size of a "normal" liver at respective time points (Korzh, Pan et al. 2008). At 6 and 8 dpf which corresponds to 2 and 4 days post treatment (dpt), larvae from each group were imaged with Zeiss Axiovert 200 M inverted microscope equipped with AxioCam HR digital camera. Liver size was calculated using Adobe Photoshop (v7.0).

2.4.3 PCNA staining of transgenic zebrafish (Tet-on EGFP-kras^{v12}) larvae liver

Larvae (8 dpf) were fixed with 30% sucrose/2% Bactoagar at room temperature. The embryos were cryo-sectioned at a thickness of 8 µm. Sections were fixed with 4% PFA/PBS, washed 3 x 5 min, blocked using 5% BSA with 1% H_2O_2 and washed using PBST 3 x 5 min. Slides were incubated in primary antibody (1 : 1000) overnight at 4 °C followed by secondary antibody (Dako Kit) conjugated with HRP for 1 h at room temperature. Slides were rinsed with PBST 3 x 10 min and

immersed in DAB colour development solution (1 : 100) for a few minutes, stained with Hoechst and finally mounted in Flurosave medium (Calbiochem). Brightfield images were taken using Olympus BX61 microscope with cell^P imaging software (v3.0).

2.4.4 TEM of zebrafish (Tet-on EGFP-kras^{v12} and wild-type) larvae liver

Larvae were pre-fixed with 2.5% glutaldehyde and 2% PFA and post-fixed with OsO_4. After a graded dehydration in 30%, 50%, 70%, 80%, 90%, 95% and 100% alcohol, larvae were treated in ethanol/propylene oxide mixture (1 : 1); 100% propylene oxide; propylene oxide/resin mixture (1 : 1) and finally embedded in 100% resin at 80 °C. Ultramicrotomy was performed using Leica Ultracut UCT with a diamond knife to obtain samples with 90 nm thickness. Samples were supported on 150 mesh copper grid, stained with uranyl acetate and lead citrate and observed using JEOL 2010-F FETEM.

2.5 Statistical analysis

Statistical analyses of the values for all experiments were expressed as mean ± standard deviation of at least 3 independent experiments. The data were analyzed using *Student's t test* where statistical significance was calculated for NPs treatment group against untreated (negative control) group. The data were subjected to unpaired one-tailed test and those with $P < 0.05$ were considered as significant.

CHAPTER 3

EVALUATING THE EFFECTS OF PLATINUM NANOPARTICLES *IN VITRO* (CELL LINES)

Publication from this chapter:

Yiwei Teow and Suresh Valiyaveettil, "Active targeting of cancer cells using folic acid-conjugated platinum nanoparticles", Nanoscale, 2010, 2, 2607–2613 (Cover article)

3.1 Introduction

In drug development, physicochemical properties such as solubility (Rytting, Lentz et al. 2005), bioavailability (Veber, Johnson et al. 2002) and drug targeting (Low 2007) are problems commonly encountered by medicinal chemists. With the development of nanomaterials, potential solutions for these issues are beginning to emerge. During drug development, especially for oral drugs, solubility is often the most difficult hurdle to overcome. Various drug-like compounds originate from natural sources such as plants and these are often huge organic molecules with low solubility in water and body fluids. A common approach to improve solubility and absorption by the body is to dissolve the compound in an organic solvent. Cremophor EL is one surfactant used to stabilize a non-polar cancer drug such as paclitaxel (Gelderblom, Verweij et al. 2001). As Cremophor EL is a huge organic molecule, it is not inert to the patient, but also exerts a range of biological side reactions. These symptoms include hypersensitivity, hyperlipidemia, abnormal lipoprotein patterns and aggregation of erythrocytes, adding to the side effects of the cancer drugs (Gelderblom, Verweij et al. 2001). Due to this reason, a biocompatible solvent or carrier which can improve drug solubility must be used.

The ultra-small size of nanoparticles (NPs) offers unique physicochemical properties such as a large surface area to mass ratio as well as high reactivity (Murakami and Tsuchida 2008; Zhang, Gu et al. 2008). Depending on the nature or materials used to synthesize NPs, the solubility of NPs in water differs greatly. A simple but effective approach to enhance solubility is to introduce biocompatible molecules, for example poly(*N*-vinyl-2-pyrrolidone) (PVP), as capping agents on the surface of nanoparticles (Chen, Falkner et al. 2005).

Bioavailability of drugs in the blood can be affected by interactions with other drug proteins, metabolism and elimination. A common way to improve drug levels is by introducing poly(ethylene glycol) (PEG) on the surface of NPs, which reduces protein-binding. By evading RES uptake, NPs have longer circulation half-life and better passive targeting outcomes for tumours can be achieved (Gaur, Sahoo et al. 2000; Li and Huang 2007).

Although passive targeting increases drug concentrations in tumour vasculature in comparison to normal tissues, this is still a non-selective process and normal tissues are also able to take up the drug, resulting in undesirable side effects. This however, can be improved by introducing targeting moieties such as antibodies on NPs which act as the carrier for the drug. Folic acid incorporated NPs are one such example which have been found to target cancerous cells which over-express folate receptors on their surface (Pan and Feng 2008; Yang, Chen et al. 2008). Taking into account solubility, passive and active targeting during the design of NPs, nanoparticulate drugs will be able to reach their targets more efficiently at a lower concentration. The end-result is faster drug onset and lesser side effects, both beneficial to the patient.

Currently, there are many reports on utilizing folic acid on nanocarriers for the active targeting of cancer cells over-expressing folate receptors, but information on the linking of folic acid to platinum nanoparticles (Pt-nps) by *in situ* reduction of hexachloroplatinic acid and investigation of toxicity have not yet been reported. We therefore demonstrate a simple method for the preparation of folic acid-capped Pt-nps (Pt-FA) which showed increased uptake and toxicity in cancer cells over PVP-capped Pt-nps (Pt-PVP). Next, we synthesized Pt-nps functionalized with folic acid, 5-fluorouracil and PVP (Pt-FA/5FU/PVP); and Pt-nps functionalized with galactose, 5-

fluorouracil and PVP (Pt-Gal/5FU/PVP), to demonstrate that adding important biomolecules could improve the viability of normal cells, while retaining the same level of toxicity toward cancer cells. The use of Pt-nps as a drug carrier was studied by introducing 5-fluorouracil *via* surface adsorption during synthesis. The rate of surface desorption of 5-fluorouracil can be studied. A simple one-pot reaction was used to prepare Pt-nps because lesser synthetic steps are required, which ensures high reproducibility and yield. Preparation of Pt-nps also involved proper purification and characterization, as factors such as purity, size, shape, surface functionalization and charge are known to affect a nanomaterial's toxicity (Teow, Asharani et al. 2011).

Here, we investigated the *in vitro* effects of Pt-nps in cell lines (normal human fibroblasts, IMR90; human cervical cancer, HeLa; human breast cancer, MCF7 and human hepatocellular carcinoma, HepG2) using the following experimental methods which were described in detail in Chapter 2 (Materials and Methods):

1. Synthesis, purification and characterization of Pt-nps (pages 30 – 36);
2. Darkfield microscopy (CytoViva) – Pt-nps uptake, cell shape, cell viability (page 37);
3. ATP assay (CellTiter-Glo) – cell proliferation (page 38);
4. Apoptosis assay – mechanism of cell death (pages 39);
5. Drug (5FU) release studies – kinetics of release of active drug 5FU (page 39).

3.2 Results

It is important for Pt-nps to maintain their stability in water, buffer and cell culture medium as aggregation or agglomeration can reduce their effective concentrations in solution. As such, we used water soluble capping agents (**Figure 3.1(a-d)**) for the synthesis of Pt-nps. As seen in **Figure 3.1(e)**, the resulting purified Pt-nps solutions showed no signs of precipitation and remained stable throughout the duration of this study.

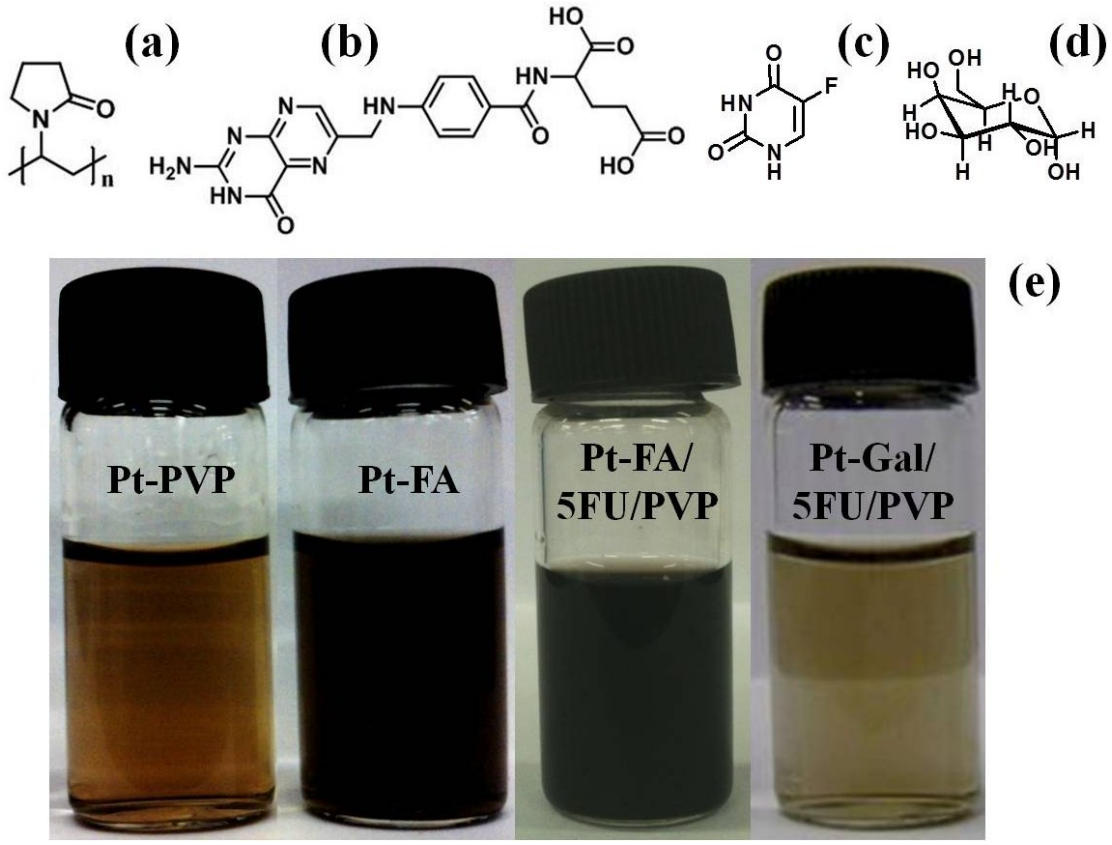

Figure 3.1: Water soluble capping agents, including PVP (a), folic acid (b), 5-fluorouracil (c) and D-galactose (d) were used for the synthesis of Pt-nps, resulting in the formation of stable colloids in solution (e).

Pt-PVP acted as the model nanoparticle in our study, as it is the simplest water-soluble and stable Pt-nps that can be synthesized. Pt-FA, on the other hand, was synthesized to prove that Pt-nps can be actively targeted toward cancer cell lines with the aid of a suitable targeting ligand, in this case, folic acid. Pt-FA/5FU/PVP and Pt-

Gal/5FU/PVP were synthesized as an attempt to improve the targeting effects and efficacy of Pt-nps and shall be discussed in the final section of this chapter.

For the synthesis of Pt-FA, hexachloroplatinic acid and folic acid were mixed and stirred before adding sodium borohydride. As for Pt-PVP, the capping agent PVP was added immediately after the introduction of sodium borohydride. A colour change from yellow to light brown indicated the formation of Pt-PVP. The nanoparticles synthesized via the former approach were too small and could not be purified using centrifugation. Alternatively, switching the sequence of reagent addition produced a pellet after centrifugation which can be easily resuspended in water. Uncapped Pt-nps are insoluble in water and appeared as a black suspension after rigorous sonication. Such solutions are not stable for long periods and are unsuitable for biological studies.

TEM images revealed that Pt-nps form homogeneous colloids in water with no signs of agglomeration (**Figure 3.2(a, b)**). This is important to make sure that individual nanoparticles can be transported across cell membranes. The core size of Pt-PVP is in the range of 2–6 nm, while Pt-FA is larger with majority of particles in the range of 10–15 nm. Pt-PVP and Pt-FA are water dispersible owing to the hydrophilic capping agents which can prevent individual particles from aggregating. It should be noted that folic acid is more soluble in buffer solutions than in ultrapure water, which is preferred for cell viability assays. DLS measurements have showed that the mean hydrodynamic diameters were 13.5 nm and 91.3 nm for Pt-PVP and Pt-FA, respectively (**Figure 3.2(c, d)**). PVP confers steric stabilization whereas folic acid gives an electrostatic stabilization. In contrast to Pt-PVP, Pt-FA has a highly-charged surface which is solvated by water molecules, which explains its increase in hydrodynamic size after dissolving in water. TEM is used to determine inner core

diameter, while the hydrodynamic size distribution includes the solid particle, its organic layers (capping agents) and the hydration shell, which explains why DLS values are always larger (Barth, Sharma et al. 2010; Kittler, Greulich et al. 2010).

The zeta potential of Pt-PVP was at -8.0 mV while that of Pt-FA was at -40.5 mV (**Figure 3.2(e, f)**). The highly-charged surface of Pt-FA arising from the ionization of acid functional groups resulted in a highly negative potential. Conversely, PVP is a neutral and hydrophilic polymer which stabilizes Pt-PVP through hydrophilic interactions with the solvent and therefore has a low surface potential. From **Figure 3.2(g)**, it is apparent that the ratio of capping agent to platinum in Pt-PVP is high (high carbon to platinum ratio). On the contrary, low carbon content was observed for Pt-FA nanoparticles. Platinum content (12.5% vs. 18.2%) of both samples were comparable which enables a fair comparison between these two nanoparticles in cell viability testing. Oxygen content (estimated) of Pt-FA was found to be higher than expected due to its hygroscopic nature.

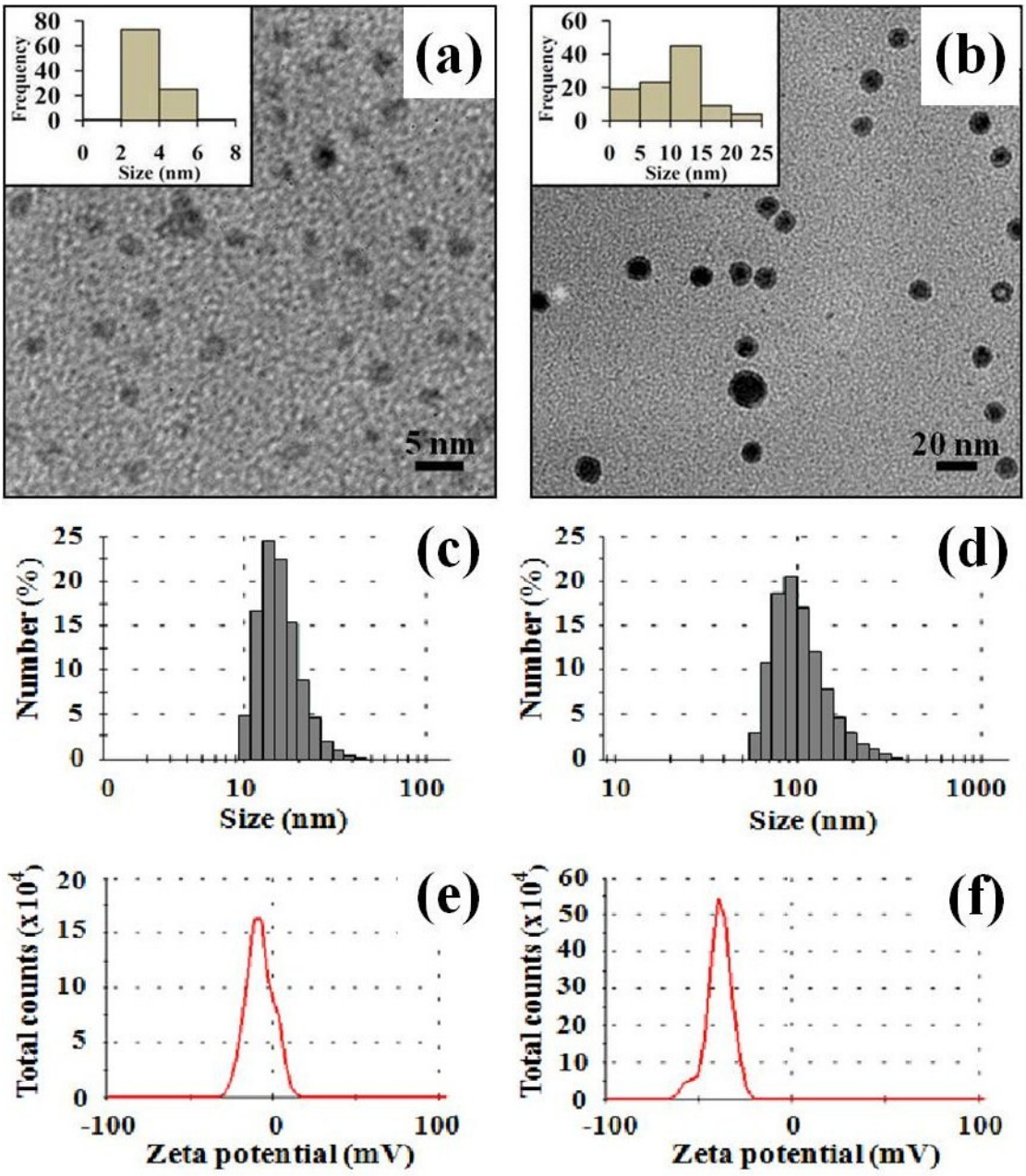

(g)

Element	Pt	C	H	N	O (est)
Pt-PVP	12.5	37.5	6.7	7.2	36.1
Pt-FA	18.2	5.35	3.1	1.2	72.15

Figure 3.2: Characterization of Pt-nps. TEM images of Pt-PVP (a) and Pt-FA (b). Insets represent size distribution of the nanoparticles. Data for the histogram were collected from 100 randomly picked particles. Dynamic light scattering histogram of Pt-PVP (c) and Pt-FA (d). Zeta potential distribution of Pt-PVP (e) and Pt-FA (f). Chemical composition (in wt%) of Pt-PVP and Pt-FA (g).

3.2.1 Darkfield microscopy (CytoViva) – Pt-nps uptake, cell shape, cell viability

Cell lines were grown on coverslips and treated with Pt-nps for 48 h before observation using CytoViva. Although the plasma membrane is vaguely observed in dark field microscopy, nuclear envelopes, cellular contents and organelles are distinct and brightly-illuminated. In the three cell types studied, untreated cells displayed a small number of bright, round circles which are evenly distributed throughout the cells (**Figure 3.3(a, d, g)**). The identity of these bright specks (yellow arrows) could be organelles or transport vesicles (endosomes) which contain high concentrations of ions and proteins. Such bright spots should not be mistaken for Pt-nps aggregates (green arrows) which are non-circular (randomly-shaped). Pt-nps are too small to be observed directly under a light microscope and therefore the bright objects seen in these images are scattered light from Pt-nps.

Pt-nps were able to enter the cytoplasm but not found inside the nucleus, which is consistent with literature findings (Komatsu, Tabata et al. 2008). With Pt-PVP treatment, cells appear to maintain their structural integrity as the membranes remained intact. In contrast, Pt-FA was found to enter cells more efficiently as indicated by more white specks. The plasma membranes became less distinct, especially in cancer cells. **Figure 3.3(c, f)** show cell debris resulting from cell death.

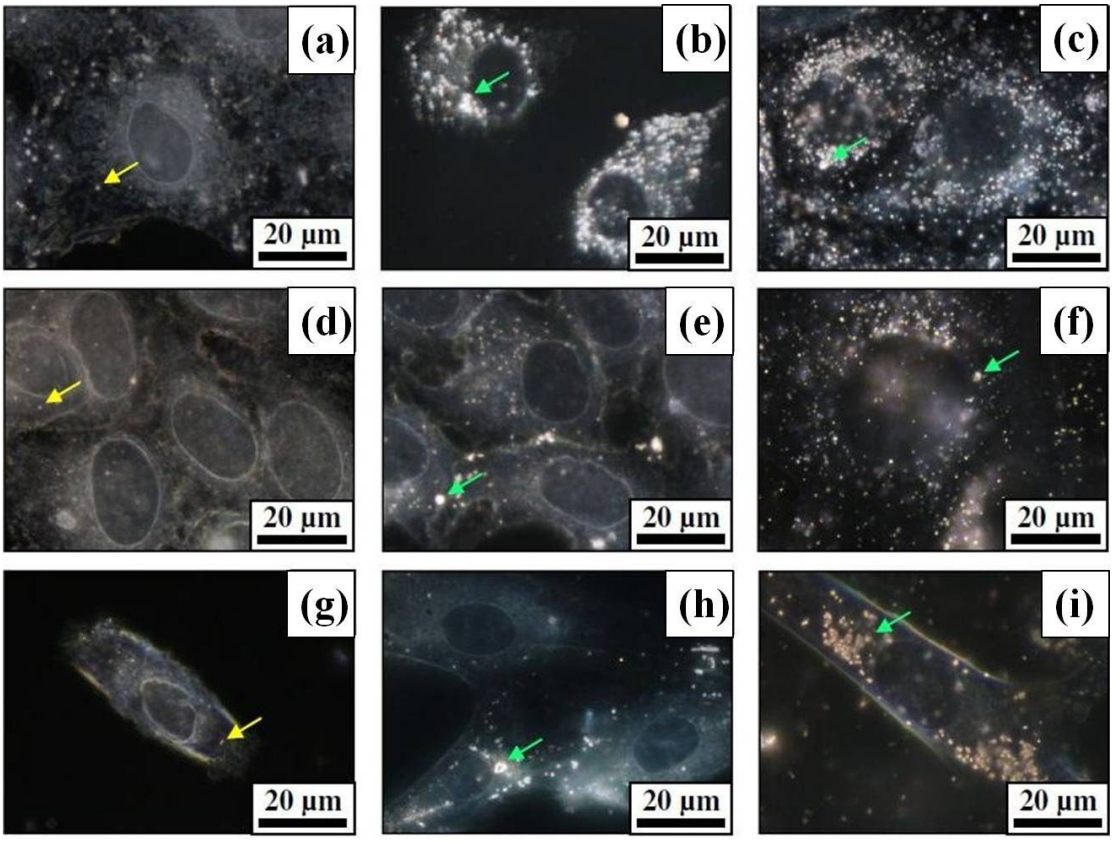

Figure 3.3: Darkfield optical images of untreated (a), Pt-PVP treated (b) and Pt-FA treated (c) HeLa cells. Untreated (d), Pt-PVP treated (e) and Pt-FA treated (f) MCF7 cells. Untreated (g), Pt-PVP treated (h) and Pt-FA treated (i) IMR90 cells. Concentration of Pt-nps = 100 µg/ml. Yellow arrows point to cellular components such as endosomes and lysosomes, while green arrows point to big Pt-nps aggregates.

3.2.2 ATP assay (CellTiter-Glo) – cell proliferation

A concentration and time-dependent study was conducted to find out the effects of Pt-nps on cell viability. Commonly-used cell viability assays are MTT (3-(4,5-dimethylthiazole-2-yl)-2,5-biphenyl tetrazolium bromide) or MTS (3-(4,5-dimethylthiazole-2-yl)-5-(3-carboxymethoxyphenyl)-2-(4-sulfophenyl)-2*H*-tetrazolium) which monitor the emission intensity of fluorescent dyes at specific wavelengths. A test substance, which might show similar optical properties to these dyes, can cause complications during the process of measurement. This is especially true when nanomaterials are being tested (Ulukaya, Ozdikicioglu et al. 2008; Doak, Griffiths et al. 2009). For example, silver and gold NPs gave distinct UV absorption

peaks due to surface plasmon resonance. Therefore, they give false-positive results when tested using the MTS or MTT assays.

The CellTiter-Glo luminescent cell viability assay is designed to monitor cytotoxicity as well as cell proliferation by measuring the number of viable cells in the culture medium. This assay measures the amount of adenosine triphosphate (ATP) present, which is directly proportional to the number of viable cells. One advantage of this assay is the short waiting time (minutes) compared to MTS or MTT (four hours or more). A comparison between the ATP and MTT assay revealed that the two assays gave different results when used to measure growth inhibition of various cancer drugs on the lung cancer cell line A549 (Ulukaya, Ozdikicioglu et al. 2008). This is because the MTT assay measures the activity of dehydrogenases, while ATP concentration was measured in the case of ATP assay. Dying cells lose ATP faster than dehydrogenase activity, hence resulting in an over-estimation of cell viability when using the MTT assay. Owing to the fact that the ATP assay is more sensitive, it was used for our measurement.

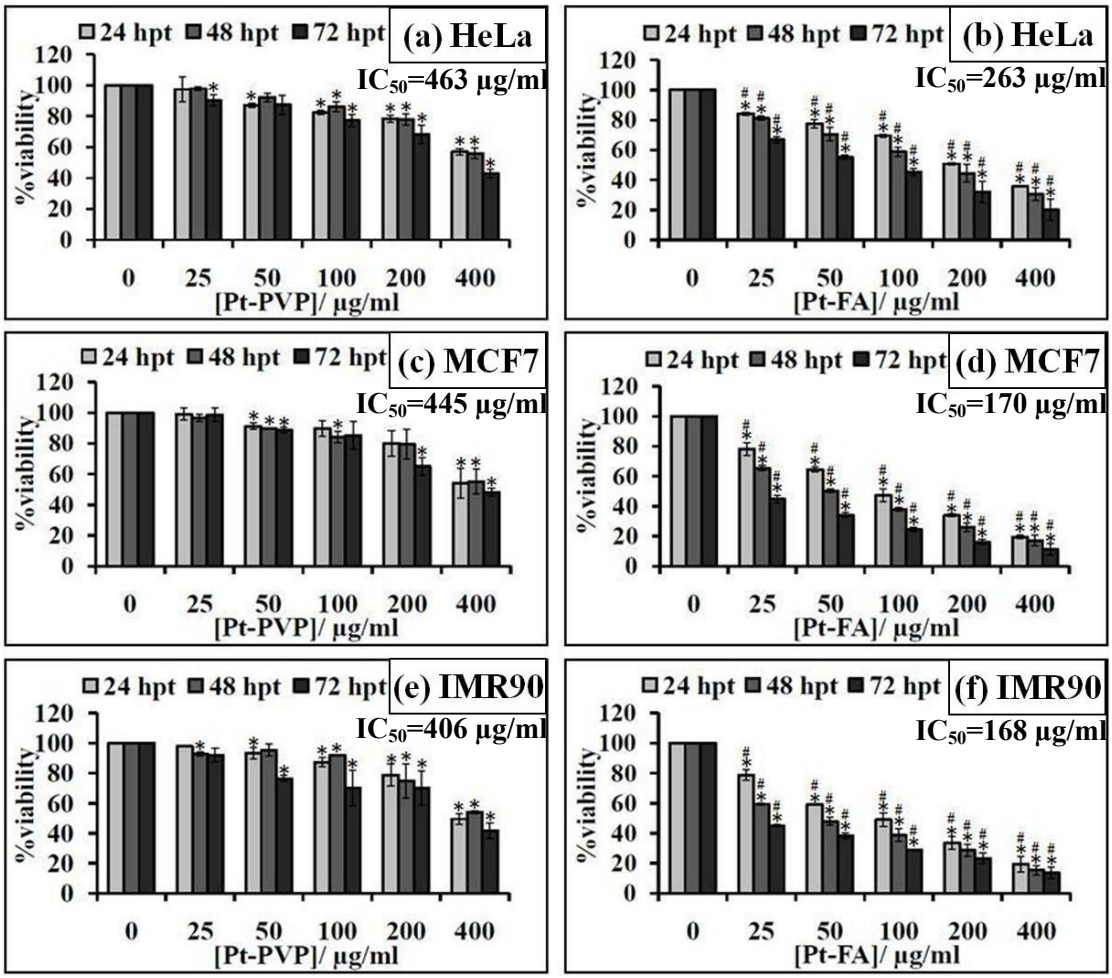

Figure 3.4: Cell viability assays of HeLa (a, b), MCF7 (c, d), and IMR90 (e, f) after exposure to various concentrations of Pt-PVP and Pt-FA 24, 48 and 72 hpt. The y-axis represents the percentage of viable cells present in the treated sample after a certain time and the x-axis represents the final Pt-nps concentration in culture. The values represent the mean ± standard deviation of three independent experiments; * denotes $P < 0.05$ with respect to the control group; # denotes $P < 0.05$ between Pt-PVP and Pt-FA using *Student's t test*.

The viability trends of Pt-PVP and Pt-FA treated cells were similar across different cell types. Generally, the viability of cells decreased with increasing Pt-nps concentration and with increasing exposure time from 24 h to 72 h (**Figure 3.4**). Pt-PVP was comparatively non-toxic compared to Pt-FA. Although Pt-PVP was internalized by all cell lines as shown by dark field microscopy, the viability of cells was not affected until a high dose of 400 µg/ml was introduced, which reduced the viability of all cell types to less than 60% after 24 h. Increasing Pt-PVP concentration

by eight-fold from 25 to 200 μg/ml did not reduce cell viability even after 72 h of exposure. On the other hand, Pt-FA is more toxic than Pt-PVP, especially to MCF7 breast cancer cells. Unlike Pt-PVP, the dose and time-dependency of Pt-FA are consistent across all cell types. At a low dose of 25 μg/ml, viability of HeLa, MCF7 and IMR90 dropped to 65%, 44%, and 43%, respectively, after 24 h, which is significantly lower than Pt-PVP. IC_{50} is defined as the half maximal inhibitory concentration of a drug and the values at 24 h were calculated using linear regression. If the drug concentration required to inhibit the growth of cells by 50% is low, the drug is said to be more effective. The calculated IC_{50} values correlated well with our observations. The inclusion of IMR90 amidst cancer cell lines allows a comparison of toxicity with normal cells. Little selectivity towards cancer cell lines over IMR90 was observed despite attaching folic acid on the Pt-nps surface. Folic acid was effective in directing Pt-nps into HeLa and MCF7 which over-expresses folate receptors as compared to NPs capped with PVP. Although IMR90 does not over-express such receptors, it was affected by the toxic effects of platinum even at low doses of Pt-FA. However, under *in vivo* conditions, Pt-FA would be expected to deposit preferentially at the tumour site due to an enhanced permeability and retention effect (EPR) which improves the selectivity (Allen and Cullis 2004; Peer, Karp et al. 2007; Byrne, Betancourt et al. 2008). This is an advantage of nanodrug delivery systems as compared to conventional molecular cancer therapeutics such as cisplatin, which has a low circulation half-life.

The increase in toxicity of Pt-FA over Pt-PVP could be due to two reasons: (i) higher platinum content; and (ii) increased receptor-mediated endocytosis. The platinum content of Pt-FA is 18.2% as compared to 12.5% in Pt-PVP. Under slightly

acidic conditions, Pt^0 can be converted to Pt^{2+} (Gao, Liang et al. 2008), which is believed to be responsible for the toxicity (Asharani, Xinyi et al. 2010).

$Pt^0 \rightleftharpoons Pt^{2+} + 2e$ $\quad E° = -1.18$ V

$H_2O_2 + 2H^+ + 2e \rightleftharpoons 2H_2O$ $\quad E° = +1.776$ V

$Pt^0 + H_2O_2 + 2H^+ \rightleftharpoons Pt^{2+} + 2H_2O$ $\quad E°_{cell} = +0.596$ V

These $E°$ values (Lide 2000) were measured at standard temperature, pressure and concentration with respect to a standard hydrogen electrode, which may not reflect the true conditions in a living cell. However, a positive $E°$ value signifies a spontaneous reaction. Gao *et al.* reported the use of FePt@CoS_2 yolk-shell nanocrystals as a potent agent to kill HeLa cells, where the FePt core was released from the shell and oxidized slowly during the process. Pt^{2+} ions can diffuse into the nucleus and mitochondria binding to DNA and leading to apoptosis of HeLa cells (Gao, Liang et al. 2007; Gao, Liang et al. 2008).

Folic acid is a low molecular weight vitamin compound (B_9) which has been shown to be an effective tumour-targeting compound, especially in cancers such as breast, lung, kidney, ovarian and epithelial mouth cancers which over-express folate receptors (Peer, Karp et al. 2007; Rosenholm, Peuhu et al. 2009; Wiradharma, Zhang et al. 2009). Unlike antibodies or hormones-tagged particles which are shuttled to the lysosome for destruction, folic acid-tagged carriers are normally retained in an endocytic vesicle or released into the cytoplasm as folic acid is essential for cell functions (Byrne, Betancourt et al. 2008). Gold nanoparticles with folic acid-linked PEG backbone and its efficiency *in vitro* have been widely reported (Byrne, Betancourt et al. 2008; Patra, Verma et al. 2008; Gullotti and Yeo 2009). Various other groups also reported the attachment of folic acid to other polymer backbones in nanocarriers (Park, Kim et al. 2005; Yoshida, Oide et al. 2006; Bhattacharya, Patra et

al. 2007; You, Li et al. 2008; Pan and Feng 2009). A simple but efficient way of directly attaching folic acid onto Pt-nps via *in situ* reduction of hexachloroplatinic acid in folic acid solution using sodium borohydride which does not require extensive organic synthesis or purification methods was described. The resulting nanoparticles were stable in water and cell medium. Also, the inherent toxicity of Pt-nps and the slow oxidation into Pt^{2+} ions as the source of anticancer activity have been incorporated into the design strategies. In fact, Pt-FA nanoparticles serve as carrier of folic acid and as a drug.

Other factors which can influence nanoparticles toxicity include size (Hussain, Hess et al. 2005; Pan, Neuss et al. 2007; Carlson, Hussain et al. 2008), surface area, surface functionalities and charge (Carlson, Hussain et al. 2008; Thevenot, Cho et al. 2008). In general, NPs toxicity was found to increase with decreasing size due to the increase in reactive surface area for interaction with biological molecules or generation of reactive oxygen species. Waters *et al.* reported that changes in gene expression in murine macrophages correlated better with total surface area of silica nanoparticles rather than particle size or concentration (Waters, Masiello et al. 2009). Thevenot *et al.* tested TiO_2 nanoparticles with different surface chemistries in various murine cell lines and found that NPs containing the amine functional group were more toxic than NPs containing hydroxyl and carboxylic acid functional groups due to strong interaction with the negatively-charged cell membrane (Thevenot, Cho et al. 2008). In fact, cationic liposomes are often used to deliver DNA with high transfection efficiencies (Torchilin 2006). Pt-FA is bigger (91.3 nm) and negatively-charged while Pt-PVP (13.5 nm) is smaller and neutral. Therefore, Pt-FA is expected to be less toxic than Pt-PVP. However, interaction with folate receptors enables Pt-FA to be internalized by cancer cells to exert its toxic effects.

3.2.3 Apoptosis assay – mechanism of cell death

The apoptosis assay was carried out to assess the extent and mode of cell death upon exposure to Pt-nps. Stained cells were passed through the flow cytometer and the percentage of unstained cells (live cells), cells with red labels (took up the red propidium iodide stain, indicating necrosis), cells with green labels (took up the green signal from Annexin V-FITC, indicating early apoptosis) and finally cells which were dual-stained (late apoptosis), were generated from dot plots.

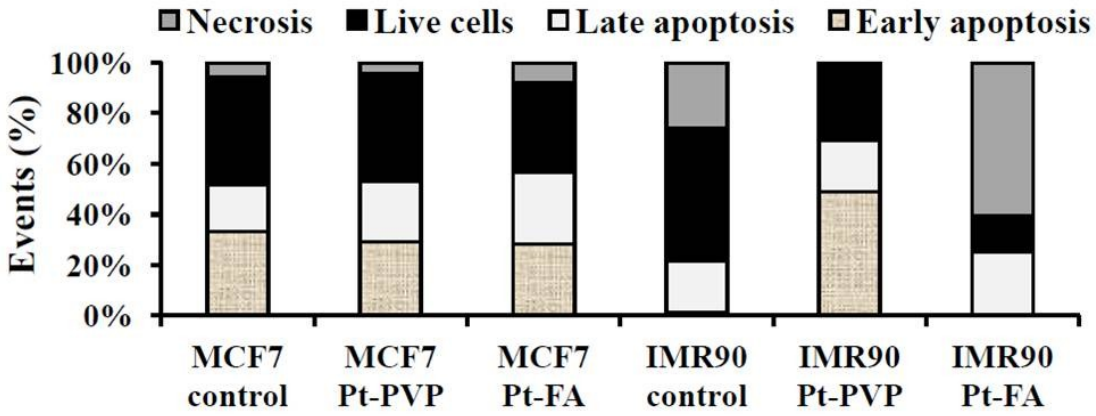

Figure 3.5: Annexin-V staining of MCF7 and IMR90 treated with 100 µg/ml Pt-nps solution for 48 h. Cells stained with PI alone are necrotic, whereas cells stained with Annexin V-FITC alone represent early apoptosis. Cells at final stages of apoptosis take up both stains.

As expected, treatment of MCF7 with Pt-PVP did not change the percentage of viable cells and is comparable to our cell viability assay results using same Pt-nps concentration (**Figure 3.5**). Treatment with Pt-FA caused the percentage of live cells to drop by 8% and the combined percentage of cells entering late apoptosis and necrosis increased by 12%.

Interestingly, the response of IMR90 is entirely different from MCF7. With Pt-PVP, there was no necrosis found in the control and the percentage of apoptotic cells observed was higher than the control by 47%. The percentage of early apoptotic cells stayed unchanged. However, with Pt-FA, the percentage of live cells decreased

drastically to 14% of the total population and cells were found to undergo only necrosis. Therefore, the mechanism of uptake of these particles and its subsequent processing by IMR90 could be different from MCF7 cells. These results were consistent with the findings from Pan *et al.*, where they reported that 1.4 nm Au-nps caused necrosis in HeLa cells whereas 1.2 nm Au-nps resulted in cell death by apoptosis predominantly, despite both Au-nps having the same surface functionality (Pan, Neuss et al. 2007). While apoptosis is usually related to caspase activation (Chipuk and Green 2005), calcium overload (Ozaki, Yamashita et al. 2009; Jahani-Asl, Germain et al. 2010) or induced by death-inducing signals, necrosis is associated with loss of lysosomal membrane integrity (Castino, Demoz et al. 2003). The mechanism of cell death can be affected by small changes in particle size and functional groups found on the surface of NPs. Such factors can have significant influence on membrane interaction, membrane damage, compartmentalization and processing of NPs after internalization.

3.2.4 Drug (5FU) release studies – kinetics of release of active drug 5FU from Pt-FA/5FU/PVP and Pt-Gal/5FU/PVP

Pt-FA/5FU/PVP was spherical with core size in the range of 10–15 nm, while Pt-Gal/5FU/PVP was less spherical but with a uniform size of 4 nm (**Figure 3.6(a, b)**). DLS measurements have showed that the mean hydrodynamic diameters were 12.2 nm and 13.3 nm for Pt-FA/5FU/PVP and Pt-Gal/5FU/PVP, respectively (**Figure 3.6(c, d)**). A similar TEM and DLS indicated that Pt-FA/5FU/PVP was not covered by a thick capping agent and hydration layer in solution. A high platinum-to-carbon ratio as showed by elemental analysis supported the data (**Figure 3.6(g)**). On the other hand, Pt-Gal/5FU/PVP had a thick capping agent layer and hydration shell when

placed in solution. The zeta potential of Pt-FA/5FU/PVP was at -39.2 mV while that of Pt-Gal/5FU/PVP was at -34.0 mV (**Figure 3.6(e, f)**).

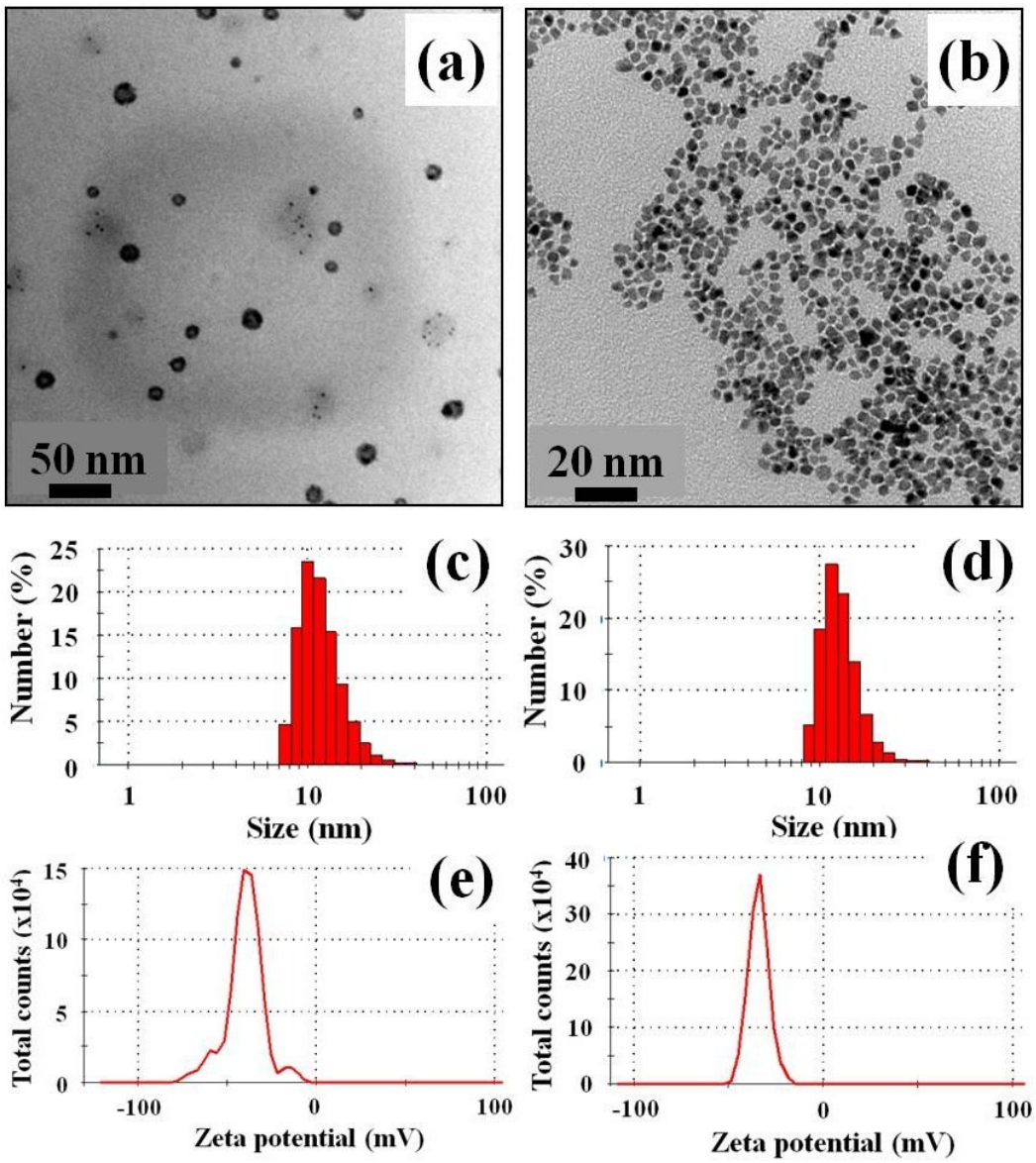

(g)

Element	Pt	C	H	N	F	O (est)
Pt-FA/ 5FU/PVP	42.3	16.4	1.1	3.6	0.3	36.3
Pt-Gal/ 5FU/PVP	31.7	17.8	2.4	7.6	1.8	38.6

Figure 3.6: Characterization of Pt-FA/5FU/PVP and Pt-Gal/5FU/PVP. TEM images of Pt-FA/5FU/PVP (a) and Pt-Gal/5FU/PVP (b). Dynamic light scattering

histogram of Pt-FA/5FU/PVP (c) and Pt-Gal/5FU/PVP (d). Zeta potential distribution of Pt-FA/5FU/PVP (e) and Pt-Gal/5FU/PVP (f). Chemical composition (in wt%) of Pt-FA/5FU/PVP and Pt-Gal/5FU/PVP (g).

Pt-FA/5FU/PVP and Pt-Gal/5FU/PVP carried 5-fluorouracil, a chemotherapeutic drug, as a capping agent. As 5FU plays an important role in the efficacy of Pt-nps against cancer cells, it is important to determine the degree and kinetics of release from Pt-nps. Here, we compared the diffusion of 5FU from 3 samples: 5FU stock solution, Pt-FA/5FU/PVP and Pt-Gal/5FU/PVP at a concentration of 1 mg/ml using the dialysis bag method (Cheng, Peng et al. 2009; Wilson, Samanta et al. 2010). Pt-nps cannot cross the membrane, while 5FU can easily diffuse out. 5FU may be entrapped, encapsulated, adsorbed or chemically attached (Wilson, Samanta et al. 2010). In our case, 5FU was expected to be primarily surface-adsorbed and possibly entrapped within the nanoparticle core.

93% of 5FU in 5FU stock solution diffused out of the dialysis membrane and reached a steady state 1 h into the study and approached 100% at 8 h (**Figure 3.7**). When bound to Pt-nps, 5FU did not diffuse out of the membrane as fast as in the case of 5FU stock solution. Pt-FA/5FU/PVP reached a percentage released value of 25% after 1 h and the total amount released after 24 h was only 42%, indicating a slow and sustained release which benefits cancer treatment. Pt-Gal/5FU/PVP released 54.5% after 1 h and the total amount released after 24 h was 64.2%. A higher percentage of 5FU was released from Pt-Gal/5FU/PVP because of a larger concentration gradient (Pt-Gal/5FU/PVP carried more 5FU than Pt-FA/5FU/PVP as seen in elemental analysis). Also, more 5FU could be entrapped within the platinum core of Pt-FA/5FU/PVP, resulting in a lower overall release.

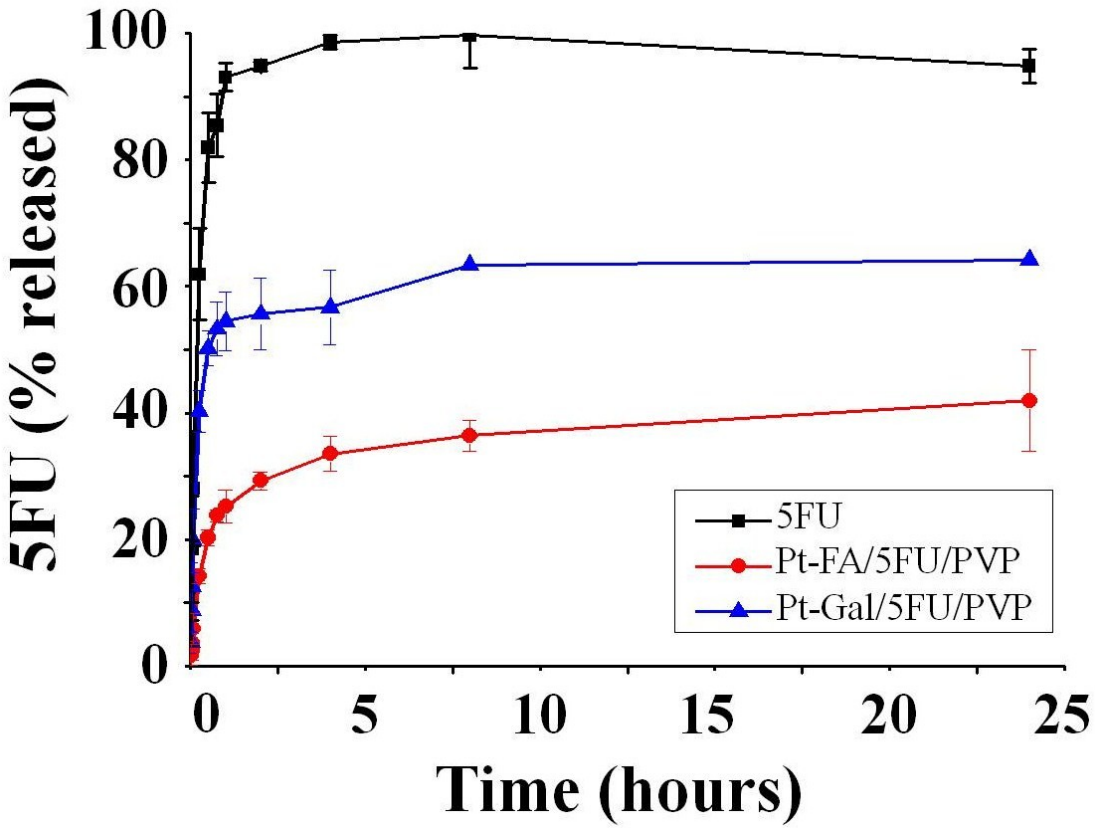

Figure 3.7: Drug release kinetics of 5FU (black), Pt-FA/5FU/PVP (red) and Pt-Gal/5FU/PVP (blue). The y-axis represents the percentage of 5FU which diffused out of the dialysis membrane and the x-axis represents specific time points.

3.2.5 Effects on cell uptake and proliferation using Pt-FA/5FU/PVP and Pt-Gal/5FU/PVP

Pt-FA/5FU/PVP carried 5FU and PVP as additional capping agents which were expected to improve the efficacy and water solubility as compared to Pt-FA. We wish to test if Pt-FA/5FU/PVP could reduce the toxic effects towards normal cells like IMR90. Zebrafish was used as an *in vivo* liver cancer model (Chapter 4). Pt-Gal/5FU/PVP was synthesized to target an *in vitro* cancer model (HepG2, hepatocellular carcinoma) and provided the necessary preliminary data. As such, we examined the cellular uptake (darkfield microscopy) and viability (ATP assay) in the same fashion as Pt-PVP and Pt-FA.

HeLa (**Figure 3.8(a, b)**), MCF7 (**Figure 3.8(c, d)**) and IMR90 (**Figure 3.8(e, f)**) were exposed to Pt-FA/5FU/PVP and checked for uptake. In cancer cell lines HeLa and MCF7, an increase in number of endosomes and white dots were observed in Pt-FA/5FU/PVP treated cells as compared to the untreated control. Pt-nps aggregates, however, were not observed as in the case of Pt-FA, which could be due to improved solubility and stability provided by PVP. The normal cell line IMR90 showed lesser uptake towards Pt-FA/5FU/PVP as compared to Pt-FA, which could mean reduced toxicity.

Pt-Gal/5FU/PVP was tested in the HCC cell line HepG2. Asialoglycoprotein receptors are expressed on the surface of liver cells and attaching galactose on Pt-nps can increase uptake. Due to the presence of galactose, a large number of endosomes were observed near the periphery of the nucleus, indicating uptake of Pt-Gal/5FU/PVP.

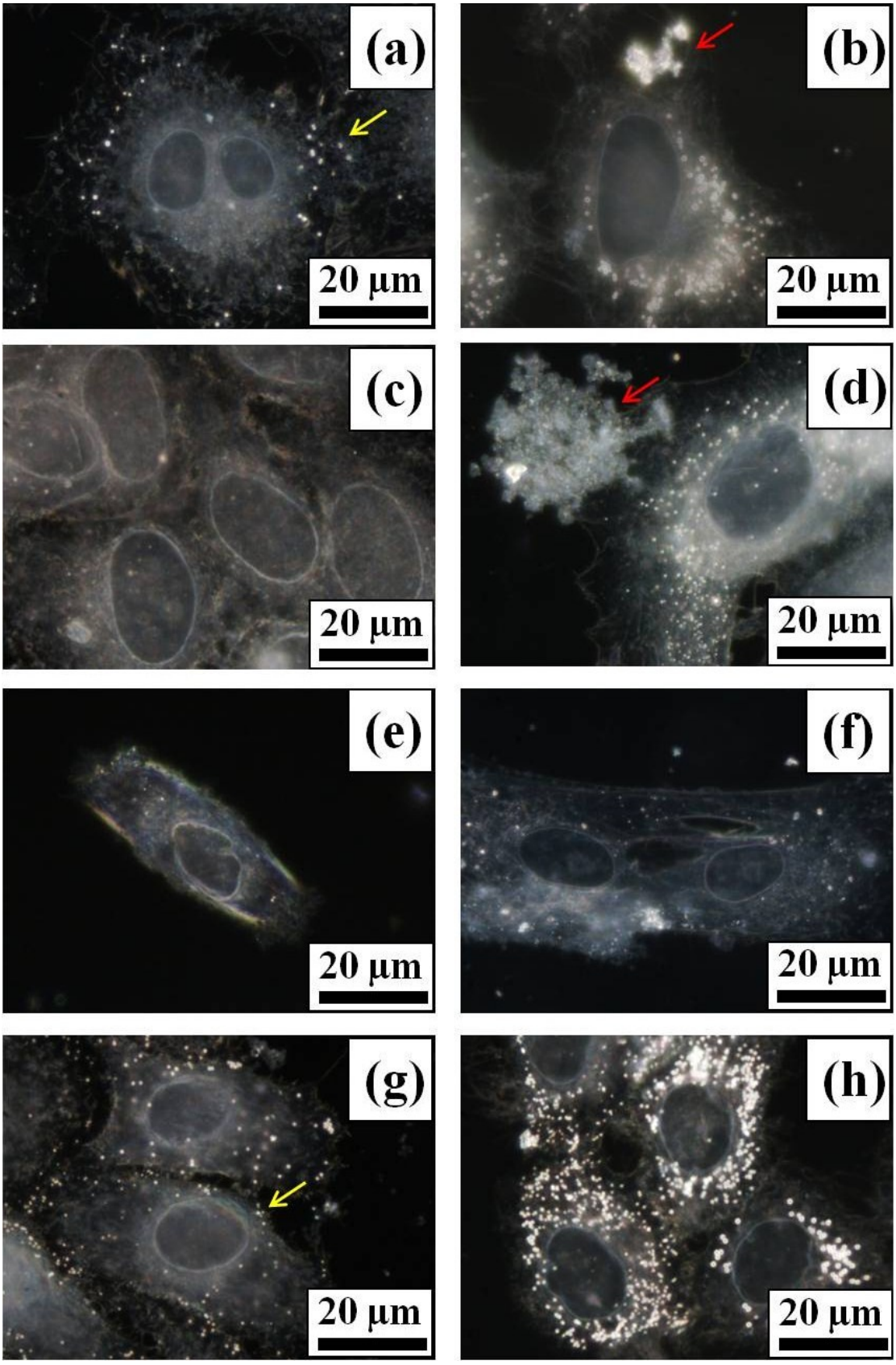

Figure 3.8: Darkfield optical images of untreated (a) and Pt-FA/5FU/PVP treated (b) HeLa cells. Untreated (c) and Pt-FA/5FU/PVP treated (d) MCF7 cells. Untreated (e) and Pt-FA/5FU/PVP treated (f) IMR90 cells. Untreated (g) and Pt-Gal/5FU/PVP

treated (h) HepG2 cells. Concentration of Pt-nps = 100 μg/ml. Yellow arrows point to cellular components such as endosomes and lysosomes, while red arrows point to dead cell debris.

Next, viabilities of HeLa and MCF7 cells were compared against IMR90 to check for cancer selectivity of Pt-FA/5FU/PVP. The efficacy of Pt-FA/5FU/PVP was also compared against the chemotherapeutic drug 5FU in these cell lines. It is important to note that the maximum concentration tested for 5FU was 200 μg/ml, while that of Pt-FA/5FU/PVP was 400 μg/ml.

The viability trends of HeLa and MCF7 were similar when exposed to 5FU. HeLa and MCF7 were insensitive to increasing concentrations of 5FU 24 hpt, until a high concentration of 100 μg/ml was introduced. The viabilities, however, began to drop drastically after 48 h, even at concentrations as low as 10 μg/ml (**Figure 3.9(a, c)**). This is possibly due to low diffusion rates of 5FU in these cells, although 5FU was highly potent. The normal cell line IMR90 showed higher viability (**Figure 3.9(e)**) when compared against HeLa and MCF7 cells, which may be because cancer cells are fast-dividing, hence higher sensitivity toward cancer drugs. This is the underlying principle of chemotherapy.

HeLa and MCF7 demonstrated different viabilities when exposed to Pt-FA/5FU/PVP, with MCF7 being more susceptible to the damages. Previously, Pt-FA was also found to reduce cell viability of MCF7 to a greater extent. This may be due to HeLa cells expressing lesser folate receptors than MCF7 cells. After 72 h of exposure at 400 μg/ml, HeLa cells had a viability of 31.6% but MCF7 had 13.0%. Pt-FA/5FU/PVP was able to cause more damages to cancer cells because they over-expressed folate receptors and take up Pt-FA/5FU/PVP *via* receptor-mediated endocytosis. The viability of IMR90 after exposure to Pt-FA/5FU/PVP was similar to that of 5FU (**Figure 3.9(f)**), but the values were improved when compared to Pt-FA

(**Figure 3.4(f)**). The increase in viabilities of IMR90 was supported by reduced uptake as shown by darkfield microscopy (**Figure 3.8(f)**). Overall, Pt-FA/5FU/PVP had the same toxicity as 5FU and Pt-FA towards cancer cells, especially MCF7, while demonstrating better compatibility towards normal cells. The IC_{50} of Pt-FA/5FU/PVP in IMR90 is calculated to be much higher as compared to Pt-FA and in other cell lines, indicating the higher biocompatibility of this nanoparticle.

As Pt-FA/5FU/PVP showed promising results, Pt-Gal/5FU/PVP was synthesized for preliminary *in vitro* testing using HepG2 before *in vivo* testing in the zebrafish. Pt-Gal/5FU/PVP showed a concentration- and time-dependent toxicity towards HepG2 cells, where cell viability decreased with increasing concentration and duration of incubation. At a concentration of 25 μg/ml and 24 h of incubation, HepG2 exhibited a reduction in cell viability and values were significantly different from control cells (**Figure 3.9(h)**). After 72 h, cell viability reduced to 6.5% in presence of 400 μg/ml Pt-nps. Pt-Gal/5FU/PVP also showed better efficacy than 5FU (**Figure 3.9(g)**) at all concentrations tested, proving to be a better nanomedicine than the conventional drug.

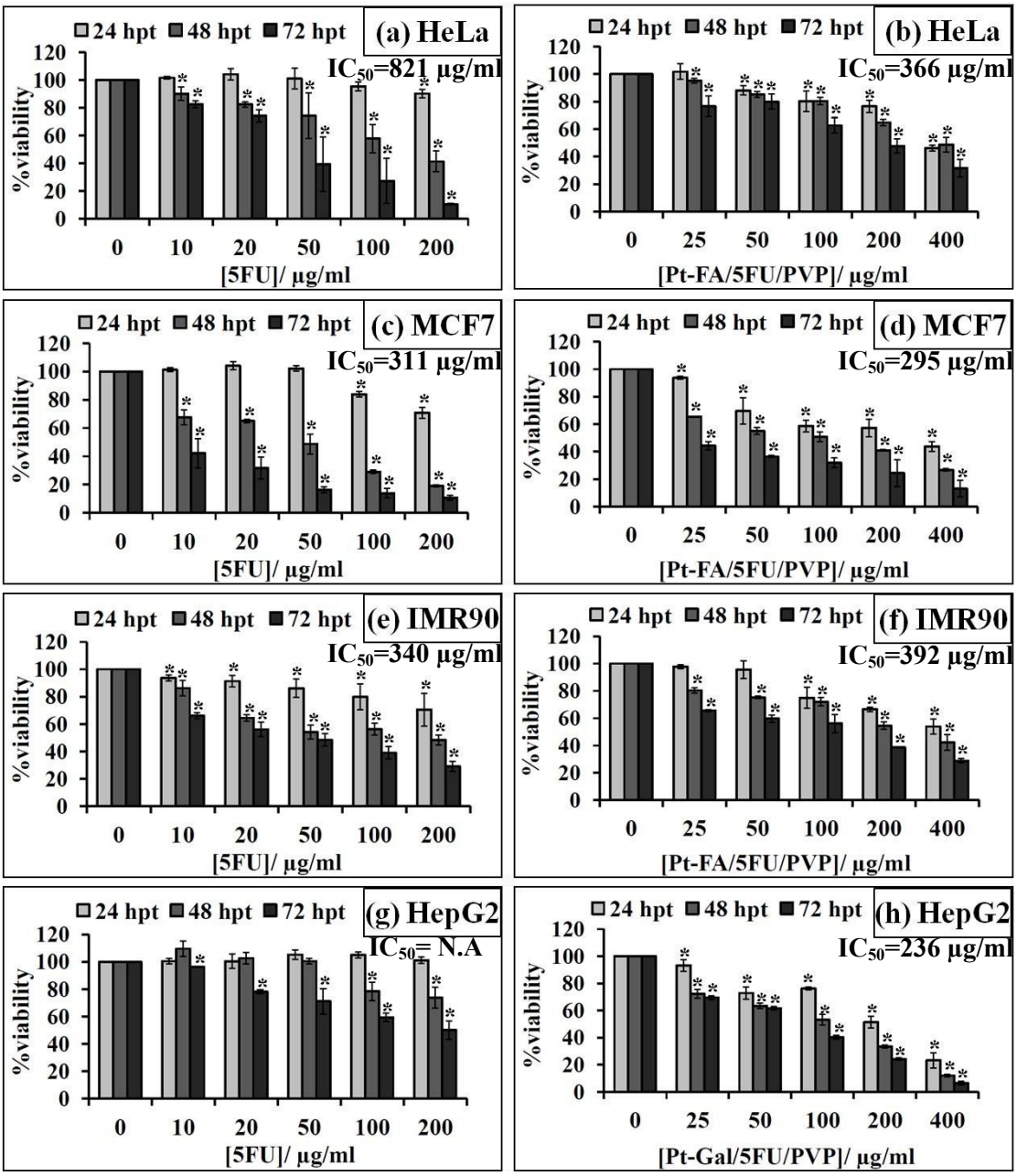

Figure 3.9: Cell viability assays of HeLa (a, b), MCF7 (c, d), IMR90 (e, f) and HepG2 (g, h) after exposure to various concentrations of 5FU, Pt-FA/5FU/PVP and Pt-Gal/5FU/PVP 24, 48 and 72 hpt. The y-axis represents the percentage of viable cells present in the treated sample after a certain time and the x-axis represents the final Pt-nps concentration in culture. The values represent the mean ± standard deviation of three independent experiments; * denotes $P < 0.05$ with respect to the control group using *Student's t test*.

The uptake of Pt-nps by cell lines and their resulting toxicities are summarized in **Table 3.10**. Using PVP or folic acid as the sole capping agent produced Pt-nps which were either non-toxic or too toxic. A combination of both capping agents,

together with a commercially available cancer drug 5FU produced Pt-FA/5FU/PVP which had similar toxicities as Pt-FA in cancer cell lines and low toxicity as Pt-PVP in IMR90. As a result of these positive properties, Pt-Gal/5FU/PVP was synthesized for *in vivo* testing in zebrafish with liver cancer.

<table>
<tr><td></td><td></td><td>Pt-PVP</td><td>Pt-FA</td><td>Pt-FA/5FU/PVP</td><td>Pt-Gal/5FU/PVP</td></tr>
<tr><td rowspan="2">HeLa</td><td>Uptake</td><td>High</td><td>High</td><td>High</td><td rowspan="6">Not applicable</td></tr>
<tr><td>Toxicity</td><td>Low</td><td>Medium</td><td>Low</td></tr>
<tr><td rowspan="2">MCF7</td><td>Uptake</td><td>Low</td><td>High</td><td>High</td></tr>
<tr><td>Toxicity</td><td>Low</td><td>High</td><td>Medium</td></tr>
<tr><td rowspan="2">IMR90</td><td>Uptake</td><td>Low</td><td>High</td><td>Low</td></tr>
<tr><td>Toxicity</td><td>Low</td><td>High</td><td>Low</td></tr>
<tr><td rowspan="2">HepG2</td><td>Uptake</td><td colspan="3" rowspan="2">Not applicable</td><td>High</td></tr>
<tr><td>Toxicity</td><td>Medium</td></tr>
<tr><td>Selectivity / targeting effects towards cancer cells</td><td></td><td>No</td><td>No</td><td>Yes</td><td>To be tested in zebrafish</td></tr>
</table>

Table 3.10: Summary of results for Pt-PVP, Pt-FA, Pt-FA/5FU/PVP, Pt-Gal/5FU/PVP and the cell lines used for *in vitro* testing. Pt-PVP had low cellular uptake and toxicity, while Pt-FA had high uptake and toxicity in both normal and cancer cell lines. A combination of capping agents: PVP, FA and 5FU, produced Pt-nps with high toxicity towards cancer cell lines and low toxicity towards IMR90. The targeting ligand was changed from folic acid to galactose to produce Pt-Gal/5FU/PVP for testing in zebrafish with liver cancer.

3.3 Conclusions

PVP and folic acid-capped Pt-nps have been synthesized to evaluate their bioactivities in commercial cell lines. The capping agents not only have an effect on the stability, shape and size distribution of NPs, but also in the uptake and toxicity of NPs by live cells. At 25 μg/ml, viability of HeLa, MCF7 and IMR90 dropped significantly to 65%, 44%, and 43%, respectively, after 24 h of incubation with Pt-FA. The observed viabilities were >90% in the cases for Pt-PVP. Darkfield optical microscope images also revealed increased accumulation of Pt-FA as compared to Pt-PVP, indicating the effectiveness of folic acid in receptor-mediated endocytosis. Pt-

nps treatment caused an increase in proportions of MCF7 cells undergoing apoptosis, especially in the case of Pt-FA. For IMR90 cells, Pt-PVP treatment caused cells to undergo apoptosis, while Pt-FA caused necrosis to take place. This suggests that different capping agents caused dissimilar cellular component targeting.

Because Pt-FA showed toxicity towards both cancer and normal cell lines, Pt-FA/5FU/PVP was synthesized as an attempt to improve the selectivity towards cancer cells and lowering damages towards normal cells. Pt-FA/5FU/PVP showed a concentration- and time-dependent relationship with both HeLa and MCF7 which was more predictable and comparable to the chemotherapeutic drug 5FU. HeLa and MCF7 were found to take up more Pt-FA/5FU/PVP from darkfield microscopy images and exhibited lower viabilities than IMR90. This subsequently translated into the development of Pt-Gal/5FU/PVP for *in vivo* testing in the zebrafish.

CHAPTER 4

EVALUATING THE EFFECTS OF PLATINUM NANOPARTICLES *IN VIVO* (*DANIO RERIO*)

Publication from this chapter:

Yiwei Teow, Boon Chuan Low, Zhiyuan Gong and Suresh Valiyaveettil, "Active targeting of liver cancer in zebrafish (*Danio rerio*) using platinum nanoparticles" (under preparation)

4.1 Introduction

As molecular drugs often face challenges from poor water solubility, stability, bioavailability and specific targeting, scientists turn to nanotechnology for answers. The solution to such issues comes in the form of drug delivery vehicles or even the drugs themselves packaged in the "nano" (10^{-9}) size range (i.e. nanomedicine) (Moghimi, Hunter et al. 2005). Successful examples which have made it to the market include Doxil (doxorubicin encapsulated in 100 nm liposomes), Abraxane (paclitaxel bound to 130 nm albumin NPs), Epaxal (liposomes functionalized with influenza virus surface proteins) and a few others which have been approved only in recent years (Zhang, Gu et al. 2008). Cancer remains one of the most devastating diseases with 10 million new cases every year (Peer, Karp et al. 2007). Despite billions of dollars had been spent on cancer research for many decades, a permanent cure for cancer is not yet achievable. Treatment methods include invasive surgical interventions, chemotherapy and radiotherapy which kill surrounding healthy tissues together with the tumour. In chemotherapy, a drug or a drug combination is introduced intravenously or orally, often accompanied by systemic adverse effects. Developing new concepts or strategies may lead to new treatments for cancer and reducing side effects by specific site targeting.

The enhanced permeability and retention effect (Matsumura and Maeda 1986) (EPR) is commonly used in passive targeting of cancers. As tumours have leaky blood vessels and poor lymphatic drainage, nanomaterials up to a threshold diameter of 400 nm can accumulate preferentially in the vicinity of the tumour; while normal blood vessels prevent these NMs from building up near healthy cells (Peer, Karp et al. 2007). A better and more specialized method to combat cancer cells is active targeting. This involves the identification of an over-expressed surface receptor present on the

surface of the cancer cells which is not found or expressed in very low levels by normal cells. Attaching a targeting moiety, often vitamins, antibodies, nucleic acids and carbohydrates on the surface of nanocarriers enhances uptake by cancer cells through specific ligand-receptor interactions (Byrne, Betancourt et al. 2008). We have discussed the use of folic acid (vitamin B_9), acting as both capping agent and targeting ligand on the surface of Pt-nps in Chapter 3 (Teow and Valiyaveettil 2011). The folate receptor is over-expressed in many types of tumours, including ovarian, breast, lung, renal and colon (Dhar, Liu et al. 2008). HeLa (human cervical cancer) and MCF7 (human breast cancer) cell lines were found to take up folic acid-capped Pt-nps to a much greater extent than Pt-nps capped with PVP, a biocompatible, water-soluble, synthetic polymer. A more detailed study is necessary to show that this active targeting property can also work *in vivo*. As such, Pt-nps functionalized with galactose (active targeting moiety), 5-fluorouracil and PVP (abbreviated as Pt-Gal/5FU/PVP hereafter) which exhibit both EPR and active targeting effects were synthesized for a comprehensive study in the zebrafish.

Hepatocellular carcinoma (HCC) is the fifth most common cause of cancer and it is occurring more often worldwide due to the dissemination of hepatitis B and C virus infection (Llovet, Burroughs et al. 2003). The tumour is generally treated by resection, liver transplantation or percutaneous treatment. With more than 500,000 new cases being diagnosed yearly and one of the top killers in some parts of Asia, HCC is a disease which entails more detailed research (Llovet, Burroughs et al. 2003).

Zebrafish (*Danio rerio*) is a powerful tool for high throughput screening of drugs and toxic chemicals (Hill, Teraoka et al. 2005; Asharani, Serina et al. 2008; Asharani, Wu et al. 2008; Nelson, Mahmoud et al. 2010). Zebrafish embryos and larvae being transparent and small, allow easy observations of the development

process using a large population that can be kept in a Petri dish or a 96-well plate. It is emerging as one of many promising animal models being used to study human cancers. This is because of high degree of similarities in terms of histopathological and molecular signatures during tumourigenesis as compared to human (Lam, Wu et al. 2006). Zebrafish can develop tumours spontaneously or in response to various chemical carcinogens. Transgenesis can be employed for zebrafish to express a mammalian oncogene. Exogenous DNA can be introduced by injection into one-cell stage embryos. An inducible system can be achieved through the use of an inducible promoter such as the Tet-on system. In the presence of the inducer (doxycycline), the reverse Tet-controlled transcriptional activator (rtTA) can bind to the Tet-response element (TRE) and transactivate the expression of a downstream transgene. An inducible Tet-on transgenic line (L-GKR: Liver specific GFP-Kras) has been created, which expresses oncogenic Kras specifically in the liver upon induction by doxycycline (Chew 2012). Upon induction, heterozygous transgenic fish are distinguished from wild-type as they can be screened by their enlarged liver and picking out GFP signals in the liver which wild-type zebrafish do not express. Aberrant Ras signalling has been implicated in the development and progression of human HCC and a high level of $kras^{v12}$ expression could initiate liver tumourigenesis (Nguyen, Emelyanov et al. 2011). The design strategy and *in vitro* efficacy of Pt-Gal/5FU/PVP was discussed previously in Chapter 3. In this chapter, the *in vivo* efficacies and mechanisms of action of Pt-Gal/5FU/PVP will be studied in the zebrafish liver cancer model which over-expressed $kras^{v12}$.

In addition to measuring liver size of zebrafish larvae, it is important to understand the mechanisms by which Pt-Gal/5FU/PVP exerts its active targeting effects due to the presence of galactose. This was achieved by performing

ultramicrotomy on Pt-np treated larvae and observation of liver cells under an electron microscope. Proliferating cell nuclear antigen (PCNA) staining of liver cells can give an indication of the number of proliferating cells before and after Pt-np treatment, providing a complementary analysis of the state of the liver. A more elaborate approach to monitor uptake by larvae is to attach a fluorescent tag on the surface of Pt-nps. As zebrafish larvae are transparent, the movement of fluorescent NPs can be observed. Although Pt-nps have a high surface area for attaching bioactive molecules, attaching a bulky fluorescent molecule in the presence of many other capping agents may be challenging. As such, we have eliminated 5-fluorouracil and PVP in the design strategy, while the presence of galactose is still required for active targeting of zebrafish liver. From this point on, platinum nanoparticles capped with galactose and the fluorescent tag will be referred to as Pt-Gal/Dye.

Here, we investigated the *in vivo* effects of Pt-nps in transgenic (Tet-on EGFP-kras^{v12} and LiPan (Korzh, Pan et al. 2008)) zebrafish larvae using the following experimental methods which were described in detail in Chapter 2 (Materials and Methods):

1. Treatment of zebrafish larvae using Pt-Gal/5FU/PVP and imaging of liver using fluorescence microscopy. Subsequently, analysis of fluorescence images using Adobe Photoshop was performed to calculate liver size (pages 40 – 41);
2. PCNA staining, ultramicrotomy and TEM images of liver (pages 41 – 42);
3. Tracking uptake of Pt-Gal/5FU/PVP by zebrafish larvae using Pt-Gal/Dye (page 34, 41);
4. Positive (cancer drug 5FU) and negative controls (Pt-nps without important capping agents: Pt-5FU/PVP, Pt-5FU/Gal, Pt-Gal/PVP and Pt-

PVP) were also set up to verify that Pt-Gal/5FU/PVP is the best combination of capping agents (pages 33 – 34, 41).

4.2 Results

Capping agents were carefully selected for their biological interactions in cell lines and in zebrafish. Galactose can be used for drug (Wang, Zhang et al. 2010; Zaman, Yang et al. 2010; Yang, Meng et al. 2011) and gene delivery (Zanta, Boussif et al. 1997; Pun and Davis 2002) as it targets asialoglycoprotein receptors on the surface of liver cells. This occurs *via* receptor-mediated endocytosis of NPs and subsequently released from the endosomes (Lai, Lin et al. 2010). PVP is a synthetic biocompatible polymer which enhances water solubility and used to modify other nanomaterials (Torchilin 2001; Torchilin 2007; Phillips, Gran et al. 2010; Parveen, Misra et al. 2012), while 5FU is an antimetabolite showing both *in vitro* (Borenfreund, Babich et al. 1990; Yamamoto, Nagano et al. 2004; Sung and Shuler 2009) and *in vivo* (Ando, Yamashita et al. 1997; Ando, Tanaka et al. 2002; Sakon, Nagano et al. 2002) effects against HCC. The presence of these capping agents can be confirmed by performing a Tollen's test (for reducing sugars) and determining the concentration of fluorine (5FU) in the final product.

4.2.1 Pt-Gal/5FU/PVP treatment and analysis of liver size

Tet-on EGFP-kras^{v12} zebrafish larvae express GFP in the liver which allows convenient measurement of liver size. 25 μg/ml and 50 μg/ml Pt-Gal/5FU/PVP were used as higher concentrations (75 μg/ml and 100 μg/ml) resulted in lethality and deformities such as bent notochord and tail malformations (**Figure 4.1**). Indeed, throughout the duration of our study, zebrafish larvae did not die or develop physical deformities after exposure to Pt-Gal/5FU/PVP (**Figure 4.2(a1-d1)**). LiPan gave an indication of the size of a "normal" liver which allows us to estimate the effectiveness of Pt-nps treatment (Korzh, Pan et al. 2008; Chew 2012).

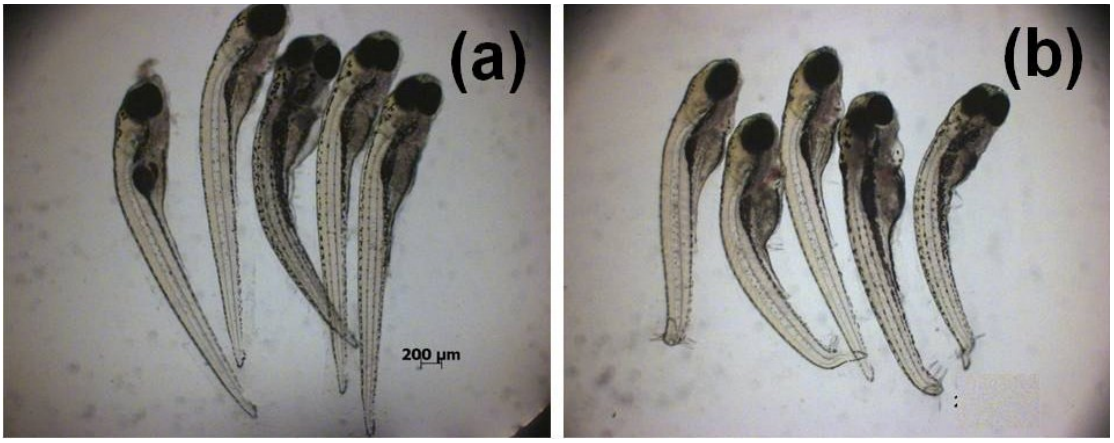

Figure 4.1: Brightfield images of Tet-on EGFP-kras^{v12} zebrafish larvae (6 dpf), larvae treated with 75 µg/ml Pt-Gal/5FU/PVP (a) and 100 µg/ml Pt-Gal/5FU/PVP (b).

Figure 4.2(a2-c2) showed a representation of the liver size of each treatment group. At 4 dpt, the average liver size of 50 larvae reduced by 8.4% and 16.0% for 25 µg/ml and 50 µg/ml Pt-Gal/5FU/PVP, respectively, as compared to control larvae (**Figure 4.2(e)**). The 50 µg/ml Pt-Gal/5FU/PVP treatment group showed a more drastic reduction in liver size and results were similar for both 2 and 4 dpt, indicating that Pt-nps concentration could be a more important factor in affecting liver size than treatment duration. However, with a longer duration (4 dpt), the average liver size of the 50 µg/ml Pt-Gal/5FU/PVP treatment group dropped lower than LiPan ("normal" liver size), which may lead to increased toxicity. A careful balance between concentration and duration must be obtained. LiPan larvae were also given 25 µg/ml and 50 µg/ml Pt-Gal/5FU/PVP in a control experiment. In this experiment, the average liver size of larvae in both treatment groups were not significantly different from untreated larvae, indicating the effects of Pt-Gal/5FU/PVP were more pronounced in rapidly proliferating liver cells, similar to the case of *in vitro* studies.

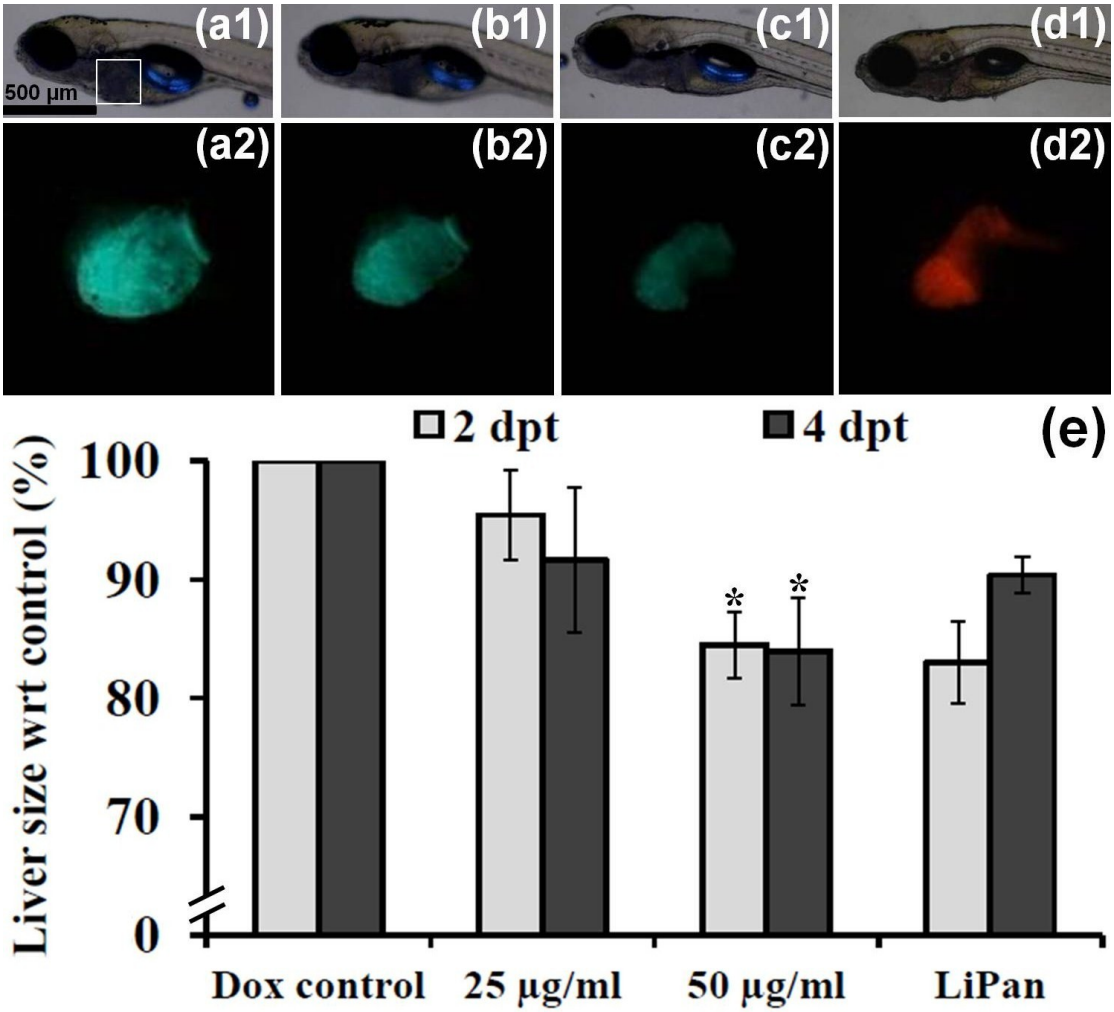

Figure 4.2: Brightfield images of Tet-on EGFP-kras^{v12} zebrafish larva (8 dpf), doxycycline control (a1), larva treated with 25 µg/ml Pt-Gal/5FU/PVP (b1) and 50 µg/ml Pt-Gal/5FU/PVP (c1), with no difference in physical appearance between each group. An image of LiPan zebrafish larva (8 dpf) was also included to give an indication of the size of a "normal" liver (d1). Respective GFP and RFP signals were imaged and enlarged, clearly indicating that liver size was reduced after exposure to increasing concentration of Pt-Gal/5FU/PVP (a2-d2). The average liver size of 50 larvae in each group was plotted (e), * indicates significant difference from control at $P < 0.05$ using *Student's t test*.

4.2.2 PCNA staining, ultramicrotomy and TEM images of liver

In order to understand how Pt-Gal/5FU/PVP can affect growth of zebrafish larvae's liver and its mechanisms, proliferating cell nuclear antigen (PCNA) staining and TEM analysis of the liver were performed. For PCNA staining, nuclei in cells that are in process of proliferating will stain brown, while cells in the resting stage (not proliferating) will not be stained. Liver cells in the doxycycline control group

displayed intense brown coloration in their nuclei as an indication of proliferation (**Figure 4.3(a)**). In contrast, liver cells of a zebrafish larva treated with 50 μg/ml Pt-Gal/5FU/PVP displayed faint coloration at 8 dpf, suggesting that Pt-Gal/5FU/PVP treatment had caused liver cells to be less active in proliferation.

To further demonstrate that a reduction in hepatocyte proliferation was due to Pt-Gal/5FU/PVP, ultramicrotomy was performed on the larvae to obtain ultra-thin transverse sections of the liver. From the TEM images, endosomes were observed to contain black particles which were later confirmed to be Pt-Gal/5FU/PVP *via* energy-dispersive X-ray spectroscopy (EDX, **Figure 4.3(e-f)**, black arrows). Black particles and EDX peaks belonging to Pt-Gal/5FU/PVP were not observed in the doxycycline treated control larva (Figure 4c-d). These evidences showed that Pt-Gal/5FU/PVP were indeed taken up by zebrafish larvae *via* active targeting and resulted in a reduction of the liver cell proliferation in our study samples.

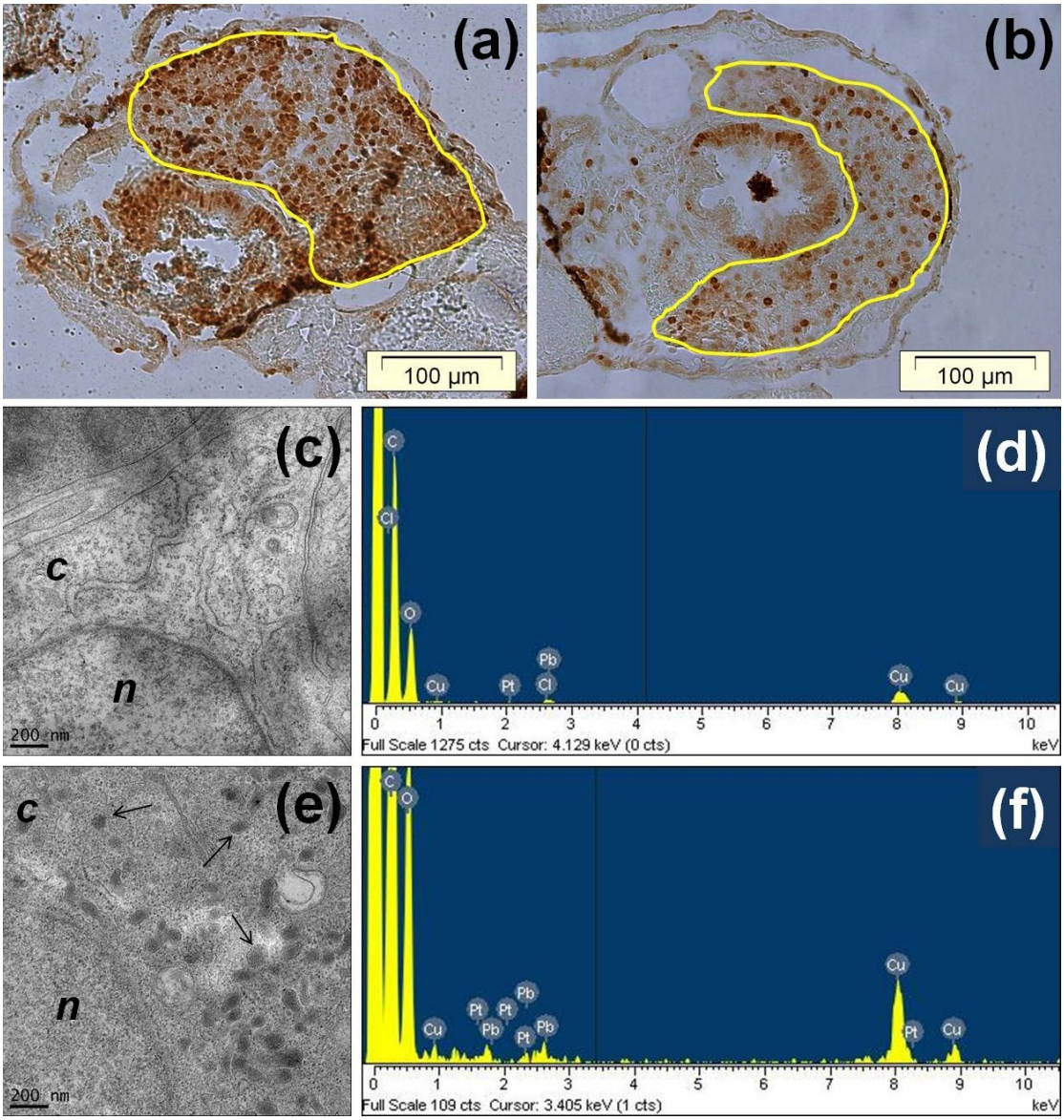

Figure 4.3: PCNA staining of Tet-on EGFP-kras^{v12} zebrafish larvae (8 dpf), doxycycline control (a) and larva treated with 50 µg/ml Pt-Gal/5FU/PVP (b), showing reduced cell proliferation in the liver of the Pt-nps-treated larva (20X magnification, liver outlined in yellow). TEM (15000X magnification) and EDX analysis of liver sections of doxycycline control (c-d) and larva treated with 50 µg/ml Pt-Gal/5FU/PVP (e-f), which indicated the presence of Pt-Gal/5FU/PVP in endosomes. Black arrows point to endosomes containing Pt-Gal/5FU/PVP, *n* represents nucleus and *c* represents cytoplasm.

4.2.3 Tracking uptake of Pt-Gal/5FU/PVP by zebrafish larvae using Pt-Gal/Dye

As TEM revealed the presence of Pt-Gal/5FU/PVP in the liver, it is interesting to study how Pt-nps were taken up by zebrafish larvae. To do this, a nanoparticle tagged with a fluorescent dye can be used to track the movement of Pt-nps in the

transparent larvae. The fluorescent nanoparticle must retain the active targeting effect of Pt-Gal/5FU/PVP, while being fluorescent. As such, Pt-nps using galactose and a fluorescent dye (Pt-Gal/Dye) were synthesized. The red fluorescent dye, Alexa Fluor 594 C_5 maleimide was chosen because it exhibits very little spectral overlap with GFP signals in the zebrafish liver and can be excited by the 568 nm line of the Ar-Kr laser and 594 nm line of the He-Ne laser. Spectrally similar to Texas Red dye, the Alexa Fluor 594 dye exhibits bright red fluorescence and have high photostability, enabling high contrast against GFP expression in the liver. The thiol-reactive maleimide group requires the use of cysteamine as a linker, as it has two functional groups with different reactivity. The thiol group (-SH) is required for reacting with the dye while the less reactive amine group (-NH_2) does not reactive with the dye but only attaches to Pt-nps. It is therefore unnecessary to use protecting groups to disguise the amine group when cysteamine is reacting with the dye.

The synthesis of Pt-Gal/Dye (**Figure 4.4(d)**) involves 3 steps: (a) synthesis of platinum nanoparticles capped with galactose (Pt-Gal); (b) synthesis of cysteamine-dye conjugate and (c) ligand exchange of cysteamine-dye conjugate with Pt-Gal. The synthesis of Pt-Gal/Dye follows a carefully planned strategy in order to avoid complications for subsequent steps downstream. For example, cysteamine should not be attached to Pt-nps before first forming a conjugate with the fluorescent dye. This is because the thiol group on cysteamine can also form bonds with Pt-nps in addition to amine group, which makes it impossible to react with the fluorescent dye next.

In the initial attempt to synthesize Pt-Gal (Step (a)), sodium borohydride was used as the reducing agent for hexachloroplatinic acid in the presence of galactose. However, resulting Pt-Gal NPs quickly agglomerated and was not suitable for subsequent synthesis steps. This is because sodium borohydride is a strong reducing

agent; while galactose with only hydroxyl groups is a weak capping agent. Therefore, a slower and weaker reduction method was used for synthesizing Pt-Gal (**Figure 4.4(a)**). This involved boiling hexachloroplatinic acid in the presence of galactose. In this case, galactose acts as both the reducing agent and the capping agent, forming a stable brown solution. For the synthesis of cysteamine-dye conjugate (Step (b)), care must be taken to prevent the reaction mixture from being exposed to light as the fluorescent dye is light-sensitive. The solution must be stirred under a nitrogen atmosphere to prevent thiol groups in cysteamine from oxidation into disulfides by molecular oxygen. In Step (c), Pt-Gal/Dye (**Figure 4.4(b-d)**) was synthesized by performing a ligand exchange between Pt-Gal and the cysteamine-dye conjugate. This can be carried out by 2 methods: stirring or ultrasonication. Using the stirring method, resulting Pt-Gal/Dye grew in size from 5 nm to around 100 nm. However, ultrasonication produced Pt-Gal/Dye which was highly aggregated (> 300 nm) and therefore unsuitable for biological studies. Hence, biological studies in the zebrafish larvae were carried out using Pt-Gal/Dye synthesized from the stirring method.

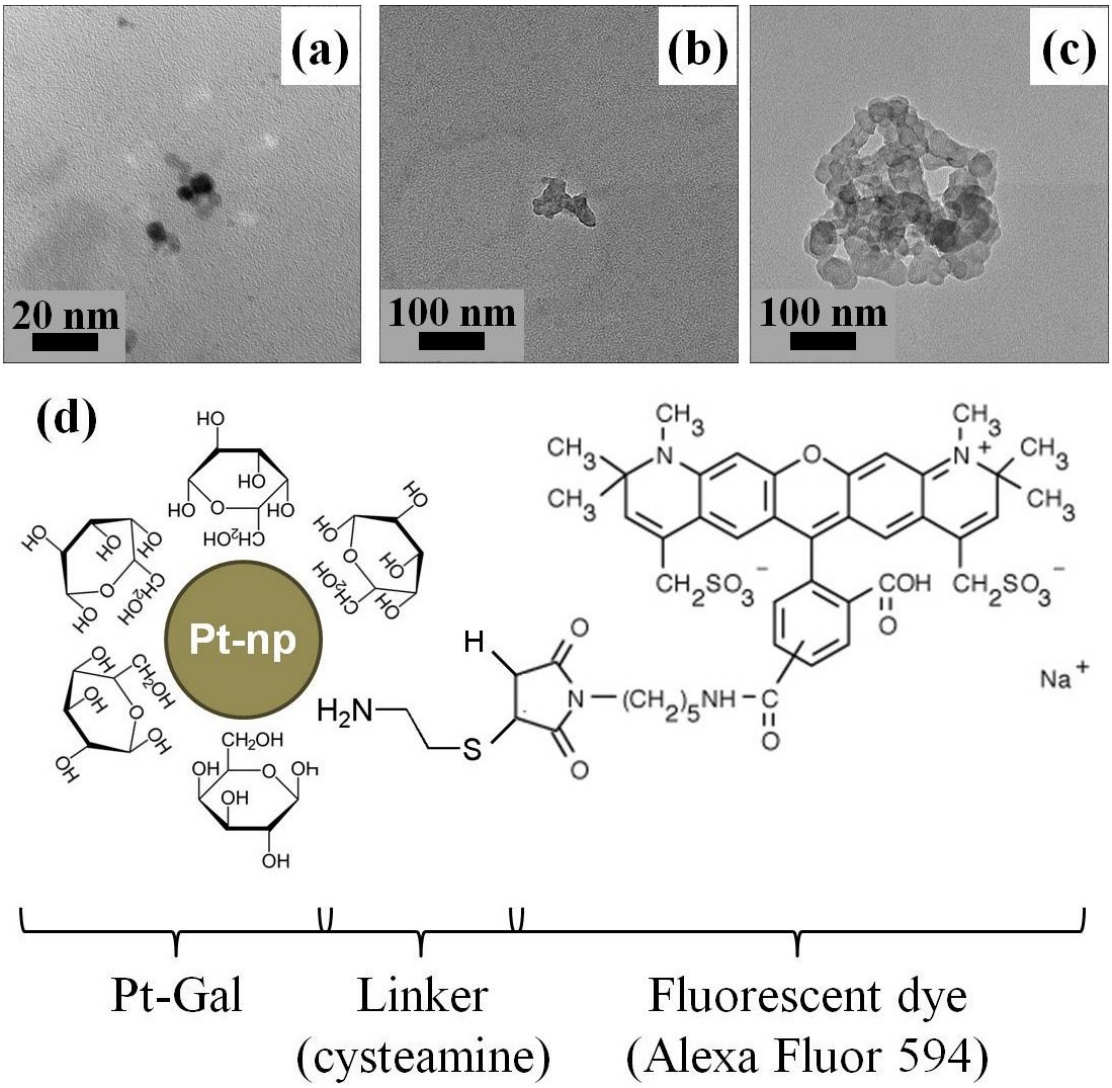

Figure 4.4: TEM image of Pt-Gal (a), Pt-Gal/Dye synthesized by stirring (b) and Pt-Gal/Dye synthesized by ultrasonication (c). Pt-Gal/Dye is made up of 4 components: Pt-np, galactose, cysteamine and the fluorescent dye (d).

To study the uptake of Pt-nps, zebrafish larvae were given Pt-Gal/Dye instead of Pt-Gal/5FU/PVP and fluorescence images were taken for the following 4 days of exposure. The liver (GFP channel) was outlined in yellow and copied onto both brightfield and RFP channels. At 1 dpt (**Figure 4.5(a3)**), little red fluorescence was observed in the pharynx, oesophagus and intestines, indicating that the larva ingested very little amounts of Pt-Gal/Dye. From 2 dpt onwards (**Figure 4.5(b3-d3)**), red fluorescence in the intestines was significantly more intense and increasing over time, indicating higher Pt-Gal/Dye uptake. The red fluorescence detected in the liver

increased over time as well, however, was very faint compared to the intestines. This shows that the Pt-nps detected in the liver by TEM was taken up by the larva from ingestion. Pt-nps accumulated in the intestines and faint fluorescence was observed in the liver from 3 dpt onwards. This could be the reason why liver size was not significantly reduced at 2 dpt (**Figure 4.2**).

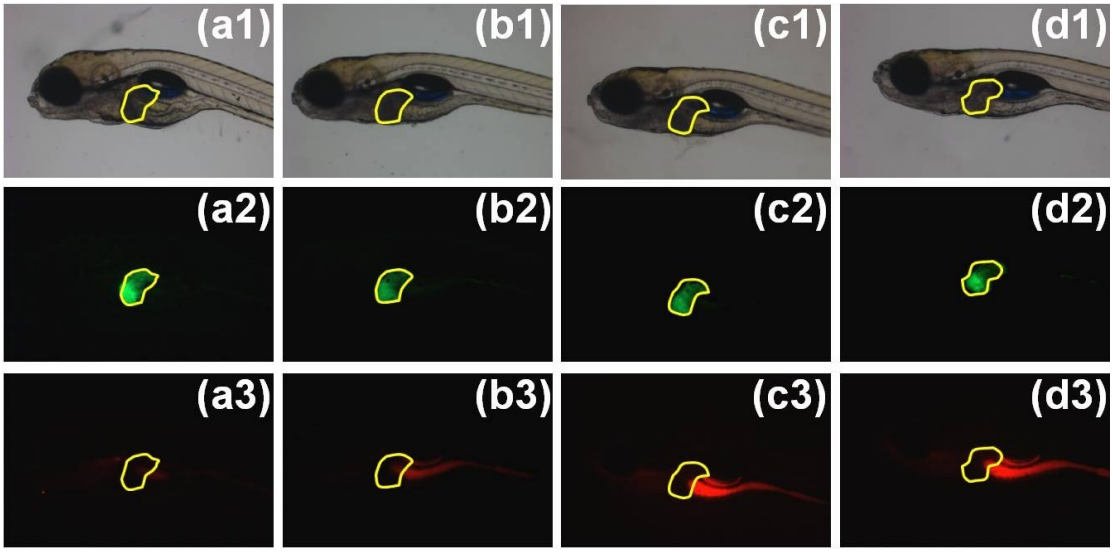

Figure 4.5: Fluorescence images of Tet-on EGFP-kras^{v12} zebrafish larvae (4 dpf) treated with Pt-Gal/Dye: 1 dpt (a), 2 dpt (b) 3 dpt (c) and 4 dpt (d). The liver's location (GFP) was outlined in yellow and copied onto the brightfield and RFP images.

4.2.4 Positive and negative controls

As 3 different capping agents were used in the synthesis of Pt-nps, additional experiments were performed to study how each capping agent could affect the overall efficacy of Pt-nps in the zebrafish liver. Four additional Pt-nps were synthesized, each lacking one of three capping agents: Pt-5FU/PVP (with capping agents 5FU and PVP), Pt-5FU/Gal (with capping agents 5FU and D-galactose), Pt-Gal/PVP (with capping agents D-galactose and PVP) and Pt-PVP (with capping agent PVP). The chemotherapeutic drug 5FU was also tested. Overall, these Pt-nps lacking essential capping agents as well as 5FU were found to be ineffective toward reducing liver

proliferation at the same concentrations and treatment duration (**Figure 4.6**). Average liver sizes from these treatment groups were between 92.7% and 104% as compared to control larvae.

5FU is used as a chemotherapeutic drug since 1957 for a wide range of solid tumours (Malet-Martino and Martino 2002). However, it is often used together with other drugs as its clinical effect is only 10 – 30%. This is because more than 80% of the injected dose is rapidly degraded by cytosolic enzymes (Malet-Martino and Martino 2002). As the intestines have high concentrations of enzymes for degradation of 5FU, it is also not common for 5FU to be administered *via* the oral route during chemotherapy (Malet-Martino and Martino 2002). These could be the reasons for the lack of activity of 5FU even though a high concentration (50 μg/ml) was administered to the larvae *via* embryo water (**Figure 4.6**). Of the Pt-nps (Pt2-Pt5) tested, only the larvae treated with Pt2 showed a slight decrease in liver size. This can be attributed to the EPR effect and without the presence of galactose for active targeting, the results were not statistically-significant. Although Pt3 (with capping agents 5FU and galactose) can be expected to show anti-proliferative effects in the liver, the absence of PVP had resulted in poor stability of the NPs, which resulted in agglomeration during the experiment. Although Pt4 was stable, it lacked the anticancer agent 5FU and did not result in a reduction of liver size. Moreover, Pt5 (Pt-PVP) did not show significant reduction in liver size. This indicates that platinum nanoparticles acted mainly as a delivery vehicle for 5FU, while PVP imparts solubility and stability. The presence of galactose was also required to improve upon the EPR effect by active targeting of the liver.

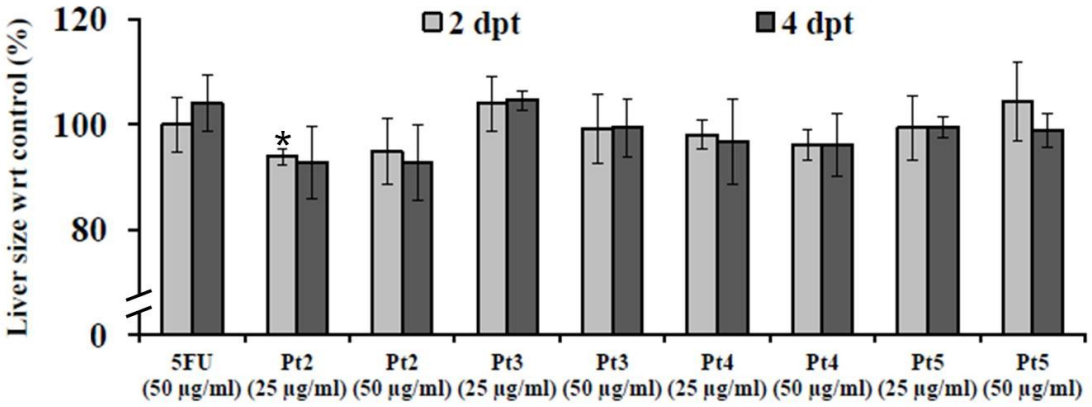

Figure 4.6: The average liver size of 50 Tet-on EGFP-kras^{v12} zebrafish larvae in each treatment group was plotted: 5FU, Pt2 (Pt-5FU/PVP), Pt3 (Pt-5FU/Gal), Pt4 (Pt-Gal/PVP) and Pt5 (Pt-PVP). * indicates significant difference from control at $P < 0.05$ using *Student's t test*.

Platinum is commonly employed in nanomedicine in its ionic form (Dhar, Gu et al. 2008; Rieter, Pott et al. 2008; Dhar, Daniel et al. 2009). The toxicity of platinum ions and their potential as fluorescence imaging agents were previously reported in zebrafish (Osterauer, Haus et al. 2009; Osterauer, Fassbender et al. 2011; Wu, Zhu et al. 2011). Our group has also reported the toxic effects of poly(vinyl alcohol)-capped Pt-nps in zebrafish embryos (Asharani, Yi et al. 2011). This study is the first report of functionalized Pt-nps as drug delivery vehicles in zebrafish larvae. Active targeting reduced the need for high concentrations of drugs to be used, saving costs, reducing side effects and enhances patient compliance. Carefully designed Pt-nps were successful in targeting liver of zebrafish larvae, showing potential applications in the treatment of human HCC.

4.2.5 Reproducibility and image analysis using ImageJ

To verify the efficacy of Pt-Gal/5FU/PVP and its experimental reproducibility in zebrafish larvae, the experiment was again performed with the help of other group members. Dr. Brahathees synthesized and purified a new batch of Pt-Gal/5FU/PVP

and performed the *in vivo* experiment with the guidance of Mr. Yan Chuan (Prof. Gong group). At 4 dpt, Dr. Brahathees captured the fluorescence images of transgenic zebrafish larvae and passed them to Mr. Yan Chuan for image analysis using ImageJ. ImageJ is a public domain software developed by the National Institute of Health and is often used for image processing. The data (**Figure 4.7**) collected by Dr. Brahathees and Mr. Yan Chuan showed significant complementarity to our previous data in terms of reproducibility.

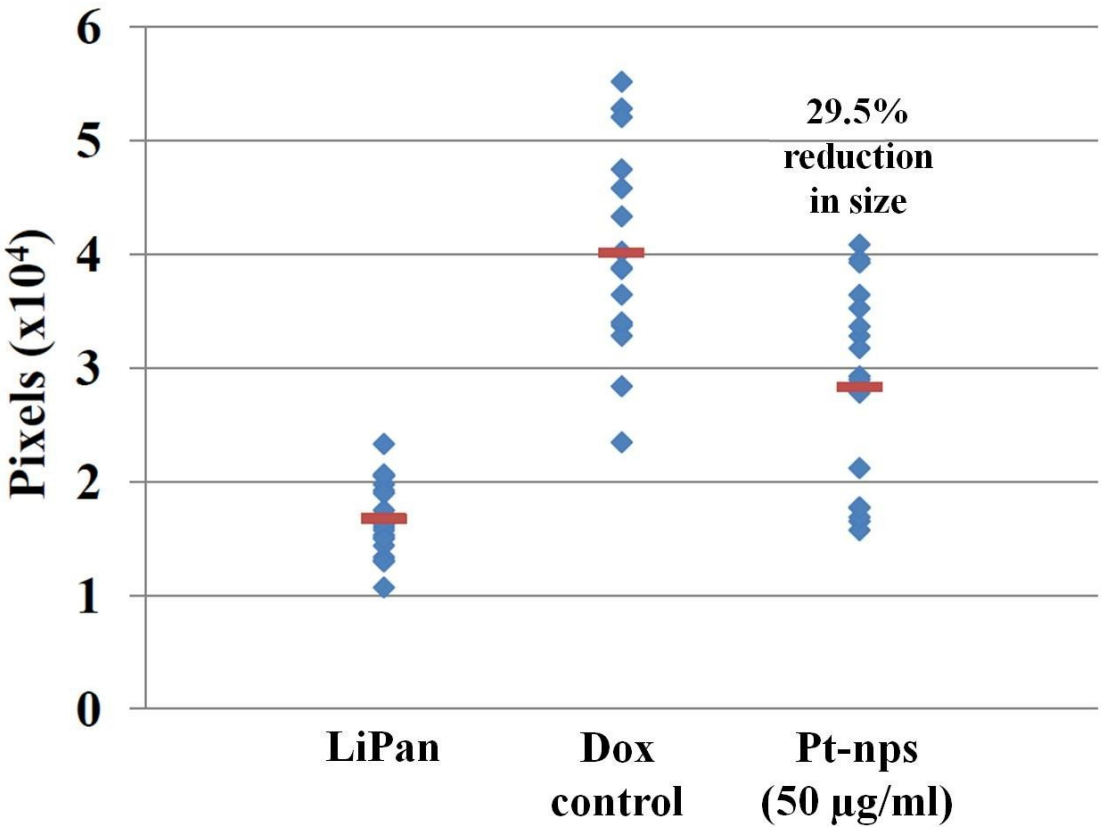

Figure 4.7: The average liver size of 20 zebrafish larvae in each treatment group was plotted: LiPan (representing "normal" liver), Dox control (representing Tet-on EGFP-kras^{v12} zebrafish larvae with liver cancer) and Pt-nps (50 µg/ml) (representing Tet-on EGFP-kras^{v12} zebrafish larvae treated with 50 µg/ml Pt-Gal/5FU/PVP). The y-axis represents the size of zebrafish larvae in pixels (ImageJ) and the x-axis represents the different treatment groups.

Similar to our previous experiments (**Figure 4.2(e)**), LiPan zebrafish larvae act as a reference to indicate whether liver size of Tet-on EGFP-kras^{v12} zebrafish larvae has reduced to the "normal" size after drug treatment. Mr. Yan Chuan has

generated a dot plot to indicate the spread of liver sizes in each treatment group. From his analysis (**Figure 4.7**), LiPan larvae displayed the lowest average liver size, while Tet-on EGFP-kras^{v12} zebrafish larvae showed the highest. After 4 days of exposure to Pt-Gal/5FU/PVP (50 μg/ml), five Tet-on EGFP-kras^{v12} zebrafish larvae showed the same average liver size as LiPan larvae and the average liver size was significantly reduced (*Student's t test*) by 29.5% when compared against untreated larvae. However, the average liver size of Pt-Gal/5FU/PVP treated Tet-on EGFP-kras^{v12} zebrafish larvae was still slightly larger than the average liver size of LiPan larvae. This is different from our previous report (**Figure 4.2(e)**) that the average liver size of Pt-Gal/5FU/PVP treated Tet-on EGFP-kras^{v12} zebrafish larvae was similar or lower than the average liver size of LiPan larvae after 4 days of exposure. This could be due to (i) different batches of adult zebrafish used for spawning and (ii) different people performing the image analysis. Overall, it was demonstrated that Pt-Gal/5FU/PVP treatment can significantly reduce liver size of zebrafish larvae (reproducible).

4.3 Conclusions

Pt-nps functionalized with galactose, 5FU and PVP were synthesized *via* a simple *in situ* reduction method. Resulting Pt-Gal/5FU/PVP nanoparticles were stable, water-soluble and were characterized. HepG2, a hepatocellular carcinoma cell line was found to take up Pt-Gal/5FU/PVP effectively and showed a concentration- and time-dependent toxicity in Chapter 3. Cell viability was reduced by increasing concentrations of Pt-Gal/5FU/PVP or incubation time and was found to be significantly reduced by as little as 25 μg/ml Pt-Gal/5FU/PVP after 24 h of incubation.

In this chapter, Tet-on EGFP-kras^{v12} zebrafish larvae were used as an animal model to further investigate the activity of Pt-Gal/5FU/PVP. This transgenic zebrafish

line was used because its liver can be induced to proliferate and express GFP in the presence of doxycycline. The effect of Pt-Gal/5FU/PVP on liver size was studied by monitoring the GFP expression in the liver. Similar to *in vitro* studies in HepG2, liver size was found to reduce with increasing concentrations of Pt-Gal/5FU/PVP or longer incubation period. However, Pt-Gal/5FU/PVP concentration was a more important factor in influencing liver size than treatment duration. At 4 dpt, the average liver size of 50 larvae was reduced by 8.4% and 16.0% for 25 µg/ml and 50 µg/ml Pt-Gal/5FU/PVP, respectively, as compared to control larvae. This was due to active targeting of liver by Pt-Gal/5FU/PVP and their subsequent uptake into the endosomes of hepatocytes, which reduced cell proliferation. Fluorescent Pt-Gal/Dye nanoparticles were used to follow uptake in larvae. Pt-Gal/Dye accumulate in the intestines over time and faint fluorescence was detected 3 dpt, accounting for the weak activity of Pt-Gal/5FU/PVP at 2 dpt. LiPan zebrafish larvae and other Pt-nps which lacked essential capping agents acted as negative controls. The controls highlighted the importance of all 3 capping agents (galactose, 5FU and PVP) in order for Pt-nps to be effective. We emphasized on reproducibility of experiment data especially in animal models. The efficacy of newly-synthesized 50 µg/ml Pt-Gal/5FU/PVP was studied in Tet-on EGFP-kras^{v12} zebrafish larvae by other colleagues following the same procedures. Newly-synthesized Pt-Gal/5FU/PVP was found to cause significant reduction in liver size of Tet-on EGFP-kras^{v12} zebrafish larvae by 29.5% after 4 days of exposure. The image analysis was performed using ImageJ, complementing our previous data. Overall, functionalized Pt-nps were an effective active targeting agent for liver cancer in zebrafish and showed promise for exploring potential nanomedicine for human HCC.

CHAPTER 5

CONCLUSIONS

5.1 Conclusions

This study made use of both *in vitro* and *in vivo* techniques to explore the use of Pt-nps as drug delivery vehicles and to be further developed as a nanomedicine. Nanomedicine provides solutions to the flaws of conventional drugs, which includes solubility, stability and targeting. Using biocompatible and water-soluble polymers like PVP in the construct solved major issues, but the resulting Pt-PVP nanoparticles were biocompatible and not an ideal nanomedicine. A careful analysis of *in vitro* and *in vivo* models reveals that additional capping agents like folic acid/galactose and 5-fluorouracil which impart active targeting and anticancer effects may be essential to synthesize better Pt-nps.

After an extensive characterization to study the size, charge, shape and elemental composition, Pt-PVP, Pt-FA, Pt-FA/5FU/PVP and Pt-Gal/5FU/PVP were tested in cell lines. Darkfield microscopy images showed that cancer cell lines were taking up both Pt-PVP and Pt-FA but significantly more in the case of Pt-FA. The normal cell line IMR90 also endocytosed Pt-FA, which resulted in toxicity and poor viability. The apoptosis assay also revealed the difference in mechanism of cell death between cancer and normal cell lines. IMR90 cells were sensitive to the effects of Pt-nps and could undergo apoptosis after exposure to Pt-PVP and necrosis in the case of Pt-FA. MCF7 cells, however, were less sensitive to the effects of Pt-FA at the same concentration and could undergo both apoptotic and necrotic pathways.

As the targeting property of Pt-FA was poor and the sensitivity of normal cell lines to Pt-nps toxicity was high, better Pt-nps must be developed. Indeed, combining capping agents to form Pt-FA/5FU/PVP has shown that it retained the same anticancer effects as Pt-FA in cancer cell lines. Most importantly, IMR90 cells endocytosed lesser particles and had higher viability than in the case of Pt-FA.

Changing the targeting ligand from folic acid to galactose allows Pt-Gal/5FU/PVP to target HepG2 HCC cells. It is important to prove that Pt-Gal/5FU/PVP is effective in HCC cell line before carrying out tests in the animal model with liver cancer. HepG2 cells showed high uptake towards Pt-Gal/5FU/PVP, lowering cell viability to a greater extent than when exposed to the cancer drug 5FU.

Tet-on EGFP-kras^{v12} (liver cancer model) and LiPan (normal liver size) zebrafish larvae were exposed to 5FU, Pt-Gal/5FU/PVP and Pt-nps which lacked important capping agents to study the effects of these chemicals on liver size. Concentrations ($\leq$ 50 μg/ml) were carefully chosen such that the chemicals were non-toxic towards developing larvae. The livers of LiPan zebrafish larvae were not growing as rapidly as Tet-on EGFP-kras^{v12} zebrafish larvae and were therefore less susceptible to the effects of Pt-Gal/5FU/PVP. Concentration (25 μg/ml *vs.* 50 μg/ml) of Pt-Gal/5FU/PVP had greater effect towards reducing liver proliferation than treatment duration (2 days *vs.* 4 days).

Pt-Gal/Dye demonstrated the increasing accumulation of Pt-nps (red fluorescence) in the intestines and liver over 4 days of exposure, which explained the greater reduction in liver size with longer durations of treatment. Pt-Gal/5FU/PVP was detected in the liver of Tet-on EGFP-kras^{v12} zebrafish larvae using TEM analysis, which resulted in the reduction of rate of hepatocytes proliferation, detected using PCNA staining. The anticancer drug 5FU and other Pt-nps lacking essential capping agents were less effective than Pt-Gal/5FU/PVP in reducing hepatocytes proliferation. Overall, Pt-Gal/5FU/PVP is an effective and non-toxic drug for treating HCC in zebrafish and may be developed into a potential nanomedicine for human HCC in future.

5.2 Future works

The main focus of our study is to develop nanoparticles for nanomedicine that can solve issues posed by conventional drugs in the treatment of cancer. The chemicals which were employed may be modified or replaced to further improve efficacy:

1. Platinum was selected because of its reported ability to bind to DNA. The anticancer drugs Cisplatin and its analogues and Pt-nps synthesized by other research groups made use of the same mechanism. Other heavy metals which possess similar properties can also be screened;
2. Folic acid and galactose are two of many possible active targeting agents. Other ligands which may possess specific actions include antibodies, aptamers and short peptides which recognize specific receptors over-expressed or expressed only on tumour cells;
3. PVP confers stability to Pt-nps in aqueous media and can prolong circulation time in the blood. Other polymers which serve the same function can also be used, including PEG, poly(cyanoacrylate), poly(D/L-lactide), poly(lactic acid) and poly(lactide-*co*-glycolide). Biopolymers from natural sources, such as gelatin and sodium alginate, may provide better biocompatibility and easier metabolism for excretion;
4. 5-Fluorouracil serves as a model anticancer drug for our studies, where efficacies of Pt-nps were compared against this drug. Anticancer drugs may be used for specific cancers and they may be synthesized in the form of nanomedicine to be tested in a suitable cancer model. Alternative drugs may include doxorubicin, paclitaxel, methotrexate, etc.;

There are an infinite number of nanoformulations which can be synthesized by altering the concentrations of these molecules. Various ratios of capping agents should be systematically studied to optimise the therapeutic effect of Pt-nps.

Tet-on EGFP-kras^{v12} zebrafish larvae can be studied more extensively to understand the mechanisms of Pt-nps. Firstly, since zebrafish larvae overexpress Kras protein, changes to the amount of protein after exposure to Pt-nps can be quantified. Secondly, an apoptosis assay can be performed to determine if Pt-nps result in apoptosis of liver cells and other tissues in the larvae. This data could complement the TEM and PCNA staining results collected previously.

REFERENCES

Ahmadi, T. S., Z. L. Wang, et al. (1996). "Shape-controlled synthesis of colloidal platinum nanoparticles." Science **272**(5270): 1924-1926.

Allen, T. M. and P. R. Cullis (2004). "Drug delivery systems: Entering the mainstream." Science **303**(5665): 1818-1822.

Ando, E., M. Tanaka, et al. (2002). "Hepatic arterial infusion chemotherapy for advanced hepatocellular carcinoma with portal vein tumor thrombosis - Analysis of 48 cases." Cancer **95**(3): 588-595.

Ando, E., F. Yamashita, et al. (1997). "A novel chemotherapy for advanced hepatocellular carcinoma with tumor thrombosis of the main trunk of the portal vein." Cancer **79**(10): 1890-1896.

Arvizo, R. R., S. Bhattacharyya, et al. (2012). "Intrinsic therapeutic applications of noble metal nanoparticles: Past, present and future." Chemical Society Reviews **41**(7): 2943-2970.

Asharani, P. V. (2009). Investigations on the toxicity of nanoparticles. Department of Chemistry. Singapore, National University of Singapore. **Doctor of Philosophy**.

Asharani, P. V., N. G. B. Serina, et al. (2008). "Impact of multi-walled carbon nanotubes on aquatic species." Journal of Nanoscience and Nanotechnology **8**(7): 3603-3609.

Asharani, P. V., S. Sethu, et al. (2010). "Investigations on the structural damage in human erythrocytes exposed to silver, gold, and platinum nanoparticles." Advanced Functional Materials **20**(8): 1233-1242.

Asharani, P. V., Y. L. Wu, et al. (2008). "Toxicity of silver nanoparticles in zebrafish models." Nanotechnology **19**(25): 255102.

Asharani, P. V., N. Xinyi, et al. (2010). "DNA damage and p53-mediated growth arrest in human cells treated with platinum nanoparticles." Nanomedicine **5**(1): 51-64.

Asharani, P. V., L. W. Yi, et al. (2011). "Comparison of the toxicity of silver, gold and platinum nanoparticles in developing zebrafish embryos." Nanotoxicology **5**(1): 43-54.

Barth, B. M., R. Sharma, et al. (2010). "Bioconjugation of calcium phosphosilicate composite nanoparticles for selective targeting of human breast and pancreatic cancers in vivo." ACS Nano **4**(3): 1279-1287.

Berry, J. P., B. Arnoux, et al. (1977). "Microanalytic study of particles transport across alveoli - Role of blood-platelets." Biomedicine Express **27**(9-10): 354-357.

Bhattacharya, R., C. R. Patra, et al. (2007). "Attaching folic acid on gold nanoparticles using noncovalent interaction via different polyethylene glycol backbones and targeting of cancer cells." Nanomedicine-Nanotechnology Biology and Medicine **3**(3): 224-238.

Boisselier, E. and D. Astruc (2009). "Gold nanoparticles in nanomedicine: Preparations, imaging, diagnostics, therapies and toxicity." Chemical Society Reviews **38**(6): 1759-1782.

Borenfreund, E., H. Babich, et al. (1990). "Rapid chemosensitivity assay with human normal and tumor-cells *invitro*." In Vitro Cellular & Developmental Biology **26**(11): 1030-1034.

Brannon-Peppas, L. and J. O. Blanchette (2004). "Nanoparticle and targeted systems for cancer therapy." Advanced Drug Delivery Reviews **56**(11): 1649-1659.

Brigger, I., C. Dubernet, et al. (2002). "Nanoparticles in cancer therapy and diagnosis." Advanced Drug Delivery Reviews **54**(5): 631-651.

Burns, A. A., J. Vider, et al. (2009). "Fluorescent silica nanoparticles with efficient urinary excretion for nanomedicine." Nano Letters **9**(1): 442-448.

Byrappa, K. and T. Adschiri (2007). "Hydrothermal technology for nanotechnology." Progress in Crystal Growth and Characterization of Materials **53**(2): 117-166.

Byrne, J. D., T. Betancourt, et al. (2008). "Active targeting schemes for nanoparticle systems in cancer therapeutics." Advanced Drug Delivery Reviews **60**(15): 1615-1626.

Carlotti, M. E., E. Ugazio, et al. (2009). "Role of particle coating in controlling skin damage photoinduced by titania nanoparticles." Free Radical Research **43**(3): 312-322.

Carlson, C., S. M. Hussain, et al. (2008). "Unique cellular interaction of silver nanoparticles: Size-dependent generation of reactive oxygen species." Journal of Physical Chemistry B **112**(43): 13608-13619.

Castino, R., M. Demoz, et al. (2003). "Destination 'lysosome': A target organelle for tumour cell killing?" Journal of Molecular Recognition **16**(5): 337-348.

Champion, J. A., A. Walker, et al. (2008). "Role of particle size in phagocytosis of polymeric microspheres." Pharmaceutical Research **25**(8): 1815-1821.

Chen, A. and P. Holt-Hindle (2010). "Platinum-based nanostructured materials: Synthesis, properties, and applications." Chemical Reviews **110**(6): 3767–3804.

Chen, M., J. Falkner, et al. (2005). "Synthesis and self-organization of soluble monodisperse palladium nanoclusters." Journal of Colloid and Interface Science **287**(1): 146-151.

Chen, Z. (2010). "Small-molecule delivery by nanoparticles for anticancer therapy." Trends in Molecular Medicine **16**(12): 594-602.

Chen, Z., H. A. Meng, et al. (2006). "Acute toxicological effects of copper nanoparticles in vivo." Toxicology Letters **163**(2): 109-120.

Cheng, K., S. Peng, et al. (2009). "Porous hollow Fe_3O_4 nanoparticles for targeted delivery and controlled release of Cisplatin." Journal of the American Chemical Society **131**(30): 10637-10644.

Chew, T. (2012). Ras and Rho coregulate liver development and HCC in zebrafish. Department of Biological Sciences. Singapore, National University of Singapore. **Doctor of Philosophy**.

Chipuk, J. E. and D. R. Green (2005). "Do inducers of apoptosis trigger caspase-independent cell death?" Nature Reviews Molecular Cell Biology **6**(3): 268-275.

Chithrani, B. D. and W. C. W. Chan (2007). "Elucidating the mechanism of cellular uptake and removal of protein-coated gold nanoparticles of different sizes and shapes." Nano Letters **7**(6): 1542-1550.

Chithrani, B. D., A. A. Ghazani, et al. (2006). "Determining the size and shape dependence of gold nanoparticle uptake into mammalian cells." Nano Letters **6**(4): 662-668.

Cho, M. J., W. S. Cho, et al. (2009). "The impact of size on tissue distribution and elimination by single intravenous injection of silica nanoparticles." Toxicology Letters **189**(3): 177-183.

Choi, C. H. J., C. A. Alabi, et al. (2010). "Mechanism of active targeting in solid tumors with transferrin-containing gold nanoparticles." Proceedings of the

National Academy of Sciences of the United States of America **107**(3): 1235-1240.

Choi, H. S., W. Liu, et al. (2007). "Renal clearance of quantum dots." Nature Biotechnology **25**(10): 1165-1170.

Daniel, M. C. and D. Astruc (2004). "Gold nanoparticles: Assembly, supramolecular chemistry, quantum-size-related properties, and applications toward biology, catalysis, and nanotechnology." Chemical Reviews **104**(1): 293-346.

Das, S. K., A. R. Das, et al. (2010). "Microbial synthesis of multishaped gold nanostructures." Small **6**(9): 1012-1021.

Dhar, S., W. L. Daniel, et al. (2009). "Polyvalent oligonucleotide gold nanoparticle conjugates as delivery vehicles for platinum(IV) warheads." Journal of the American Chemical Society **131**(41): 14652-+.

Dhar, S., F. X. Gu, et al. (2008). "Targeted delivery of cisplatin to prostate cancer cells by aptamer functionalized Pt(IV) prodrug-PLGA-PEG nanoparticles." Proceedings of the National Academy of Sciences of the United States of America **105**(45): 17356-17361.

Dhar, S., Z. Liu, et al. (2008). "Targeted single-wall carbon nanotube-mediated Pt(IV) prodrug delivery using folate as a homing device." Journal of the American Chemical Society **130**(34): 11467-11476.

Doak, S. H., S. M. Griffiths, et al. (2009). "Confounding experimental considerations in nanogenotoxicology." Mutagenesis **24**(4): 285-293.

Dutta, N. and D. Green (2008). "Nanoparticle stability in semidilute and concentrated polymer solutions." Langmuir **24**(10): 5260-5269.

Edwards-Jones, V. (2009). "The benefits of silver in hygiene, personal care and healthcare." Letters in Applied Microbiology **49**(2): 147-152.

Eklund, S. E. and D. E. Cliffel (2004). "Synthesis and catalytic properties of soluble platinum nanoparticles protected by a thiol monolayer." Langmuir **20**(14): 6012-6018.

Elder, A., H. Yang, et al. (2007). "Testing nanomaterials of unknown toxicity: An example based on platinum nanoparticles of different shapes." Advanced Materials **19**(20): 3124-3129.

Filon, F. L., G. Maina, et al. (2004). "In vitro percutaneous absorption of cobalt." International Archives of Occupational and Environmental Health **77**(2): 85-89.

Furuyama, A., S. Kanno, et al. (2009). "Extrapulmonary translocation of intratracheally instilled fine and ultrafine particles via direct and alveolar macrophage-associated routes." Archives of Toxicology **83**(5): 429-437.

Gajbhiye, M., J. Kesharwani, et al. (2009). "Fungus-mediated synthesis of silver nanoparticles and their activity against pathogenic fungi in combination with fluconazole." Nanomedicine-Nanotechnology Biology and Medicine **5**(4): 382-386.

Gao, J. H., G. L. Liang, et al. (2008). "Multifunctional yolk-shell nanoparticles: A potential MRI contrast and anticancer agent." Journal of the American Chemical Society **130**(35): 11828-11833.

Gao, J. H., G. L. Liang, et al. (2007). "FePt@CoS_2 yolk-shell nanocrystals as a potent agent to kill HeLa cells." Journal of the American Chemical Society **129**(5): 1428-1433.

Gaur, U., S. K. Sahoo, et al. (2000). "Biodistribution of fluoresceinated dextran using novel nanoparticles evading reticuloendothelial system." International Journal of Pharmaceutics **202**(1-2): 1-10.

Gehrke, H., J. Pelka, et al. (2011). "Platinum nanoparticles and their cellular uptake and DNA platination at non-cytotoxic concentrations." Archives of Toxicology **85**(7): 799-812.

Gelderblom, H., J. Verweij, et al. (2001). "Cremophor EL: The drawbacks and advantages of vehicle selection for drug formulation." European Journal of Cancer **37**(13): 1590-1598.

Gullotti, E. and Y. Yeo (2009). "Extracellularly activated nanocarriers: A new paradigm of tumor targeted drug delivery." Molecular Pharmaceutics **6**(4): 1041-1051.

Guo, J. W., T. S. Zhao, et al. (2005). "Preparation and the physical/electrochemical properties of a Pt/C nanocatalyst stabilized by citric acid for polymer electrolyte fuel cells." Electrochimica Acta **50**(10): 1973-1983.

He, Q. J., Z. W. Zhang, et al. (2009). "Intracellular localization and cytotoxicity of spherical mesoporous silica nano- and microparticles." Small **5**(23): 2722-2729.

Herricks, T., J. Y. Chen, et al. (2004). "Polyol synthesis of platinum nanoparticles: Control of morphology with sodium nitrate." Nano Letters **4**(12): 2367-2371.

Hill, A. J., H. Teraoka, et al. (2005). "Zebrafish as a model vertebrate for investigating chemical toxicity." Toxicological Sciences **86**(1): 6-19.

Hillyer, J. F. and R. M. Albrecht (2001). "Gastrointestinal persorption and tissue distribution of differently sized colloidal gold nanoparticles." Journal of Pharmaceutical Sciences **90**(12): 1927-1936.

Hoet, P. H. M., I. Brüske-Hohlfeld, et al. (2004). "Nanoparticles – Known and unknown health risks." Journal of Nanobiotechnology **2**: 12.

Huang, M., Z. S. Ma, et al. (2002). "Uptake of FITC-chitosan nanoparticles by A549 cells." Pharmaceutical Research **19**(10): 1488-1494.

Huczko, A. (2000). "Template-based synthesis of nanomaterials." Applied Physics A-Materials Science & Processing **70**(4): 365-376.

Hussain, S. M., L. K. Braydich-Stolle, et al. (2009). "Toxicity evaluation for safe use of nanomaterials: Recent achievements and technical challenges." Advanced Materials **21**(16): 1549-1559.

Hussain, S. M., K. L. Hess, et al. (2005). "In vitro toxicity of nanoparticles in BRL 3A rat liver cells." Toxicology in Vitro **19**(7): 975-983.

Hyun, J. S., B. S. Lee, et al. (2008). "Effects of repeated silver nanoparticles exposure on the histological structure and mucins of nasal respiratory mucosa in rats." Toxicology Letters **182**(1-3): 24-28.

Jahani-Asl, A., M. Germain, et al. (2010). "Mitochondria: Joining forces to thwart cell death." Biochimica Et Biophysica Acta-Molecular Basis of Disease **1802**(1): 162-166.

Jani, P., G. W. Halbert, et al. (1990). "Nanoparticle uptake by the rat gastrointestinal mucosa - Quantitation and particle-size dependency." Journal of Pharmacy and Pharmacology **42**(12): 821-826.

Jarvie, H. P., H. Al-Obaidi, et al. (2009). "Fate of silica nanoparticles in simulated primary wastewater treatment." Environmental Science & Technology **43**(22): 8622-8628.

Jarvie, H. P. and S. M. King (2010). "Just scratching the surface? New techniques show how surface functionality of nanoparticles influences their environmental fate." Nano Today **5**(4): 248-250.

Jin, H., D. A. Heller, et al. (2009). "Size-dependent cellular uptake and expulsion of single-walled carbon nanotubes: Single particle tracking and a generic uptake model for nanoparticles." ACS Nano **3**(1): 149-158.
Johnston, H. J., G. Hutchison, et al. (2010). "A review of the *in vivo* and *in vitro* toxicity of silver and gold particulates: Particle attributes and biological mechanisms responsible for the observed toxicity." Critical Reviews in Toxicology **40**(4): 328-346.
Jones, C. F. and D. W. Grainger (2009). "*In vitro* assessments of nanomaterial toxicity." Advanced Drug Delivery Reviews **61**(6): 438-456.
Kang, B., M. A. Mackey, et al. (2010). "Nuclear targeting of gold nanoparticles in cancer cells induces DNA damage, causing cytokinesis arrest and apoptosis." Journal of the American Chemical Society **132**(5): 1517-1519.
Kang, S. J., C. Kocabas, et al. (2007). "High-performance electronics using dense, perfectly aligned arrays of single-walled carbon nanotubes." Nature Nanotechnology **2**(4): 230-236.
Kim, D. H., E. A. Rozhkova, et al. (2010). "Biofunctionalized magnetic-vortex microdiscs for targeted cancer-cell destruction." Nature Materials **9**(2): 165-171.
Kim, J. H., H. H. Jang, et al. (2010). "A functionalized gold nanoparticles-assisted universal carrier for antisense DNA." Chemical Communications **46**: 4151-4153.
Kim, W. Y., J. Kim, et al. (2009). "Histological study of gender differences in accumulation of silver nanoparticles in kidneys of Fischer 344 rats." Journal of Toxicology and Environmental Health-Part a-Current Issues **72**(21-22): 1279-1284.
Kittler, S., C. Greulich, et al. (2010). "The influence of proteins on the dispersability and cell-biological activity of silver nanoparticles." Journal of Materials Chemistry **20**(3): 512-518.
Klein, J. (2007). "Probing the interactions of proteins and nanoparticles." Proceedings of the National Academy of Sciences of the United States of America **104**(7): 2029-2030.
Kocbek, P., N. Obermajer, et al. (2007). "Targeting cancer cells using PLGA nanoparticles surface modified with monoclonal antibody." Journal of Controlled Release **120**(1-2): 18-26.
Komatsu, T., M. Tabata, et al. (2008). "The effects of nanoparticles on mouse testis Leydig cells *in vitro*." Toxicology in Vitro **22**(8): 1825-1831.
Korzh, S., X. F. Pan, et al. (2008). "Requirement of vasculogenesis and blood circulation in late stages of liver growth in zebrafish." BMC Developmental Biology **8**: 15.
Kowshik, M., S. Ashtaputre, et al. (2003). "Extracellular synthesis of silver nanoparticles by a silver-tolerant yeast strain MKY3." Nanotechnology **14**(1): 95-100.
Lacerda, L., M. A. Herrero, et al. (2008). "Carbon-nanotube shape and individualization critical for renal excretion." Small **4**(8): 1130-1132.
Lademann, J., H. J. Weigmann, et al. (1999). "Penetration of titanium dioxide microparticles in a sunscreen formulation into the horny layer and the follicular orifice." Skin Pharmacology and Applied Skin Physiology **12**(5): 247-256.

Lai, C. H., C. Y. Lin, et al. (2010). "Galactose encapsulated multifunctional nanoparticle for HepG2 cell internalization." Advanced Functional Materials **20**(22): 3948-3958.

Lam, S. H., Y. L. Wu, et al. (2006). "Conservation of gene expression signatures between zebrafish and human liver tumors and tumor progression." Nature Biotechnology **24**(1): 73-75.

Larese, F. F., F. D'Agostin, et al. (2009). "Human skin penetration of silver nanoparticles through intact and damaged skin." Toxicology **255**(1-2): 33-37.

Leonov, A. P., J. W. Zheng, et al. (2008). "Detoxification of gold nanorods by treatment with polystyrenesulfonate." ACS Nano **2**(12): 2481-2488.

Li, S. D. and L. Huang (2007). Pharmacokinetics and biodistribution of nanoparticles, Valencia, SPAIN, Amer Chemical Soc.

Liang, M., I. C. Lin, et al. (2010). "Cellular uptake of densely packed polymer coatings on gold nanoparticles." ACS Nano **4**(1): 403-413.

Lide, D. R. (2000). CRC Handbook of Chemistry and Physics, CRC Press.

Lim, S. I., I. Ojea-Jimenez, et al. (2010). "Synthesis of platinum cubes, polypods, cuboctahedrons, and raspberries assisted by cobalt nanocrystals." Nano Letters **10**(3): 964-973.

Liu, Z. H., Y. P. Jiao, et al. (2008). "Polysaccharides-based nanoparticles as drug delivery systems." Advanced Drug Delivery Reviews **60**(15): 1650-1662.

Llovet, J. M., A. Burroughs, et al. (2003). "Hepatocellular carcinoma." Lancet **362**(9399): 1907-1917.

Low, P. S. (2007). "The optimal strategy for drug targeting." Molecular Pharmaceutics **4**(5): 629-630.

Lynch, I. and K. A. Dawson (2008). "Protein-nanoparticle interactions." Nano Today **3**(1-2): 40-47.

Lynch, I., A. Salvati, et al. (2009). "Protein-nanoparticle interactions - What does the cell see?" Nature Nanotechnology **4**(9): 546-547.

Maeda, H. (2001). The enhanced permeability and retention (EPR) effect in tumor vasculature: The key role of tumor-selective macromolecular drug targeting. Advances in Enzyme Regulation, Vol 41. G. Weber. Oxford, Pergamon-Elsevier Science Ltd. **41:** 189-207.

Maeda, H., J. Wu, et al. (2000). "Tumor vascular permeability and the EPR effect in macromolecular therapeutics: A review." Journal of Controlled Release **65**(1-2): 271-284.

Malet-Martino, M. and R. Martino (2002). "Clinical studies of three oral prodrugs of 5-fluorouracil (capecitabine, UFT, S-1): A review." Oncologist **7**(4): 288-323.

Mandal, B. B. and S. C. Kundu (2009). "Self-assembled silk sericin/poloxamer nanoparticles as nanocarriers of hydrophobic and hydrophilic drugs for targeted delivery." Nanotechnology **20**(35): 14.

Mang, S. H., N. Won, et al. (2009). "Hyaluronic acid-quantum dot conjugates for *in vivo* lymphatic vessel imaging." ACS Nano **3**(6): 1389-1398.

Matsumura, Y. and H. Maeda (1986). "A new concept for macromolecular therapeutics in cancer-chemotherapy - Mechanism of tumoritropic accumulation of proteins and the antitumor agent smancs." Cancer Research **46**(12): 6387-6392.

Mavon, A., C. Miquel, et al. (2007). "*In vitro* percutaneous absorption and *in vivo* stratum corneum distribution of an organic and a mineral sunscreen." Skin Pharmacology and Physiology **20**(1): 10-20.

Mishra, B., B. B. Patel, et al. (2010). "Colloidal nanocarriers: A review on formulation technology, types and applications toward targeted drug delivery." Nanomedicine-Nanotechnology Biology and Medicine **6**(1): 9-24.
Misra, R. and S. K. Sahoo (2010). "Intracellular trafficking of nuclear localization signal conjugated nanoparticles for cancer therapy." European Journal of Pharmaceutical Sciences **39**(1-3): 152-163.
Moghimi, S. M., A. C. Hunter, et al. (2005). "Nanomedicine: Current status and future prospects." FASEB Journal **19**(3): 311-330.
Molema, G., D. K. F. Meijer, et al. (1998). "Tumor vasculature targeted therapies - Getting the players organized." Biochemical Pharmacology **55**(12): 1939-1945.
Murakami, T. and K. Tsuchida (2008). "Recent advances in inorganic nanoparticle-based drug delivery systems." Mini-Reviews in Medicinal Chemistry **8**(2): 175-183.
Nanda, A. and M. Saravanan (2009). "Biosynthesis of silver nanoparticles from Staphylococcus aureus and its antimicrobial activity against MRSA and MRSE." Nanomedicine-Nanotechnology Biology and Medicine **5**(4): 452-456.
Nel, A., T. Xia, et al. (2006). "Toxic potential of materials at the nanolevel." Science **311**(5761): 622-627.
Nelson, S. M., T. Mahmoud, et al. (2010). "Toxic and teratogenic silica nanowires in developing vertebrate embryos." Nanomedicine-Nanotechnology Biology and Medicine **6**(1): 93-102.
Nemmar, A., S. Al-Maskari, et al. (2007). "Cardiovascular and lung inflammatory effects induced by systemically administered diesel exhaust particles in rats." American Journal of Physiology-Lung Cellular and Molecular Physiology **292**(3): L664-L670.
Nemmar, A., H. Vanbilloen, et al. (2001). "Passage of intratracheally instilled ultrafine particles from the lung into the systemic circulation in hamster." American Journal of Respiratory and Critical Care Medicine **164**(9): 1665-1668.
Nguyen, A. T., A. Emelyanov, et al. (2011). "A high level of liver-specific expression of oncogenic Kras(V12) drives robust liver tumorigenesis in transgenic zebrafish." Disease Models & Mechanisms **4**(6): 801-813.
Nichols, B. J. and J. Lippincott-Schwartz (2001). "Endocytosis without clathrin coats." Trends in Cell Biology **11**(10): 406-412.
Oberdorster, G., E. Oberdorster, et al. (2005). "Nanotoxicology: An emerging discipline evolving from studies of ultrafine particles." Environmental Health Perspectives **113**(7): 823-839.
Oberdorster, G., Z. Sharp, et al. (2004). "Translocation of inhaled ultrafine particles to the brain." Inhalation Toxicology **16**(6-7): 437-445.
Oh, W. K., S. Kim, et al. (2010). "Shape-dependent cytotoxicity and proinflammatory response of poly(3,4-ethylenedioxythiophene) nanomaterials." Small **6**(7): 872-879.
Osterauer, R., C. Fassbender, et al. (2011). "Genotoxicity of platinum in embryos of zebrafish (*Danio rerio*) and ramshorn snail (*Marisa cornuarietis*)." Science of the Total Environment **409**(11): 2114-2119.
Osterauer, R., N. Haus, et al. (2009). "Uptake of platinum by zebrafish (*Danio rerio*) and ramshorn snail (*Marisa cornuarietis*) and resulting effects on early embryogenesis." Chemosphere **77**(7): 975-982.
Ozaki, T., T. Yamashita, et al. (2009). "Mitochondrial m-calpain plays a role in the release of truncated apoptosis-inducing factor from the mitochondria."

Biochimica Et Biophysica Acta-Molecular Cell Research **1793**(12): 1848-1859.

Pan, J. and S. S. Feng (2008). "Targeted delivery of paclitaxel using folate-decorated poly(lactide) - vitamin E TPGS nanoparticles." Biomaterials **29**(17): 2663-2672.

Pan, J. and S. S. Feng (2009). "Targeting and imaging cancer cells by folate-decorated, quantum dots (QDs)-loaded nanoparticles of biodegradable polymers." Biomaterials **30**(6): 1176-1183.

Pan, Y., S. Neuss, et al. (2007). "Size-dependent cytotoxicity of gold nanoparticles." Small **3**(11): 1941-1949.

Park, E. K., S. Y. Kim, et al. (2005). "Folate-conjugated methoxy poly(ethylene glycol)/poly(e-caprolactone) amphiphilic block copolymeric micelles for tumor-targeted drug delivery." Journal of Controlled Release **109**: 158-168.

Parveen, S., R. Misra, et al. (2012). "Nanoparticles: A boon to drug delivery, therapeutics, diagnostics and imaging." Nanomedicine-Nanotechnology Biology and Medicine **8**(2): 147-166.

Patra, C. R., R. Verma, et al. (2008). "Fabrication of gold nanoparticle for potential application in multiple myeloma." Journal of Biomedical Nanotechnology **4**(4): 499-507.

Pauluhn, J., A. Hahn, et al. (2008). "Assessment of early acute lung injury in rats exposed to aerosols of consumer products: Attempt to disentangle the "Magic Nano" conundrum." Inhalation Toxicology **20**(14): 1245-1262.

Pazos-Perez, N., B. Rodriguez-Gonzalez, et al. (2010). "Gold encapsulation of star-shaped FePt nanoparticles." Journal of Materials Chemistry **20**(1): 61-64.

Peer, D., J. M. Karp, et al. (2007). "Nanocarriers as an emerging platform for cancer therapy." Nature Nanotechnology **2**(12): 751-760.

Phillips, M. A., M. L. Gran, et al. (2010). "Targeted nanodelivery of drugs and diagnostics." Nano Today **5**(2): 143-159.

Pun, S. H. and M. E. Davis (2002). "Development of a nonviral gene delivery vehicle for systemic application." Bioconjugate Chemistry **13**(3): 630-639.

Rai, M., A. Yadav, et al. (2009). "Silver nanoparticles as a new generation of antimicrobials." Biotechnology Advances **27**(1): 76-83.

Reddy, A. S., C. Y. Chen, et al. (2010). "Biological synthesis of gold and silver nanoparticles mediated by the bacteria *Bacillus Subtilis*." Journal of Nanoscience and Nanotechnology **10**(10): 6567-6574.

Rejman, J., V. Oberle, et al. (2004). "Size-dependent internalization of particles via the pathways of clathrin-and caveolae-mediated endocytosis." Biochemical Journal **377**: 159-169.

Rieter, W. J., K. M. Pott, et al. (2008). "Nanoscale coordination polymers for platinum-based anticancer drug delivery." Journal of the American Chemical Society **130**(35): 11584-+.

Rodriguez-Hernandez, J., F. Checot, et al. (2005). "Toward 'smart' nano-objects by self-assembly of block copolymers in solution." Progress in Polymer Science **30**(7): 691-724.

Rosenholm, J. M., E. Peuhu, et al. (2009). "Targeted intracellular delivery of hydrophobic agents using mesoporous hybrid silica nanoparticles as carrier systems." Nano Letters **9**(9): 3308-3311.

Rupper, A. and J. Cardelli (2001). "Regulation of phagocytosis and endo-phagosomal trafficking pathways in Dictyostelium discoideum." Biochimica Et Biophysica Acta-General Subjects **1525**(3): 205-216.

Rytting, E., K. A. Lentz, et al. (2005). "Aqueous and cosolvent solubility data for drug-like organic compounds." AAPS Journal **7**(1): E78-E105.

Sakon, M., H. Nagano, et al. (2002). "Combined intraarterial 5-fluorouracil and subcutaneous interferon-alpha therapy for advanced hepatocellular carcinoma with tumor thrombi in the major portal branches." Cancer **94**(2): 435-442.

Sarin, H., A. S. Kanevsky, et al. (2008). "Effective transvascular delivery of nanoparticles across the blood-brain tumor barrier into malignant glioma cells." Journal of Translational Medicine **6**: 15.

Scholars, W. W. I. C. f. (25/08/09). "Consumer Products: An inventory of nanotechnology-based consumer products currently on the market." Retrieved 04/06/2012, 2012, from http://www.nanotechproject.org/inventories/consumer/.

Semmler-Behnke, M., W. G. Kreyling, et al. (2008). "Biodistribution of 1.4- and 18-nm gold particles in rats." Small **4**(12): 2108-2111.

Shrivastava, S., T. Bera, et al. (2009). "Characterization of antiplatelet properties of silver nanoparticles." ACS Nano **3**(6): 1357-1364.

Shvedova, A. A., J. P. Fabisiak, et al. (2008). "Sequential exposure to carbon nanotubes and bacteria enhances pulmonary inflammation and infectivity." American Journal of Respiratory Cell and Molecular Biology **38**(5): 579-590.

Sonavane, G., K. Tomoda, et al. (2008). "*In vitro* permeation of gold nanoparticles through rat skin and rat intestine: Effect of particle size." Colloids and Surfaces B-Biointerfaces **65**(1): 1-10.

Song, Y., X. Li, et al. (2009). "Exposure to nanoparticles is related to pleural effusion, pulmonary fibrosis and granuloma." European Respiratory Journal **34**(3): 559-567.

Souris, J. S., C. H. Lee, et al. (2010). "Surface charge-mediated rapid hepatobiliary excretion of mesoporous silica nanoparticles." Biomaterials **31**(21): 5564-5574.

Storm, G., S. O. Belliot, et al. (1995). "Surface modifications of nanoparticles to oppose uptake by the mononuclear phagocyte system." Advanced Drug Delivery Reviews **17**(1): 31-48.

Sung, J. H. and M. L. Shuler (2009). "A micro cell culture analog (mu CCA) with 3-D hydrogel culture of multiple cell lines to assess metabolism-dependent cytotoxicity of anti-cancer drugs." Lab on a Chip **9**(10): 1385-1394.

Szarpak, A., D. Cui, et al. (2010). "Designing hyaluronic acid-based layer-by-layer capsules as a carrier for intracellular drug delivery." Biomacromolecules **11**(3): 713-720.

Teow, Y., P. V. Asharani, et al. (2011). "Health impact and safety of engineered nanomaterials." Chemical Communications **47**(25): 7025-7038.

Teow, Y. and S. Valiyaveettil (2011). "Active targeting of cancer cells using folic acid-conjugated platinum nanoparticles." Nanoscale **2**(12): 2607-2613.

Thakkar, K. N., S. S. Mhatre, et al. (2010). "Biological synthesis of metallic nanoparticles." Nanomedicine-Nanotechnology Biology and Medicine **6**(2): 257-262.

Thanh, N. T. K. and L. A. W. Green (2010). "Functionalisation of nanoparticles for biomedical applications." Nano Today **5**(3): 213-230.

Thevenot, P., J. Cho, et al. (2008). "Surface chemistry influences cancer killing effect of TiO_2 nanoparticles." Nanomedicine-Nanotechnology Biology and Medicine **4**(3): 226-236.

Thomas, M. and A. M. Klibanov (2003). "Conjugation to gold nanoparticles enhances polyethylenimine's transfer of plasmid DNA into mammalian cells." Proceedings of the National Academy of Sciences of the United States of America **100**(16): 9138-9143.
Thorpe, P. E. (2004). "Vascular targeting agents as cancer therapeutics." Clinical Cancer Research **10**(2): 415-427.
Torchilin, V. P. (2001). "Structure and design of polymeric surfactant-based drug delivery systems." Journal of Controlled Release **73**(2-3): 137-172.
Torchilin, V. P. (2006). "Multifunctional nanocarriers." Advanced Drug Delivery Reviews **58**(14): 1532-1555.
Torchilin, V. P. (2007). "Micellar nanocarriers: Pharmaceutical perspectives." Pharmaceutical Research **24**(1): 1-16.
Ulukaya, E., F. Ozdikicioglu, et al. (2008). "The MTT assay yields a relatively lower result of growth inhibition than the ATP assay depending on the chemotherapeutic drugs tested." Toxicology in Vitro **22**(1): 232-239.
van Rheenen, P. R., M. J. McKelvy, et al. (1987). "Synthesis and characterization of small platinum particles formed by the chemical reduction of chloroplatinic acid." Journal of Solid State Chemistry **67**(1): 151-169.
Veber, D. F., S. R. Johnson, et al. (2002). "Molecular properties that influence the oral bioavailability of drug candidates." Journal of Medicinal Chemistry **45**(12): 2615-2623.
Walsh, M., M. Tangney, et al. (2006). "Evaluation of cellular uptake and gene transfer efficiency of pegylated poly-L-lysine compacted DNA: Implications for cancer gene therapy." Molecular Pharmaceutics **3**(6): 644-653.
Wang, B., W. Y. Feng, et al. (2006). "Acute toxicity of nano- and micro-scale zinc powder in healthy adult mice." Toxicology Letters **161**(2): 115-123.
Wang, L., H. J. Wang, et al. (2010). "Rapid and efficient synthesis of platinum nanodendrites with high surface area by chemical reduction with formic acid." Chemistry of Materials **22**(9): 2835-2841.
Wang, Q., L. Zhang, et al. (2010). "Norcantharidin-associated galactosylated chitosan nanoparticles for hepatocyte-targeted delivery." Nanomedicine-Nanotechnology Biology and Medicine **6**(2): 371-381.
Wang, X., F. Liu, et al. (2006). "Carbon nanotube-DNA nanoarchitectures and electronic functionality." Small **2**(11): 1356-1365.
Wang, Y. and G. Z. Cao (2006). "Synthesis and enhanced intercalation properties of nanostructured vanadium oxides." Chemistry of Materials **18**(12): 2787-2804.
Waters, K. M., L. M. Masiello, et al. (2009). "Macrophage responses to silica nanoparticles are highly conserved across particle sizes." Toxicological Sciences **107**(2): 553-569.
Westerfield, M. (2000). The zebrafish book: A guide for the laboratory use of zebrafish (*Danio rerio*), Inst of Neuro Science.
Wiley, B., Y. G. Sun, et al. (2007). "Synthesis of silver nanostructures with controlled shapes and properties." Accounts of Chemical Research **40**(10): 1067-1076.
Wilson, B., M. K. Samanta, et al. (2010). "Chitosan nanoparticles as a new delivery system for the anti-Alzheimer drug tacrine." Nanomedicine-Nanotechnology Biology and Medicine **6**(1): 144-152.
Wiradharma, N., Y. Zhang, et al. (2009). "Self-assembled polymer nanostructures for delivery of anticancer therapeutics." Nano Today **4**: 302-317.

Wu, S. D., C. C. Zhu, et al. (2011). "*In vitro* and *in vivo* fluorescent imaging of a monofunctional chelated platinum complex excitable using visible light." Inorganic Chemistry **50**(23): 11847-11849.

Xia, T., N. Li, et al. (2009). "Potential health impact of nanoparticles." Annual Review of Public Health **30**: 137-150.

Xing, X. L., X. X. He, et al. (2005). "Uptake of silica-coated nanoparticles by HeLa cells." Journal of Nanoscience and Nanotechnology **5**(10): 1688-1693.

Yamago, S., H. Tokuyama, et al. (1995). "*In-vivo* biological behavior of a water-miscible fullerene - C-14 labeling, absorption, distribution, excretion and acute toxicity." Chemistry & Biology **2**(6): 385-389.

Yamamoto, T., H. Nagano, et al. (2004). "Partial contribution of tumor necrosis factor-related apoptosis-inducing ligand (TRAIL)/TRAIL receptor pathway to antitumor effects of interferon-alpha/5-fluorouracil against hepatocellular carcinoma." Clinical Cancer Research **10**(23): 7884-7895.

Yanagisawa, R., H. Takano, et al. (2009). "Titanium dioxide nanoparticles aggravate atopic dermatitis-like skin lesions in NC/Nga mice." Experimental Biology and Medicine **234**(3): 314-322.

Yang, R., F. H. Meng, et al. (2011). "Galactose-decorated cross-linked biodegradable poly(ethylene glycol)-b-poly(epsilon-caprolactone) block copolymer micelles for enhanced hepatoma-targeting delivery of Paclitaxel." Biomacromolecules **12**(8): 3047-3055.

Yang, X. Q., Y. H. Chen, et al. (2008). "Folate-encoded and Fe_3O_4-loaded polymeric micelles for dual targeting of cancer cells." Polymer **49**(16): 3477-3485.

Yih, T. C. and M. Al-Fandi (2006). "Engineered nanoparticles as precise drug delivery systems." Journal of Cellular Biochemistry **97**(6): 1184-1190.

Yoshida, T., N. Oide, et al. (2006). "Induction of cancer cell-specific apoptosis by folate-labeled cationic liposomes." Journal of Controlled Release **111**(3): 325-332.

You, J., X. Li, et al. (2008). "Folate-conjugated polymer micelles for active targeting to cancer cells: preparation, in vitro evaluation of targeting ability and cytotoxicity." Nanotechnology **19**(4): 9.

Zalipsky, S. (1995). "Chemistry of polyethylene-glycol conjugates with biologically-active molecules." Advanced Drug Delivery Reviews **16**(2-3): 157-182.

Zaman, N. T., Y. Y. Yang, et al. (2010). "Stimuli-responsive polymers for the targeted delivery of paclitaxel to hepatocytes." Nano Today **5**(1): 9-14.

Zanta, M. A., O. Boussif, et al. (1997). "*In vitro* gene delivery to hepatocytes with galactosylated polyethylenimine." Bioconjugate Chemistry **8**(6): 839-844.

Zhang, L., F. X. Gu, et al. (2008). "Nanoparticles in medicine: Therapeutic applications and developments." Clinical Pharmacology & Therapeutics **83**(5): 761-769.

Zhang, L. W. and N. A. Monteiro-Riviere (2008). "Assessment of quantum dot penetration into intact, tape-stripped, abraded and flexed rat skin." Skin Pharmacology and Physiology **21**(3): 166-180.

Zhou, J. F., J. Ralston, et al. (2009). "Functionalized gold nanoparticles: Synthesis, structure and colloid stability." Journal of Colloid and Interface Science **331**(2): 251-262.

Zhu, M. T., W. Y. Feng, et al. (2009). "Particokinetics and extrapulmonary translocation of intratracheally instilled ferric oxide nanoparticles in rats and the potential health risk assessment." Toxicological Sciences **107**(2): 342-351.

Zhu, X. S., L. Zhu, et al. (2008). "Comparative toxicity of several metal oxide nanoparticle aqueous suspensions to zebrafish (*Danio rerio*) early developmental stage." Journal of Environmental Science and Health Part a-Toxic/Hazardous Substances & Environmental Engineering **43**(3): 278-284.

APPENDIX